UNIVERSITY OF THESSALY

SCHOOL OF ENGINEERING

DEPARTMENT OF MECHANICAL ENGINEERING

Diploma Thesis

CONSIDERATION OF CREEP AND CARBURIZATION IN OIL REFINERIES

by

Georgios F. Samaras

A thesis submitted in partial fulfilment of the requirements for the degree of Diploma in Mechanical Engineering, University of Thessaly

2015

Approved by the members of the Examination Committee

Dr. Gregory Haidemenopoulos (Supervisor)

Professor of Physical Metallurgy

Department of Mechanical Engineering, University of Thessaly

Dr. Nikolaos Aravas

Professor of Computational Mechanics of Structures

Department of Mechanical Engineering, University of Thessaly

Dr. Alexis Kermanidis

Assistant Professor of Mechanical Behavior of Metallic Materials

Department of Mechanical Engineering, University of Thessaly

Acknowledgments

First of all, I would to thank my thesis supervisor, Prof. Gregory Haidemenopoulos, for his valuable assistance and guidance during my studies at the Department of Mechanical Engineering. His high level of knowledge and teaching attracted me in the Material's field. I'm also grateful for the assignment of this thesis which opened more my horizons.

I would also like to express my deeper thanks to Prof. Nikolaos Aravas for his support and encouragement all these five years of my studies. He provided me a strong scientific bridge between materials and mechanics through undergraduate and postgraduate courses, taught by him at an exceptional level.

I am also grateful to the 3rd member of the thesis committee, Ass. Prof. Alexis Kermanidis for his valuable suggestions and for the careful reading of my work.

In addition upon the completion of my studies, I would also like to thank the members of the Academic Staff of the Department for providing me knowledge and foundations in the field of Mechanical Engineering. Special thanks to Professors Spyros Karamanos, Vasilios Bontozoglou, Georgios Kozanidis, Nikolaos Andritsos, Anna Zervaki, Georgios Perantzakis, Nikolaos Hassiotis, Helen Kamoutsi and Tasos Stamatis.

Moreover, I would like to thank the members of the Materials Laboratory, for their cooperation and kind support during my stay at the Lab.

I would like also like to mention and to express my deepest gratitude's to my classmates but mostly friends, Mitsos, Agapitos, Nikos, Stamatis, Stelios and Elias, Eleni for their friendship, collaboration and continuous support. We've shared a lot of unforgettable moments at the Department, and in Volos, at this very important period of our life, and I think that this is a strong guarantee for our friendship in the future, independently of the place where everyone will proceed to the next step. Last but not least, I would like to thank Chryssa for her support and understanding during the completion of this Thesis.

Above all, I am grateful to my parents, Filippos and Anna and my brother Dimitris for their love and constant support over the years.

CONSIDERATION OF CREEP AND CARBURIZATION

IN OIL REFINERIES

Georgios F. Samaras

University of Thessaly, Department of Mechanical Engineering, 2015

Supervisor: Dr. Gregory Haidemenopoulos, Professor of Physical Metallurgy

ABSTRACT

The scope of this Diploma Thesis was to study the different creep phenomena which may cause catastrophic failures if evolved out of control, in equipment used in oil refineries. Towards this scope specific API codes were studied, analyzed and adopted for simulations of several case studies which were taken from Greek Refineries.

API 530 standard was used for the determination of the thickness in tubes used in high temperature. In addition the Larson- Miller approach was employed in order to predict the remaining life and to calculate the accumulated creep damage in components which had been exposed in the creep range for extended time periods.

API 579 was used in order to implement Fitness- For- Service assessment in components which had experienced a temperature excursion during service. In addition experimental evaluation based on microstructural analysis and tensile testing was also performed in order to support FFS assessment. The calculations provided reliable results, which may be used for the determination of the operational conditions for the future life time of the components.

Finally, an attempt was made concerning carburization simulations for the heat-resistant steels referred to API-530. It is worth noting that the code doesn't take into account the carburization phenomena encountered in high temperature applications in oil refineries. Computational thermodynamics and kinetics (Thermo-Calc and DICTRA) were employed to model the carbon diffusion with the concurrent formation of alloy carbides so as to categorize the materials according to their resistance to carburization. The results can be exploited, for material selection for carburization resistance and for the maintenance procedures for the timely replacement of tubes.

The calculations provided in each chapter of the current thesis, may be exploited by the end users (oil refineries) in order to develop certain rules on the re-rating of components worked in the creep range.

Table of Contents

List of Figures

List of Tables

1. Introduction

The general aim of this thesis is to generate know-how in the area of creep for components operating at high temperature in oil refineries, based on the operative API codes, failure analysis cases and scientific knowledge in the area of materials and mechanics. The specific aim is to develop procedures for Fitness-For-Service (FFS) assessment for the continued operation of equipment in the creep range.

The work consists of four parts:

- In part 1 the procedures for the design for creep resistance are reviewed (API 530).
- In part 2 the procedures for estimation of remaining creep life (API 530) are reviewed.
- In part 3, procedures for FFS assessments per API 579 are applied.
- In part 4, a ranking of carburization resistance for the materials used in refineries is provided.

Analytically the structure of the thesis is presented as follows:

Part 1 Design for creep resistance

Aim: to review thickness calculation procedure and to present basic guidelines on elastic and creep rupture design

- API 530 Elastic design and creep rupture design of tubes
- Materials: carbon steels, Cr-Mo steels, P3,P5,P9, austenitic stainless steels (304,316,321,347), heat resistant steels (HK type), Incolloy 800, 800H, 800HT
- Elastic and rupture allowable stresses
- Develop procedure and computer code for minimum thickness calculation per API 530 for elastic and creep rupture design

Part 2 Estimation of remaining life (API 530)

Aim: to review basic knowledge on creep, as well as to provide reaming life assessment procedure based on Larson-Miller method.

- Larson-Miller parameter curves
- Limiting design metal temperature
- Estimation of accumulated creep damage (application of Larson-Miller plots)
- Estimation of consumed life fractions
- Estimation of remaining life
- Develop procedure and computer code for estimation of remaining life

Part 3 Fitness-for-Service Assessment of components operating in the creep range creep (API 579, Part 10)

Aim: to determine the suitability for continued operation and the remaining life of a component operating in the creep range

- Required data for FFS assessment (Loads, stresses, temperatures, Maintenance and operational history, material properties, damage characterization)
- Level II assessment
- Remaining life assessment (Larson-Miller / Project Omega procedures)
- Special cases (Creep bulging)
- Microstructural effects
- Develop procedure for FFS creep assessment

Part 4 Carburization of High- Temperature steels: A simulation- based ranking of materials carburization resistance

Aim: to provide guidelines for material selection for carburization resistance as well as to develop a maintenance tool for the timely replacement of tubes.

- Simulation of carburization by employing computational thermodynamic and kinetic (Thermo-Calc and DICTRA)
- Experimental validation
- Representative calculations for the 316 austenitic stainless steel
- Ranking of the carburization resistance

In the following chapters each part is presented, the methodology adopted is given and case studies taken from Greek refineries are also incorporated.

The thesis is completed by summarizing the progress achieved and providing the main results from each task.

2. Design for Creep Resistance

2.1 Introduction

The thickness calculation of tubes, against creep, in oil refineries, is a very important factor for the right operation and the safety of the plant. The tubes are designed to withstand the rupture design pressure and the design temperature for long periods of operation.

API STANDARD 530 [2.1], *"Calculation of Heater-Tube Thickness in Petroleum Refineries"*, is an inspection code, written and published by the American Petroleum Institute (API), to establish recommendations and requirements for the procedures used for calculating the required wall thickness of new tubes and associated component fittings for petroleum-refinery heaters and determining design criteria as well. The first edition of the code was originally published in October of 1997 and the most recent release was the 7th edition, published in April of 2015.

These procedures laid out in API 530 were specifically developed for the design of refinery and related process-fired heater tubes (direct-fired, heat-absorbing tubes within enclosures). On the other hand, they were not intended to be used for the design or inspection of external piping. The standard also does not specify recommendations or requirements for tube retirement thickness.

The main limitations of API 530 are:

- Can be applied to thin tubes with thickness to diameter ratio less than 0.15.
- Apply to seamless tubes. When applied to welded tubes multiply allowable stress with joint efficiency.
- There is no consideration for graphitization, carburization or hydrogen attack.

This is the main reason that carburization of tubes was given special consideration in Section 4.

Heater tubes are designed in two different design conditions:

- Elastic design (lower Temperatures)
- Creep rupture design (higher Temperatures)

$$\delta_\sigma = \frac{p_{el} D_i}{2\sigma_{el} - p_{el}} \tag{2.1}$$

Besides API, code ASME B31 [2.2] provides also methodology for tube thickness determination. The equation stands for this case is:

$$t = t_e + t_{th} + \left[\frac{Pd_0}{2(SE + PY)}\right]\left[\frac{100}{100 - T_{ol}}\right] \quad (2.2)$$

In case of a seamless tube the above equation simplifies:

$$t = t_e + \left[\frac{Pd_0}{2(SE + PY)}\right] \quad (2.3)$$

There is a similarity with equation (2.1) but ASME code is stringer in comparison to API 530.

2.2 Methodology

The methodology followed for the thickness calculation depends on the design temperature:

- There is a transition temperature, which has a characteristic value for each alloy, according to the relevant equations used.
- For higher temperatures the creep phenomenon influences the life of the tube increasing the possibilities of failure under a certain stress. At lower temperatures the effect of creep is negligible.

The two approaches, described below, concern rupture and elastic design. It is worth noting that the temperature set to separate the elastic and the creep rupture design is not a single value but it is a range of values depending on the alloy, the elastic design pressure, the rupture design pressure, the design life and the corrosion allowance. The whole procedure is fully described in the flow chart of Fig. 2.1 and is given in detail per case hereinafter:

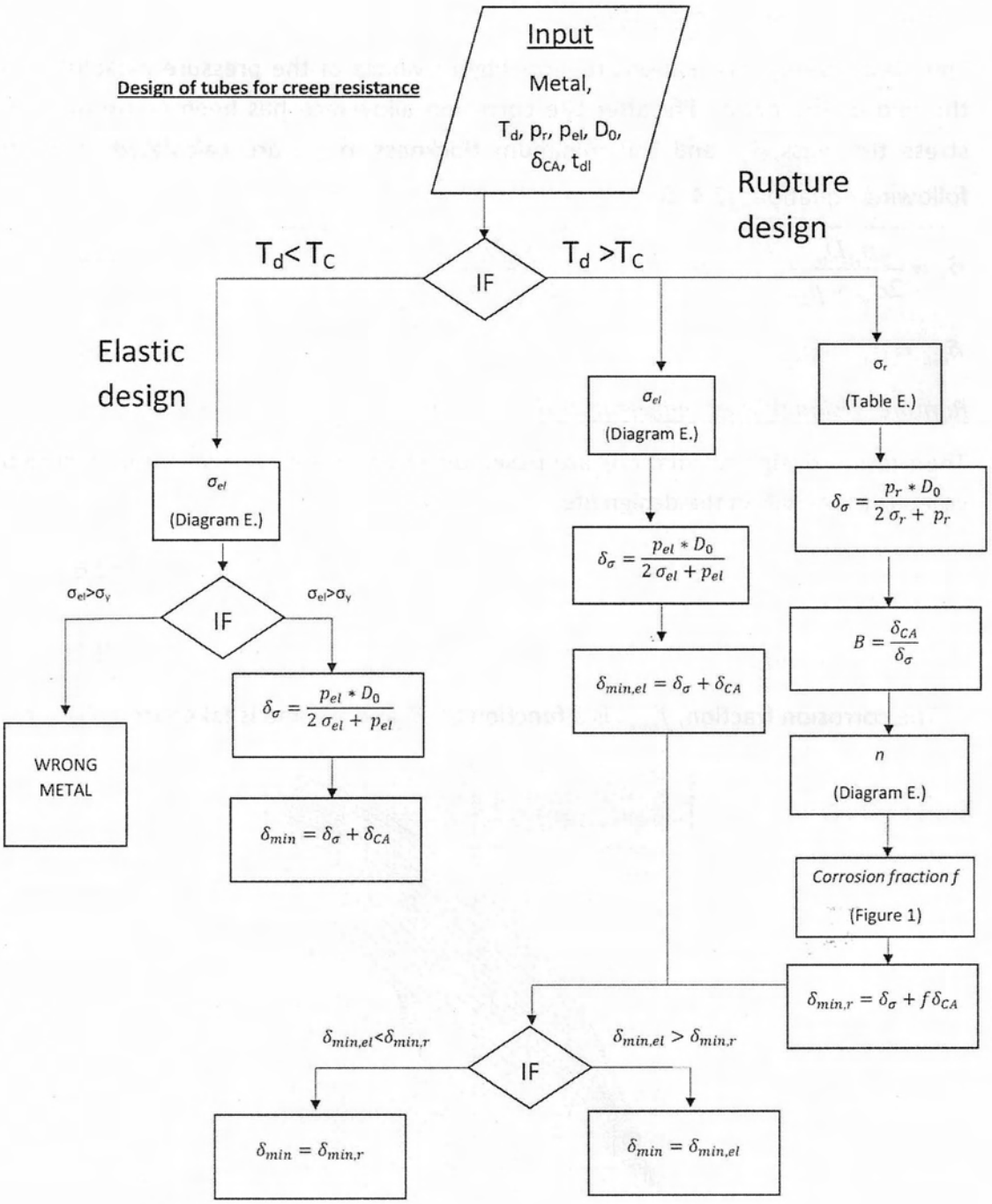

Figure 2.1: Design for creep resistance according to API 530 [2.1]. The terms appearing in the flow chart are defined in Section 2.5

Elastic design (lower temperatures)

The elastic design calculations regards higher values of the pressure established at the end of the design life after the corrosion allowance has been consumed. The stress thickness, δ_σ, and the minimum thickness, $\delta_{\min}$, are calculated from the following equations (2.4) & (2.5):

$$\delta_\sigma = \frac{p_{el} D_0}{2\sigma_{el} + p_{el}} \quad \text{or} \quad \delta_\sigma = \frac{p_{el} D_i}{2\sigma_{el} - p_{el}} \tag{2.4}$$

$$\delta_{\min} = \delta_\sigma + \delta_{CA} \tag{2.5}$$

Rupture design (higher temperatures)

The rupture design calculations are based on the criterion for preventing failure by creep rupture within the design life.

$$\delta_\sigma = \frac{p_r D_0}{2\sigma_r + p_r} \tag{2.6}$$

$$\delta_{\min} = \delta_\sigma + f_{corr}\delta_{CA} \tag{2.7}$$

The corrosion fraction, f_{corr}, is a function of B and n, and is taken from Fig.2.2.

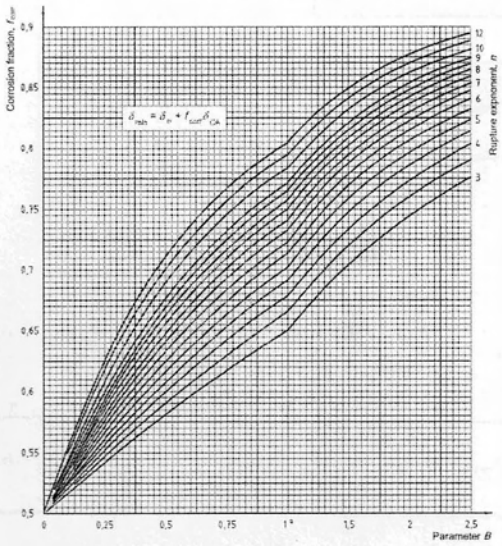

Figure 2.2: Corrosion fraction [2.1]

In the current thesis two case studies are examined based on: (a) elastic design and (b) rupture design. The calculations were performed in Mathematica. The relevant commands list is provided in the Annex.

2.3 Case Studies

1. Elastic design

The following example illustrates the thickness calculation of austenitic stainless steel 347 tubes in elastic range used in refineries. The required information is given bellow.

- Material = 18Cr-10Ni-Nb, Type 347 stainless steel
- Outside Diameter (D_0) = 150 mm
- Elastic design gauge pressure (p_{el}) = 6 MPa
- Corrosion Allowance (δ_{ca}) = 3.2 mm
- Design Temperature (T_d) = 500 °C

Since the design temperature is lower than the temperature limit of Type 347 stainless steel which is 590 °C, then calculation according to elastic design is required. From Fig. 2.3:

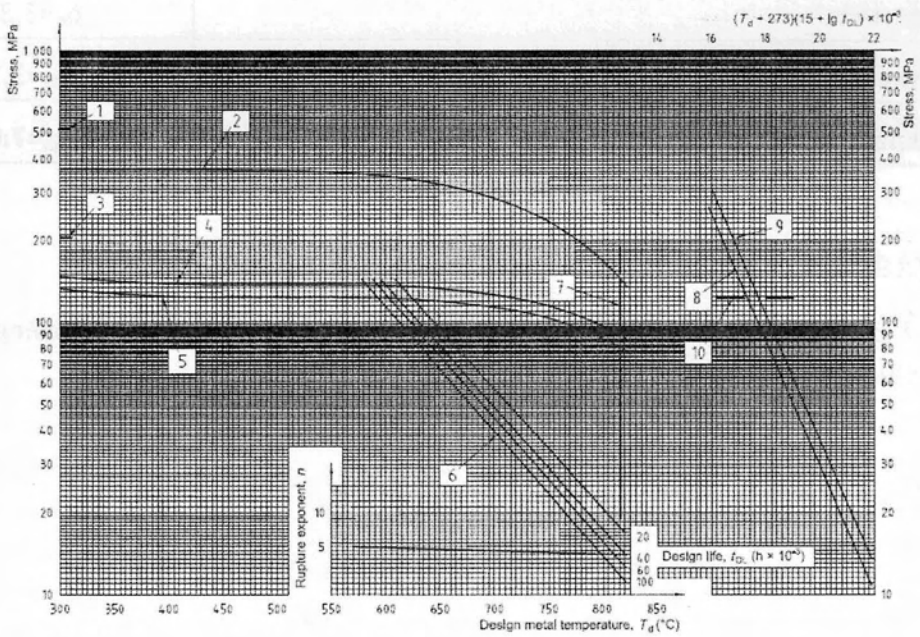

Figure 2.3: Stress curves (SI units) for ASTM A 213, ASTM A 271, ASTM A 312 and ASTM A 376 types 347 and 347H (18Cr-10Ni-Nb) stainless steels

$$\sigma_{el} = 124MPa$$
$$\sigma_{y} = 139MPa$$

Using the equations (2.4) and (2.5) for elastic design:

$$\delta_\sigma = \frac{p_{el} D_0}{2\sigma_{el} + p_{el}} = \frac{(6)(150)}{2(124)+6} = 3.83mm$$

$$\delta_{\min} = \delta_\sigma + \delta_{CA} = 3.83 + 3.2 = 7.03mm$$

The design calculations are summarized in Table 2.1

Table 2.1: Calculation sheet for elastic design, according to API 530

CALCULATION SHEET SI units	
Material: Type 347	
Calculation of minimum thickness	**Elastic design**
Outside diameter, mm	D_0=150
Design pressure, MPa	P_{el}=6
Design metal Temperature, °C	T_d=500
Elastic allowable stress, MPa	σ_{el}=124
Stress thickness, mm	δ_σ=3.83
Corrosion allowance, mm	δ_{ca}=3.2
Minimum thickness, mm	**δ_{min}=7.03**

2. Rupture design

The same steel as in the previous example is going to be designed for the following operating conditions:

$T_d = 800^0 C$

$t_{DL} = 100000h$

$p_r = 4.5MPa$

From Fig. 2.3:

$\sigma_r = 14.03MPa$

$n = 4.4$

Using the equation (2.6) for rupture design:

$$\delta_\sigma = \frac{p_r D_0}{2\sigma_r + p_r} = \frac{(4.5)(150)}{2(14.03)+4.5} = 20.72mm$$

In addition the parameter B is calculated as follows:

$$B = \frac{\delta_{CA}}{\delta_{\sigma}} = \frac{3.2}{20.72} = 0.1544$$

The corrosion fraction f_{corr} is given from Fig.2.2, combining the values for B and n:

$$f_{corr} = 0.4343$$

From equation (2.4):

$$\delta_{\min} = \delta_{\sigma} + f_{corr}\delta_{CA} = 20.72 + (0.4343 \times 3.2) = 22.11\,\text{mm}$$

The tube thickness is also calculated using the equations from the elastic range in order to verify the method.

$$\sigma_{el} = 88MPa$$

$$\delta_{\sigma} = \frac{(6)(150)}{2(88) + 6} = 4.95mm$$

$$\delta_{\min} = 4.95 + 3.2 = 8.15mm$$

The minimum design thickness $\delta_{\min}$ based on the elastic design criterion is approximately 1/3 of the required from the rupture design that reliable. The results are summed up in Table 2.2.

Table 2.2: Calculation sheet for rupture design, according to API 530

CALCULATION SHEET SI units		
Material: Type 347		
Calculation of minimum thickness	**Elastic design**	**Rupture design**
Outside diameter, mm	D_0=150	D_0=150
Design pressure, MPa	P_{el}=6	P_r=4.5
Design metal Temperature, °C	T_d=800	T_d=800
Design Life, h	-	t_{DL}=100000
Allowable stress, MPa	σ_{el}=88	σ_r=14.03
Stress thickness, mm	δ_σ=4.95	δ_σ=20.72
Corrosion allowance, mm	δ_{ca}=3.2	δ_{ca}=3.2
Corrosion Fraction	-	f_{corr}=0.4343
Minimum thickness, mm	**δ_{min}=8.15**	**δ_{min}=22.11**

The results presented above suggest that the temperature plays a major role at thickness calculation.

It is well known the exponential correlation of temperature with creep rate for the steady state creep i.e.:

$$\dot{\varepsilon} = D_0 \exp\left(-\frac{\Delta G}{kT}\right)\sigma^m \qquad [1.3]$$

The influence of temperature on the thickness of the tube, especially above 600 °C is depicted in Fig. 2.4. Data were retrieved from a series of calculations run similar to the above for different Temperatures.

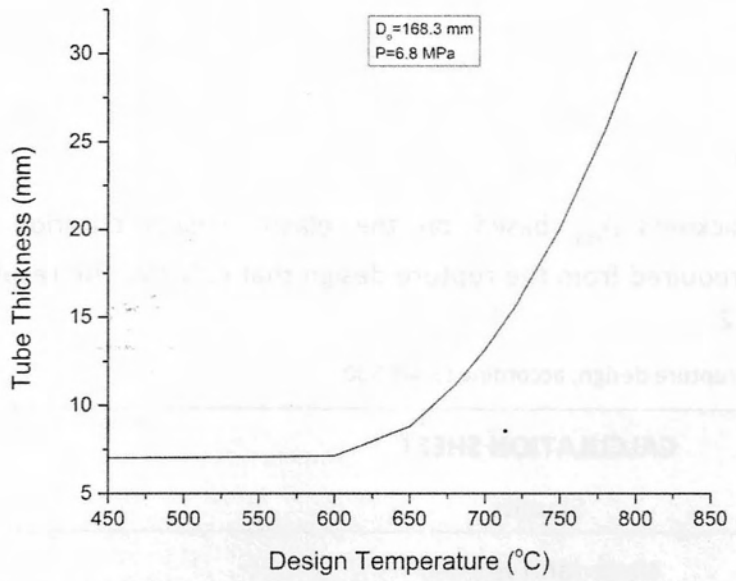

Figure 2.4: Tube thickness vs design temperature. Tube thickness vs design temperature.

2.4 Conclusions

API 530 was adopted for the minimum thickness evaluation of 347 austenitic stainless steel.

The whole procedure was demonstrated in detail and the influence of the working temperature, as well as the initial design consideration, on the tube thickness were demonstrated.

Mathematica was employed for the calculations. The relevant commands list is provided in the Annex.

2.5 Terms & Definitions

t minimum design wall thickness, in.

t_e corrosion allowance, in

t_{th} thread or groove depth, in.

P allowable internal pressure in pipe, psi

d_0 outside diameter of pipe, in

S allowable stress for pipe, psi

E longitudinal weld-joint factor [1.0 seamless, 0.95 electric fusion weld, double butt, straight or spiral seam APL 5L, 0.85 electric resistance weld (ERW), 0.60 furnace butt weld]

Y derating factor (0.4 for ferrous materials operating below 900°F)

T_{ol} manufacturers allowable tolerance, % (12.5 pipe up to 20 in.-OD, 10 pipe > 20 in. OD, API 5L)

δ_σ stress thickness, expressed in millimetres

p_{el} elastic design gauge pressure, expressed in megapascals

p_r rupture design rupture pressure, expressed in megapascals

D_0 outside diameter, expressed in millimeters

D_i^* inside diameter, expressed in millimetres, with the corrosion allowance removed

σ_{el} elastic allowable stress, expressed in megapascals, at the design metal temperature

σ_r rupture allowable stress, expressed in megapascals, at the design metal temperature

$\delta_{\min}$ minimum thickness, expressed in millimetres, including corrosion allowance

δ_{CA} corrosion allowance, expressed in millimetres

f_{corr} corrosion fraction, given in figure 1 as a function of B and n

$$B = \frac{\delta_{CA}}{\delta_\sigma}$$

n rupture exponent at the design metal temperature

t_{DL} operating time used as a basis for tube design

2.6 References

[2.1] API Standard 530. Calculation of heater tube thickness in petroleum refineries. 5th Edition, American Petroleum Institute. 2003

[2.2]ASME B31. Code for pressure piping, section on power piping. The American Society of Mechanical Engineers. 2007

[2.3] Haidemenopoulos GN. Physical Metallurgy. Tziolas Publications.2007

3. Evaluation of Remaining Life based on LM parameter

3.1 Introduction

Metallic materials often experience service at elevated temperatures and are exposed to static mechanical stresses (e.g., turbine rotors in jet engines and steam generators, high-pressure steam lines, as well as gasifiers, steam reformers, steam generators in refineries etc.), that can cause the type of deformation termed **creep.** Defined as the time-dependent and permanent deformation of materials when subjected to a constant load or stress, creep is an undesirable phenomenon and is usually the limiting factor in the equipment's lifetime. It is observed in all materials types; for metals it evolves for temperatures greater than $0.4T_m$ (T_m = absolute melting temperature). The creep strain is accumulated gradually and its kinetics can be described for each material as creep strain vs time at specific temperature [3.1].

The creep curve (Fig. 3.1) consists of three regions, each of which has its own distinctive strain–time features. *Primary* or *transient creep* occurs first, characterized by a continuously decreasing creep rate; that is, the slope of the curve diminishes with time. This suggests that the material is experiencing an increase in creep resistance or strain hardening—deformation becomes more difficult as the material is strained. For *secondary creep*, sometimes termed *steady-state creep*, the rate is almost constant; that is, the plot becomes linear. This is often the stage of creep that is of the longest duration. The constancy of creep rate is explained on the basis of a balance between the competing processes of strain hardening and recovery, recovery being the process whereby a material becomes softer and retains its ability to experience deformation. Finally, for *tertiary creep*, there is an acceleration of the rate leading to failure in short time periods. This failure is frequently termed *rupture* and results from microstructural and/or metallurgical changes, for example, grain boundary separation, and the formation of internal cracks, cavities, and voids [3.1].

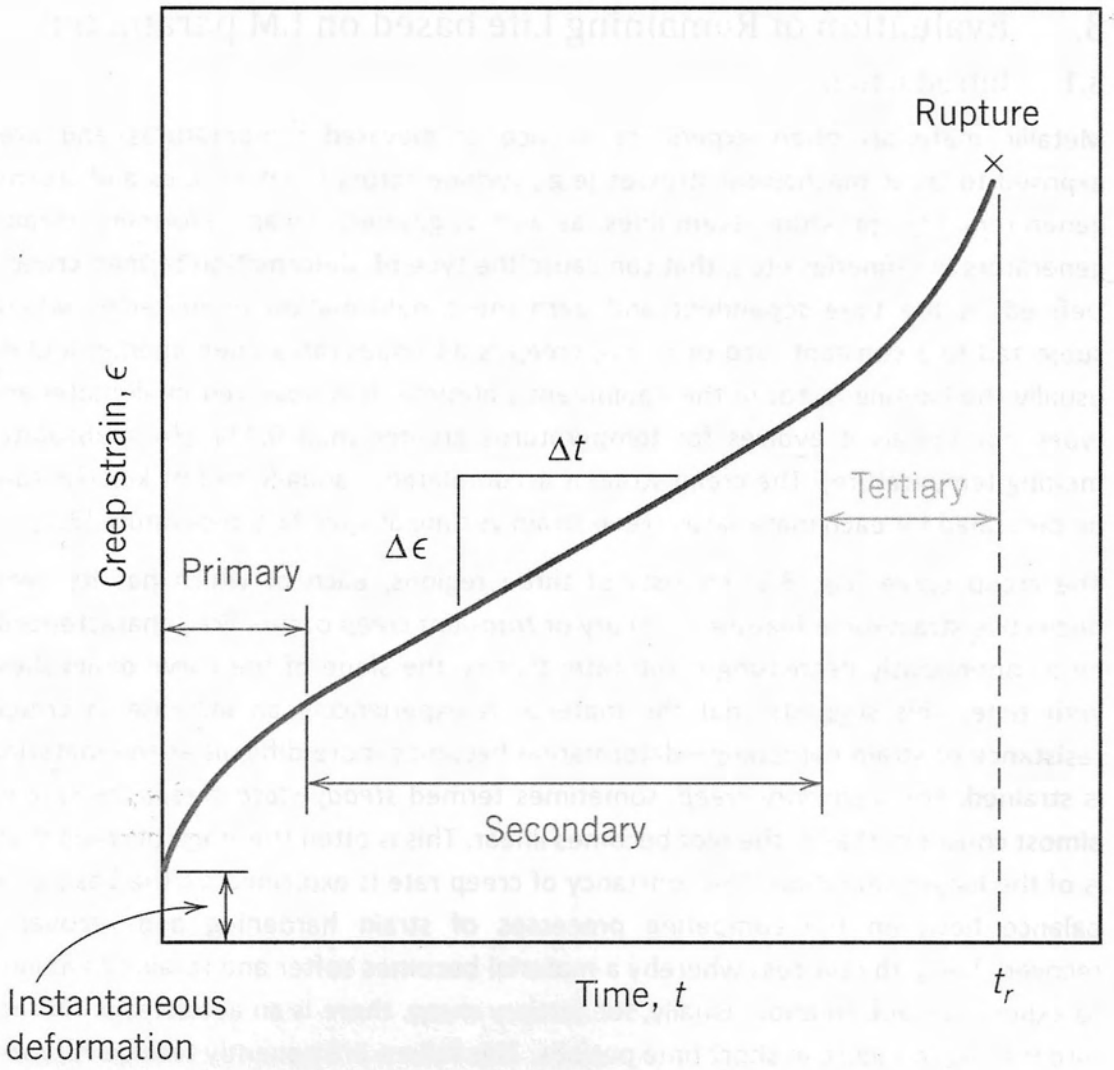

Figure 3.1: Typical curve of creep strain vs time at constant load and constant temperature ($T>0.4T_m$) [3.1]

Creep deformation and rupture are initiated in the grain boundaries and proceed by sliding, separation and microcracking (Fig. 3.2). Thus, creep rupture failures are intercrystalline, in contrast, for example, to the transcrystalline failure surface exhibited by room temperature fatigue failures. Although creep is a plastic flow phenomenon, the intercrystalline failure path results in a rupture surface that has the appearance of brittle fracture.

The creep life of structural components can be determined from the standard creep curve shown in Fig 3.1. However this may require extremely long testing times and there has been a requirement of accelerated testing at extreme conditions to predict creep life at milder service conditions. Extrapolation methods work by establishing correlations between temperature, time to rupture and stress such that the least possible number of accelerated tests are used to determined life under service conditions.

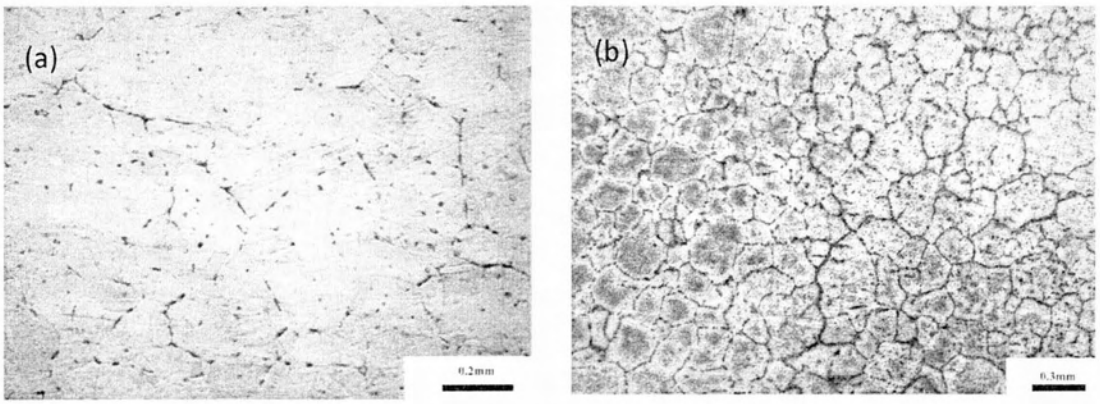

Figure 3.2: (a) Initial stage of secondary creep, with cavities at the triple points of the material, (b) Tertiary creep, with grain separation and microcracks [3.2].

In the engineering practice the following problems have to be solved:

• The working stress and the working temperature T are given. The problem is to determine the time to rupture t_R

•The time to rupture t_R and the working temperature T are given. The problem is to determine the working stress σ,, at which the material will be failed for time t_R

Various approaches, demonstrating the dependences of these parameters can be found in the open literature and the most known of them are provided in Table 3.1:

Table 3.1: Relevant equations correlating proposed parameters to remaining time t_R according to various approaches

Parameter of:	Relevant equation	Material constants to be determined	Reference
Larson- Miller	$LM = T(C + \log t_R)$	C	[3.3]
Manson- Haferd	$MH = \frac{\log t_R - \log t_a}{T - T_a}$	T_a, t_a	[3.4]
Manson- Brown	$MB = \frac{\log t_R - \log t_a}{(T - T_a)^n}$	T_a, t_a, n	[3.5]
Manson- Succop	$MS = \log t_R + C \times T$	C	[3.6]
Orr- Sherby- Dorn	$OSD = \log t_R - \frac{B}{T}$	B	[3.7]

The parameters, referred in Table 3.1, have been determined experimentally at elevated temperatures and stress, when the time to rupture is short. After that, they are used to predict the time to rupture at lower temperatures, for which the same stress level will give considerably higher values of t_R. The procedure is carried out in three steps. For example when t_R is to be defined:

1. A creep experiment is performed and the time to rupture is determined for different loads and temperatures. The parameter that gives the best relation

among the values t, T, and σ is determined. A graph of the function $P = f(\sigma)$ is drawn.

2. The value of P is determined for a given value of σ from the graph constructed in the previous step.
3. t_R is calculated from the relevant equation

The most precise and most frequently used methods in practice are those proposed by Larson- Miller [3.3] and Manson- Haferd [3.4]. The parameter *MH* is more precise than *LM* but it contains two constants. *LM* contains only one constant which makes it preferable and easier to use in practice and this is the main reason, why it was adopted by API 530 [3.8].

The Larson–Miller method [3.3] postulates that for each combination of material and stress level a unique value of a parameter *LM* exists, that is related to temperature and time by the equation:

$$LM = (T_d + 273)(20 + \log t_r)$$

(3.1)

This equation was investigated for both creep and rupture for 28 different materials by Larson and Miller with remarkable success. By using (3.1) it is a simple matter to find a short-term combination of temperature and time that is equivalent to any desired long-term service prediction requirement.

In the recent literature a significant number of research papers applying the L-M method in order to estimate the remaining life of various components, can be found. For example, Sivaprasad et al. [3.9] estimated the stress rupture life through Larson-Miller method on reformer furnace heater tubes made of cast austenitic alloy steels and serve in the temperature range of 1073–1173 K and pressure around 3-4 MPa. Marahleh et al. [3.10] used Larson-Miller parameter to extrapolate the stress–rupture test results to the actual operating conditions of turbine blades. Vikrant et al. [3.11] estimated the residual life of T22 steel (2.25Cr-1Mo) service exposed Super heater tube using Larson-Miller Parametric method. Endo [3.12] studied the creep rupture life of fossil power plant components while Shrestha et al. [3.13] studied the creep deformation behavior of Grade 91 steel in the temperature range of 600–700 °C and at stresses of 35–350 MPa.

Ferritic heat resistant steels are the most widely used materials in oil refineries.

Industrial practice and research have shown that, after long time high-temperature (550-650 °C) operation, microstructure and properties of ferritic-type low carbon-low alloy heat resistant steel will deteriorate. The microstructure changes include the dilution of alloy elements, the transformation of carbide type and coarsening, the spheroidizing of pearlite and the degradation of mechanical properties relatively, which will lead finally to progressive creep damage and rupture [3.14].

In the current thesis LM method was employed for the estimation of the remaining life of components being in service in refineries. A case study has been undertaken and microstructural assessment was also carried out in order to support the computational results.

3.2 Methodology adopted in this thesis

API 530 [3.8] besides the instructions for the design of new tubes, provides also guidelines for the estimation of remaining life for various pressurized components used in refineries. It is, thus, used to help engineers to get answers on re-rating and retirement questions arising on existing tubes that have operated in the creep-rupture range. A detail procedure based on Larson- Miller method was applied and is shown in the flow chart of Fig. 3.3. Because of the uncertainties inhered in these calculations, decisions about component retirement should not be based solely on those results. Other factors such as thickness or diameter strain measurements as well as microstructural characteristics combined with in-situ hardness measurements should be taken into account as regards the decision about component management (retirement, replacement, repair).

The main route of the calculation procedure can be outlined as follows:

- The operating history is divided into periods of time in which the pressure, metal temperature, and corrosion rate are assumed constant.
- For each of these periods, the life fraction used up is calculated. The sum of these calculated life fractions is the total accumulated component damage.
- The fraction remaining is calculated by subtracting this sum from unity.
- Finally, the remaining life fraction is transformed into an estimation of the expected life at specified operating conditions.

In the next paragraph this procedure is presented as applied for the remaining life calculation of a gasifier shell, which exhibited local plastic deformation due to the refractory damage during service. In addition to the calculations microstructural assessment based on replica metallography as well as common metallography of selected specimens is also given. The calculations were performed in Mathematica. The relevant commands lists is provided in the Annex.

Estimation of remaining tube life

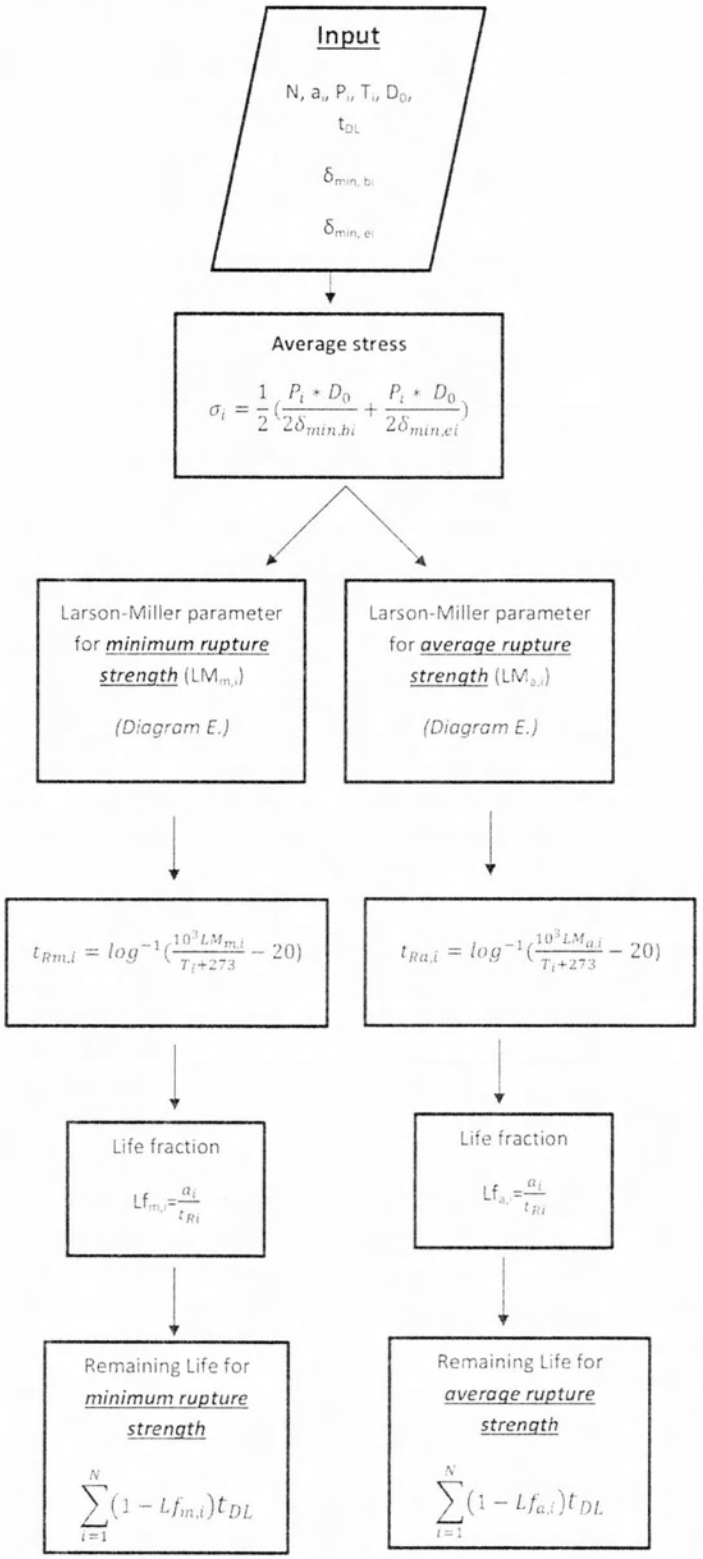

Figure 3.3: Flow Chart demonstrating the Remaining Life procedure according to API 530 Annex A [3.8]. Definition of terms is given in Section 3.4.

3.3 Case Study: Remaining Life evaluation of a gasifier shell based on LM method

A gasifier unit in a Greek refinery has experienced several hot spots (temperature exceeded 343°C) in certain areas of the shell, due to refractory damage. The areas of the hot spots are cooled by steam flow until the refractory is healed and the temperature drops to normal values. In the area of the hot spot the shell material is exposed to a thermal cycle which may last several hours.

Operating as well as design data of the gasifier are provided below.

- Component = Cylinder
- Material = SA-516 Grade 70
- Typical Condition (j=1) = 0.38 MPa @ 343°C
- Internal Diameter = 13666 mm
- Fabricated Thickness = 26 mm
- Future Corrosion Allowance (FCA) = 1.5 mm
- Weight = 31625.7 kg
- Capacity = 486904.63 liters
- Operating Time = 87600 hours= 10years

Refractory: thickness 203mm, density 1315Kg/m^3, weight 40744.7Kg

The chemical composition of the steel material in presented in Table 3.2

Table 3.2: Chemical composition of SA-516 Grade 70

C	Mn	Si	Cr	Al	Cu	Ni	Mo	Nb	Ti	V
0.15	1.5	0.6	0.3	0.02	0.3	0.3	0.08	0.01	0.03	0.02

3.3.1 Remaining Life calculation

In the following paragraphs, calculations on the remaining life assessment of the shell material after the high temperature exposure are provided. In addition an estimation of time-to-rupture as a function of temperature is also given.

The first step of the calculations comprises the estimation of the remaining life fraction from the first period (Table 3.3)

Table 3.3: Operational data retrieved for the 1st period according to the refinery

Operation period	Time period (years)	Thickness (mm)/ Pressure (Kg/cm²)	Temperature (°C)	Stress (MPa)
1	0-10	26 / 3.94	343	107.7

The remaining time, t_R, is computed rearranging equation (3.1)

$$t_R = \log^{-1}\left(\frac{10^3 LM}{T+273} - 20\right) \qquad (3.2)$$

The actual stress corresponding to the actual wall thickness is 107.7 MPa.

The Larson- Miller parameter based on curve 8 (minimum strength), corresponding to this value, is LM=16.5 (Fig. 3.4)

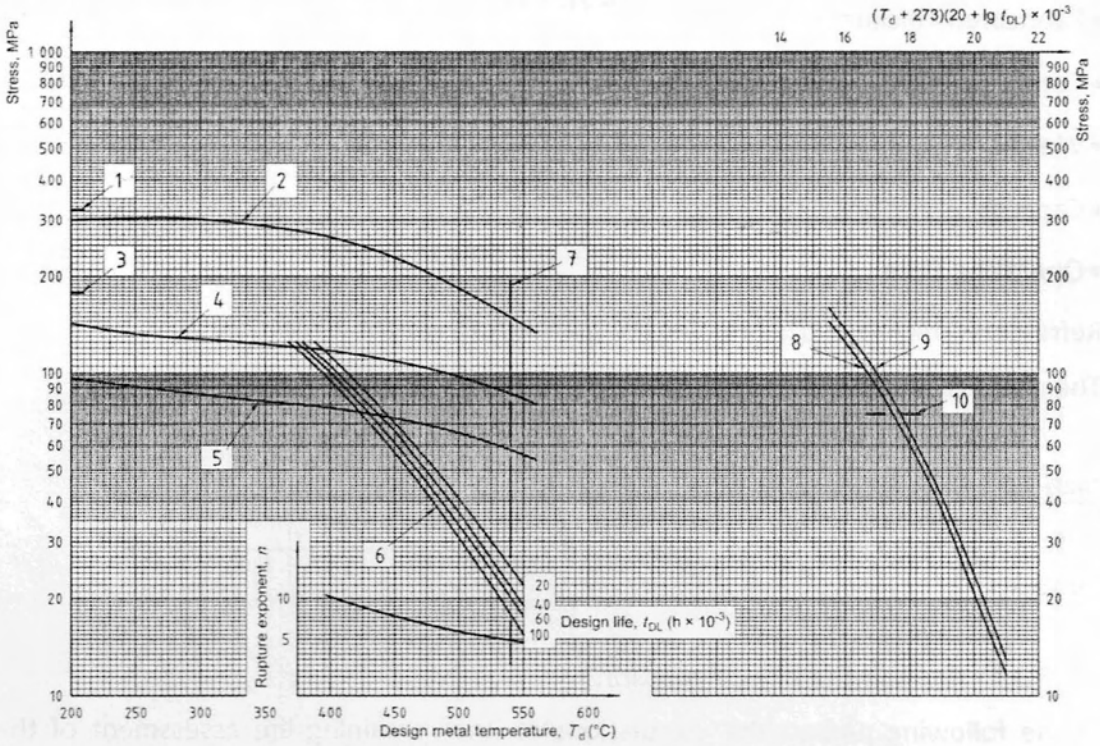

Figure 3.4: Stress curves for low-carbon steels [3.8]

$$t_R = \log^{-1}\left(\frac{10^3(16.5)}{343+273} - 20\right)$$

$$t_R = 6\times10^6 hours = 685 years$$

The life fraction is the duration of the operating period divided by the rupture time corresponding to that period.

Utilizing the minimum-strength rupture time calculated above, the life fraction for the first period is:

$$LM_{m,1} = 10 / 685 = 0.015$$

This result suggests that a very small time fraction has been consumed up to the bulging incidence. Because of this small number, and the fact that calculations refer to two periods, the rupture time of the second period will be the remaining life of the component. The same calculations employing equation (3.2) were conducted in order to calculate the rupture time based on the average stress. The Larson- Miller parameter, in this case, is LM=16.7 according to the curve 9 of Fig.3.4

A summary of the results is presented in the Table 3.4.

Table 3.4: Estimated rupture time, based either on minimum or on average strength

Temperature (°C)	Rupture time (h) based on minimum strength	Rupture time (h) based on average strength
343	6×10^6	40×10^6
380	185350	10^6
400	32890	182000
430	2950	15200
450	660	3260
480	82	378
500	22	98
540 (limiting design metal temperature)	2	8

The results of Table 3.4 show a rapid reduction of rupture time with the increase of temperature (Fig. 3.5), due to creep under the applied loads. It is worth noting that above the limiting design temperature (540°C for CS) the LM cannot be applied. In case the carbon steel (CS) is exposed to temperatures above 540°C then the microstructure changes and other metallurgical phenomena has to be considered. For temperatures up to 720°C, carbide spherodization or graphitization can occur (depending on the time the CS remains at that temperature), which result in weakening of the steel (permanent reduction of tensile strength). At temperatures above 720°C, phase transformations take place (austenitization), which alter the microstructure and properties, the most important being severe softening.

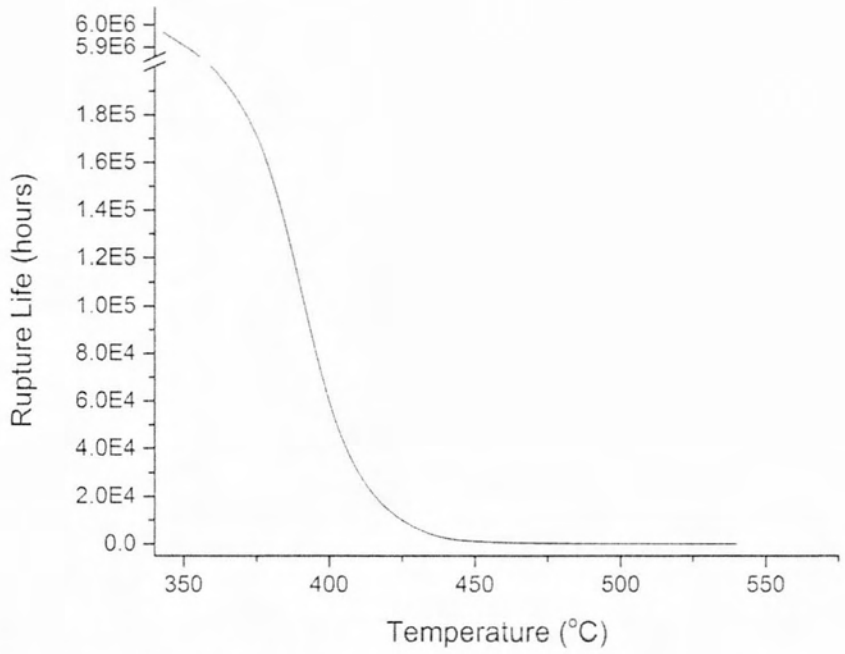

Figure 3.5: Predicted rupture time vs Temperature

The results of Table 3.4 could be used from the refinery during the repair period, since they provide quantitative results on the time to rupture according to the temperature exposure.

3.3.2 Assessment of microstructure

Shell microstructure was evaluated in situ by using replica metallography, as well as, at the laboratory after the removal of a sample from the shell. In addition, tensile tests were carried out in order to determine the current tensile properties of the shell material [3.15].

Replica Metallography was performed on selected areas of the shell's Outer Surface (OS) using Nital 5% for etching. The replicas correspond to the areas depicted in Fig 3.6

Metallography: The specimens were cut perpendicular to the shell and they were prepared with standard metallographic procedure (grinding with SiC papers 120, 220, 300, 500, 1000, 2000 grit, and polishing with diamond paste of 1 and 3 μm. Chemical etching was performed with Nital 5%. Evaluation of the microstructure was carried out by using the optical microscope available at the Lab (Leitz Aristomet).

Mechanical Properties: Tensile tests were performed on a servohydraulic tensile machine according to ASTM E8M. Microhardness measurements were also carried out on selected areas of the metallographic specimens on the microhardness tester available at the Materials Lab (Woolpert-402MVD, load 300 gr)

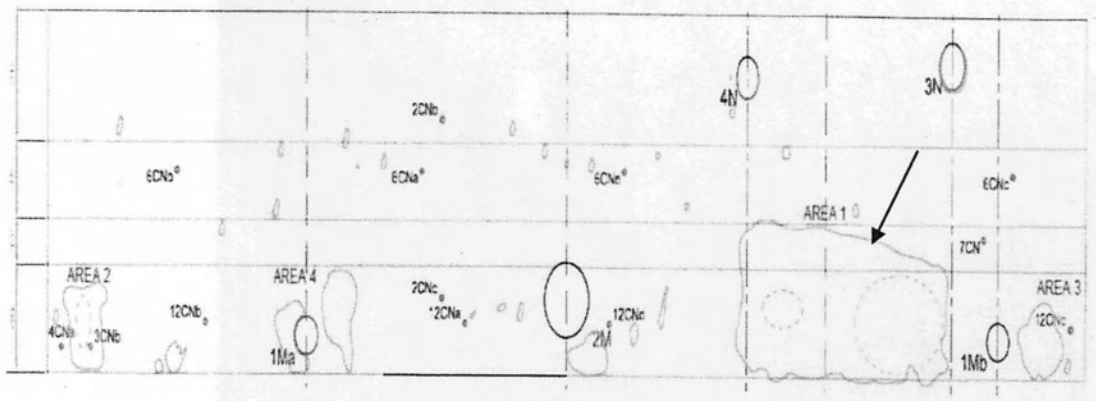

Figure 3.6: Bulge area (shown by the arrow), associated with several hot spots on the shell. Replication was performed on A1, A2, A4, and on unaffected material

3.3.2.1 Replica evaluation

Reference replicas: These replicas were taken from a shell region that was not suffered by temperature excursions. Characteristic results are presented in Figs. 3.7 & 3.8. The microstructure consists of ferrite and pearlite as expected for this CS. Perlite has lamellar structure, indicating that there has been no heat effect in this area.

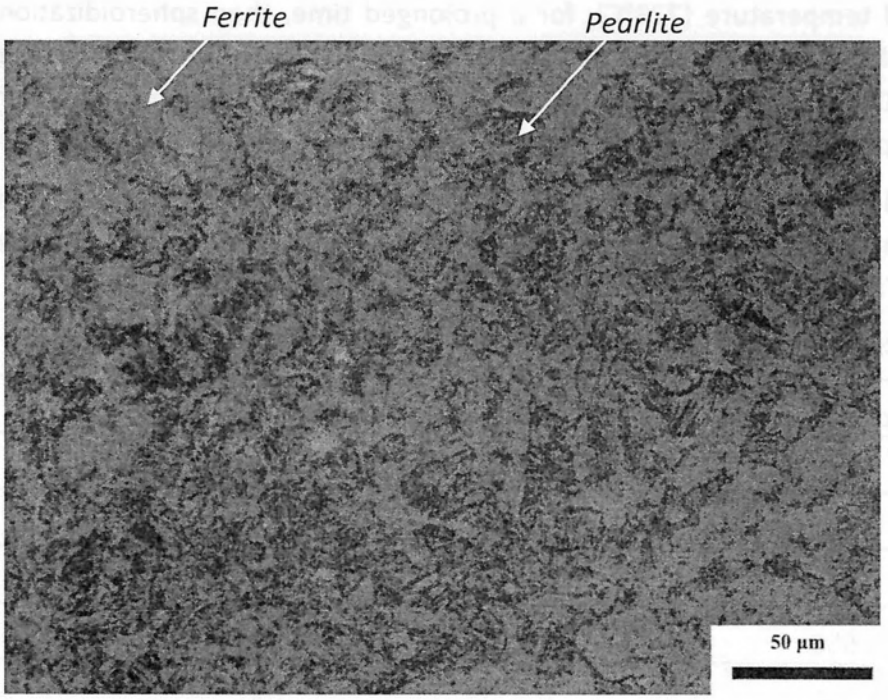

Figure 3.7: Microstructure from the reference area

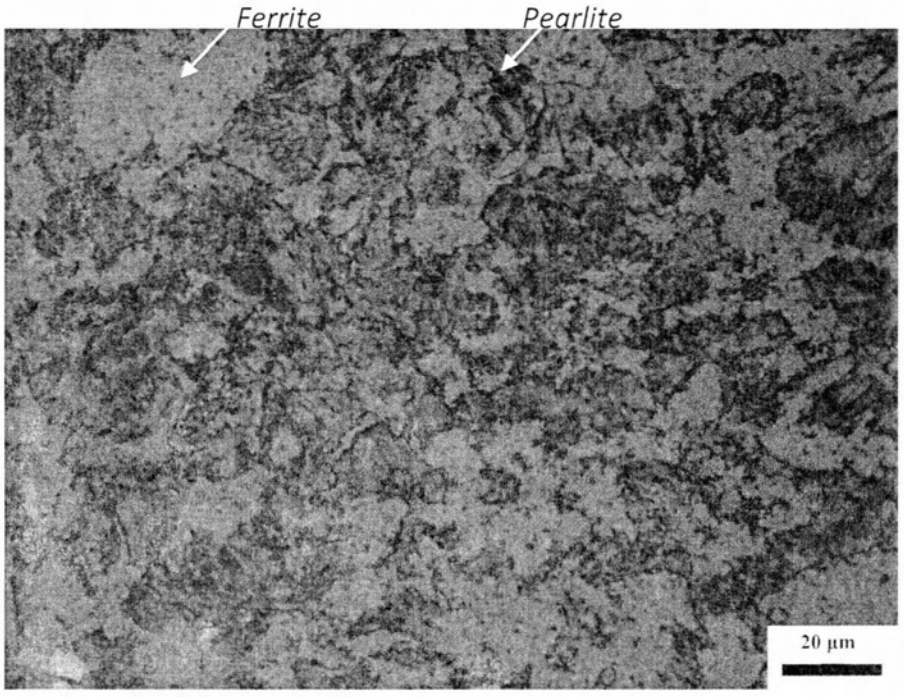

Figure 3.8: Microstructure from the reference area

Replicas from the Bulged area: Representative results are given in Figs. 3.9 and 3.10. In comparison to the unaffected area, it is obvious that the microstructure has undergone extensive cementite spheroidization (Fig. 3.10). This is an indication of the high temperature exposure since it is known that when a CS with a ferrite-pearlite microstructure is heated at a relatively high temperature, below the A1 critical eutectoid temperature (723°C), for a prolonged time, then spheroidization takes place. The lamellar structure of pearlite consists of alternate lamellar of ferrite and cementite. During spheroidization the cementite is converted from a lamellar morphology to spheroidal particle morphology.

According to calculations performed at the Materials Laboratory [3.15] the time required for spheroidization depends strongly on the Temperature and is of the order of hours (Table 3.5).

Table 3.5: Time for complete spheroidization at various temperatures [3.14]

Speroidization Temperature (°C)	Speroidization Time (h)
700	25
650	33
600	46
550	65
500	100

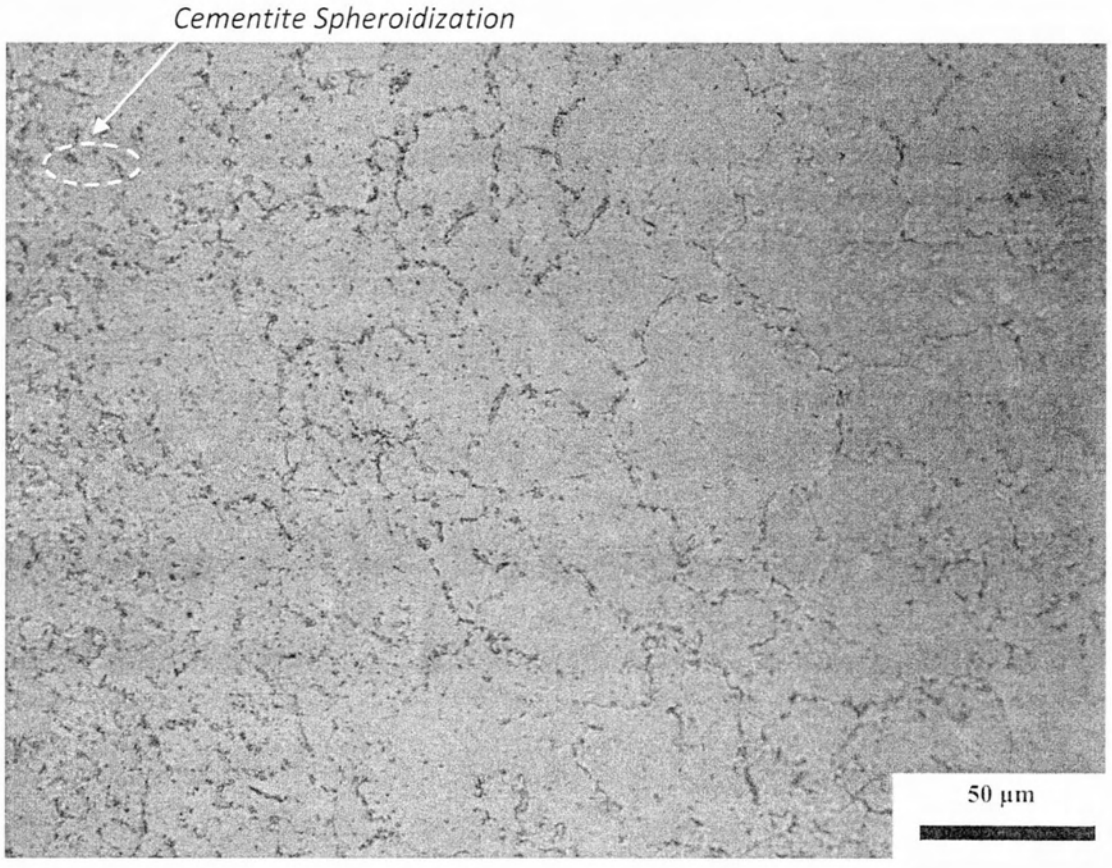

Figure 3.9: Microstructure from the bulged area

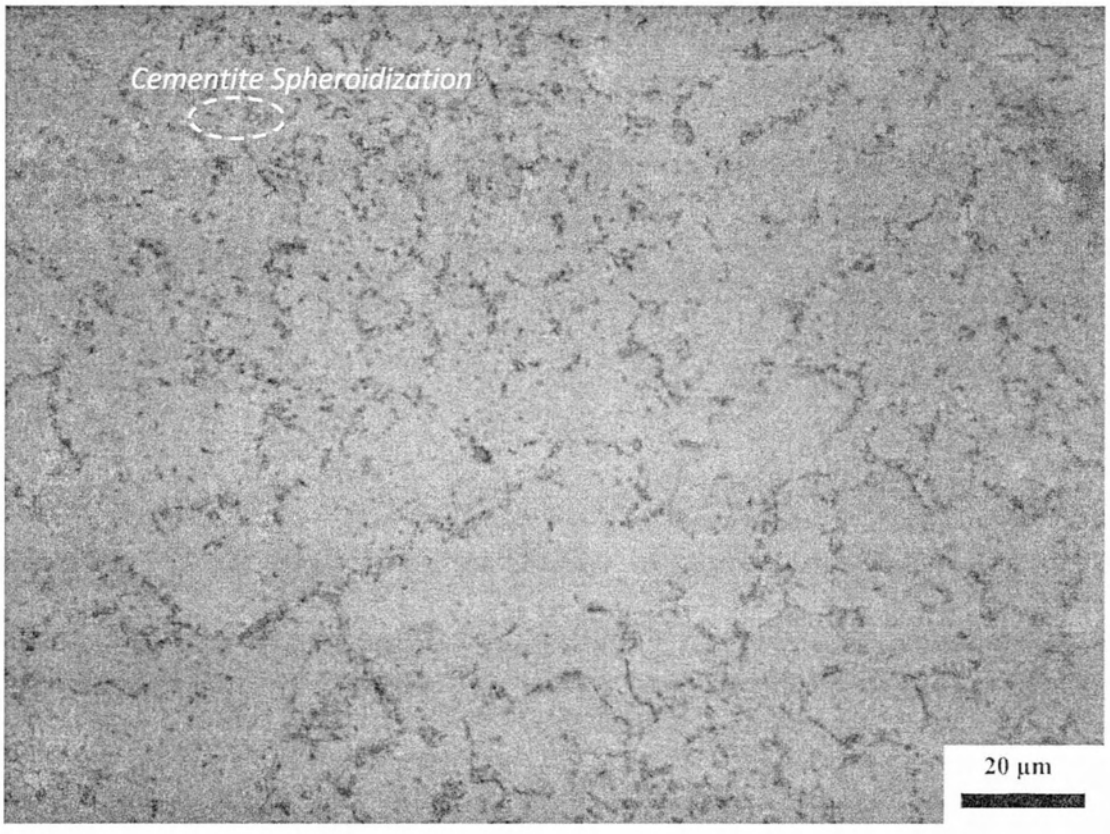

Figure 3.10: Microstructure from Failure area

3.3.2.2 Tensile Properties in the bulged area

A part of the Area 1 (Fig. 3.6) was removed from the gasifier and was then subjected to destructive testing i.e. tensile tests and metallography. The circumferential direction was marked as θ, while the axial direction was marked as z. Two tensile test specimens were extracted parallel to the circumferential direction (θ1, θ2) and two specimens were extracted parallel to the axial direction (z1, z2). The tensile test results are shown in Table 3.6, and are compared with the manufacturer inspection certificate issued during commissioning, and the requirements of the relevant specification. Regarding the comparison with the certificate of the manufacturer, the yield strength as well as the ultimate tensile strength exhibit a reduction after the high temperature exposure while the elongation exhibits an increase, in line with the spheroidization process of the material. From the comparison with the ASTM standard it is concluded that three of the specimens conform to the requirements of the specification, while specimen θ2 exhibited a reduction of 12 MPa in its tensile strength value, in relation to the minimum specified requirement. The average value of tensile strength of θ1 and θ2 is 487.5MPa, which is above the minimum specified value [3.15].

Table 3.6: Tensile properties and comparison to the specification requirements.

	Yield Strength $R_{p0.2}$ [MPa]	Tensile Strength **R_m [MPa]**	Elongation **A_{50} (%)**
z_1 (axial)	324	504	35.6
z_2 (axial)	327	499	33.9
θ_1(circumfer.)	321	502	30.8
θ_2(circumfer.)	325	473	31.8
Manufacturer Inspection Certificate	355	491	26.5
	378	514	30.0
	373	512	27.5
ASTM A516 Gr 70	260 min	485-620	21 min

3.3.2.3 Metallography

Inner surface (IS): The microstructure at the IS of the shell consists of ferrite and pearlite. The metallographies of Figures 3.11-3.12 indicate that some pearlite grains have lamellar structure, while others have partial cementite spheroidization. The average microhardness in this area was measured 170$HV_{0.3}$

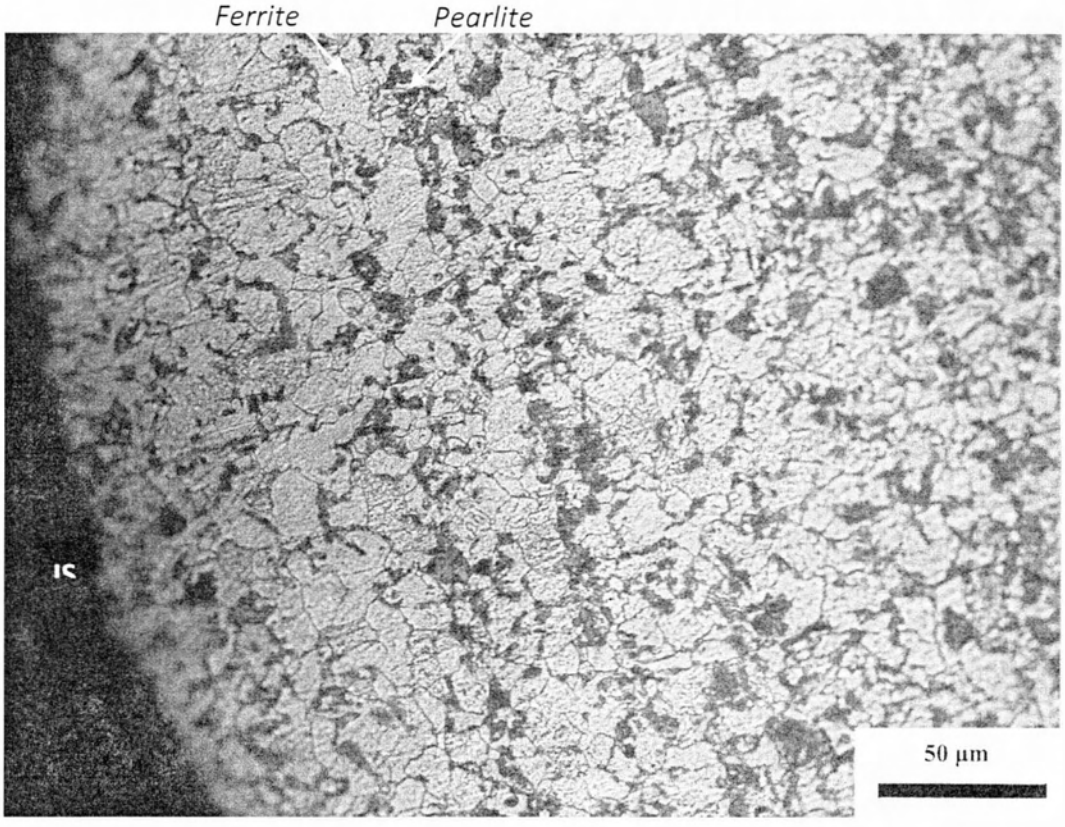

Figure 3.11: Microstructure at the inner surface

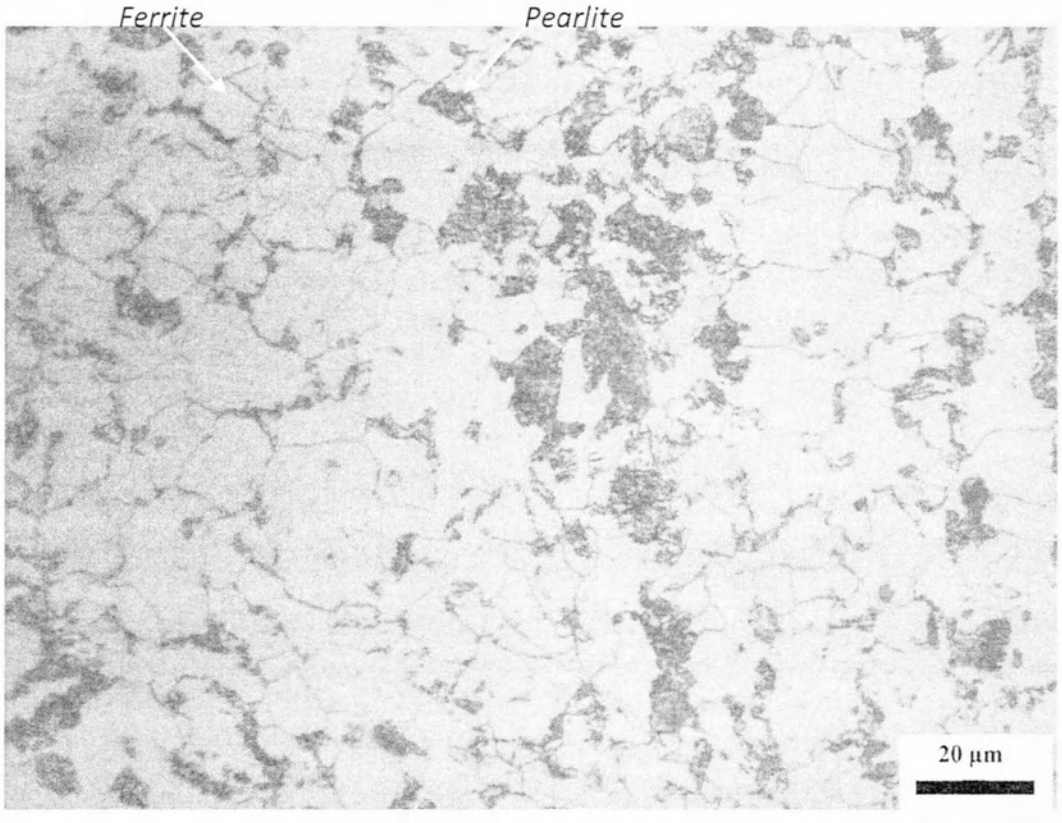

Figure 3.12: Microstructure at the inner surface. Ferrite and pearlite with cementite speroidization

Outer surface (OS): The outer surface has undergone cementite spheroidization (Fig. 3.13). Also the dissolution of pearlite is more pronounced in the direction towards the OS at a zone with a width ~ 50μm (Fig. 3.14). The microhardness within this zone has an average value of 130 $HV_{0,3}$. Below that zone the average microhardness was measured $150HV_{0.3}$.

In conclusion the results from common metallography are identical to the replica observations.

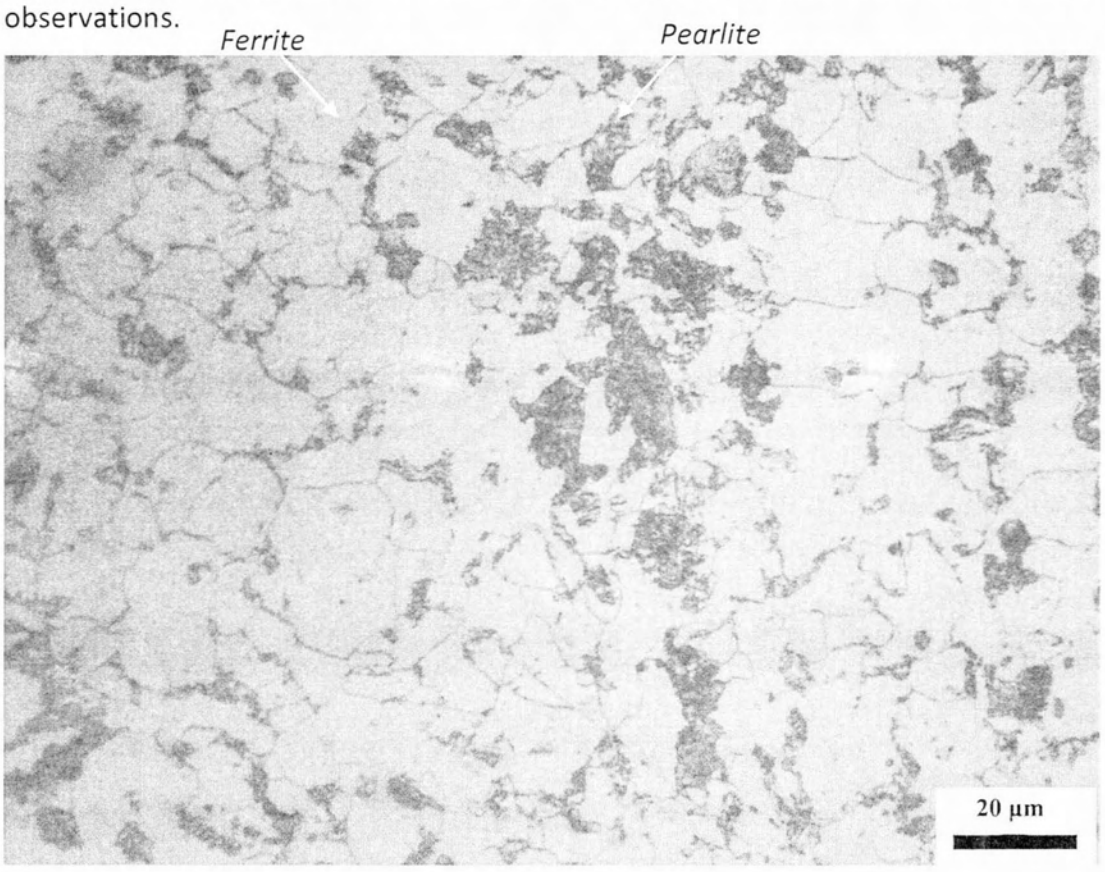

Figure 3.13: Microstructure at the outer surface. Pearlite with cementite spheroidization

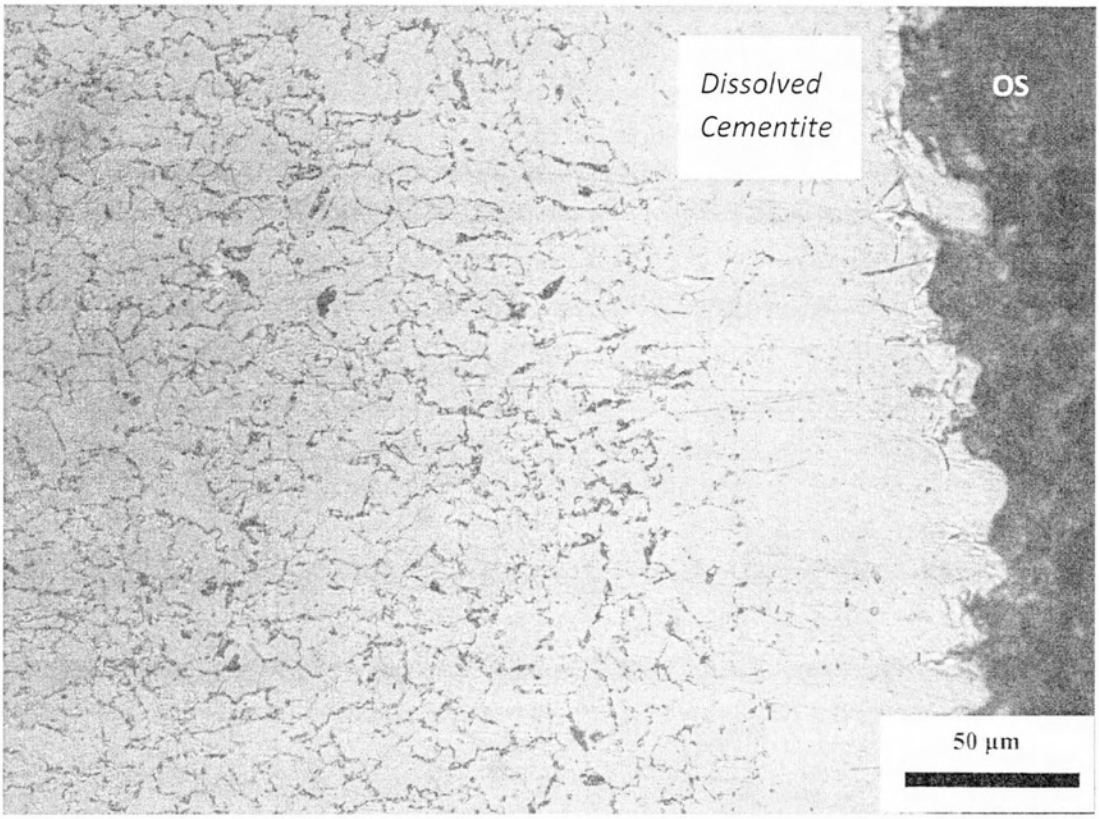

Figure 3.14: Microstructure below the OS

3.3.3 Conclusions

The remaining life fraction of a gasifier shell was calculated according to API 530 using the LM method. Taking into account the results the shell has consumed a small portion of its service life before the temperature excursions.

API 530 suggests safe operational time periods in strong relation to the maximum temperature attained, while above the design limit (540 °C) cannot be used for any prediction purposes.

Microstructural assessment performed both by replica and common metallography technics indicated that locally the maximum temperature during the incidence excided the design limit of the CS. Phenomena as pearlite spheroidization, as well as grain coarsening were detected associated with local softening.

The bulk tensile properties showed that the CS's tensile properties are maintained well above the specified limits.

3.4 Terms & definitions- Estimation of Remaining Tube Life

N number of operating periods

a_i duration for the *i* operating period

P_i operation gauge pressure for the *i* operating period, expressed in megapascals

D_0 outside diameter, expressed in mm

t_{DL} operating time used as a basis for tube design, expressed in h

σ_i average stress for the *i* operating period, expressed in MPa

$\delta_{\min,bi}$ minimum thickness, expressed in mm, at the *beginning* of the *i* operating period

$\delta_{\min,ei}$ minimum thickness, expressed in mm, at the *end* of the *i* operating period

$LM_{m,i}$ Larson-Miller value, according to *minimum* rupture strength curve (*Diagram E.*), for the *i* operating period

$LM_{a,i}$ Larson-Miller value, according to *average* rupture strength curve (*Diagram E.*), for the *i* operating period

$t_{Rm,i}$ minimum-strength rupture time for the *i* operating period

$t_{Ra,i}$ average-strength rupture time for the *i* operating period

$Lf_{m,i}$ life fraction based on minimum strength for the *i* operating period

$Lf_{a,i}$ life fraction based on average strength for the *i* operating period

3.5 References

[3.1] Calister WD, Rethwisch DG. Fundamentals of Materials Science and Engineering. John Wiley & Sons, Inc. 2008

[3.2]Evaluation of creep damage with Replica, Report No. 55, Laboratory of Materials, April 2006

[3.3] Larson F, Miller J. A Time-Temperature Relationship for Rupture and Creep Stresses. Trans. ASME.1952; 74:765

[3.4]Manson S, Haferd A. A Linear Time-temperature Relation for Extrapolation of Creep and Stress Rupture Data. NACA TN 2890, 1953

[3.5] ISO Standard TR 7468

[3.6] Manson, S., Succop, G.: Stress-Rupture Properties of Inconel 700 and Correlation on the Basis of Several Time Temperature Parameters. ASTM STP 174: 405.

[3.7] Orr R, Sherby O, Dorn J. Correlations of rupture data for metals at elevated temperatures. Trans. ASME.1954;46:113

[3.8]API Standard 530. Calculation of heater tube thickness in petroleum refineries. 5th Edition, American Petroleum Institute, 2003

[3.9] Swaminathan J, Prasad P, Gunjan MK, Gugloth K, Roy PK, Singh R, Ghosh R. Mechanical strength and microstructural observations for remaining life assessment of service exposed 24Ni–24Cr–1.5Nb cast austenitic steel reformer tubes. Eng Fail Anal.2008;15:723-735

[3.10] Marahleh G, Kheder ARI, Hamad HF. Creep life prediction of service-exposed turbine blades. Mater Sci and Eng A.2006;433:305–309

[3.11] Vikrant KSN, Ramareddy GV, Pavan AHV, Singh K. Estimation of residual life of boiler tubes using steamside oxide scale thickness. Int J. Pres. Ves. Pip. 2013;104:69-75

[3.12] Endo T. Progress in life assessment and design methodology for fossil power plant components. Int J. Pres. Ves. Pip.1994;57:7-20

[3.13] Shrestha T, Basirat M, Charit I, Potirniche GP , Rink KK. Creep rupture behavior of Grade 91 steel. Mater Sci and Eng A.2013;565:382-391

[3.14] Lemaitre J, Desmorat R. Engineering Damage Mechanics. Springer Berlin Heidelberg New York.2005

[3.15] Material evaluation of the main hot spot area in the shell of Gasifier Unit 32-R-003, Report No. 174, Laboratory of Materials, March 2014.

4. Fitness- For- Service for components operating in the creep range

4.1 Introduction

Structural integrity is of considerable importance in order to avoid failures of mechanical components and structures in a number of industrial sectors. The ability to demonstrate the structural integrity of in service component that sustained some damage or contains a flaw is termed as integrity assessment or fitness-for-service (FFS) and is extensively dealt with by assessment procedures. The FFS evaluations are conducted periodically to determine whether a component with existing damage is suitable for continued service until the end of a pre-specified period of operation such as the next shutdown, a specific future date or the end of its useful life.

Such assessments include:

- Determination of current serviceability to ensure safe operation in the present condition, and
- Assessment of remaining service life of the equipment.

The FFS of any material is determined by performing a FFS assessment. Performing accurate FFS evaluations is an integral aspect of fixed equipment asset integrity management. On the other hand, failing to perform evaluations can lead to equipment failures which can further result in injury, loss of life, and severe financial and economic consequences. The reason these examinations are performed is because that even if a piece of equipment has a crack or other defect, this doesn't necessarily mean that it's inappropriate for service. Most equipment can continue their service life despite small flaws, and to repair or replace equipment that can still be used would be an unnecessary and costly expense. Besides that unnecessary weld repairs can actually cause more damage than the initial situation.

There are several ways to evaluate if a flaw can cause a piece of equipment to be no longer fit for service. For cracks, fracture mechanics provides the mathematical framework for the examination by quantifying combinations of stress, flaw size, and fracture toughness of the material. While cracks tend to be the most dangerous, they're not the only flaw that might needs evaluation. Volumetric flaws such as corrosion pits, porosity, and slag may reduce the load-bearing capacity of a structure. Likewise, structural integrity may also be compromised by locally thinned areas which come grinding out cracks, thus FFS methodologies have been developed to evaluate local thinning. In these cases acceptance criteria are based on limit load analyses rather than fracture mechanics models. Some examples of these different FFS methodologies are the BS 7910 method, the API RP 579-1/ASME FFS-1 method, as well as the R5, R6 methods (Table 1).

There have been several Fitness for Service (FFS) applications published in the recent literature. Tantichattanont et al. [4.2] conducted FFS assessment of spherical pressure vessel with hot spot. Sisha et al. [4.3] implemented FFS in Pressurized

Heavy Water Reactor (PHWR) which operates under the environment of high pressure and temperature (typically 10 MPa and 573 K), and fast neutron flux. Under this operating environment, the material of the pressure tube undergoes degradation over a period of time, and eventually needs to be assessed for fitness for continuing operation, without jeopardizing the safety of the reactor. Shekari et al. [4.4] presented a new FFS assessment methodology for tracking and predicting pitting corrosion. Dogan [4.5] provides an overview of the high temperature assessment procedures with recent developments in his approach. Alegre et al. [4.6] present the procedure followed to calculate the number of design cycles, employing the fracture mechanics approach and the structural integrity concepts. In particular, the API 579-1/ASME FFS-1 procedure has been used to analyze the structural integrity of the vessel through the crack propagation stage.

It is important to note though that FFS evaluation can't provide an absolute delineation between safe and unsafe operating conditions. Uncertainties in input parameters such as stress, flaw size, and toughness often lead to a large uncertainty in the prediction of the critical conditions for failure. In general there are two approaches to address this uncertainty. The more traditional approach has been to use conservative input values in a deterministic analysis. The result of such an analysis is a pessimistic prediction of critical flaw size or remaining life. An alternative approach, which is becoming more common, entails performing a probabilistic analysis that incorporates the uncertainties in the input data. The latter type of analysis does not result in an absolute yes/no answer as to whether or not a structure is safe for continued operation. Rather, a probabilistic analysis estimates the relative likelihood of failure, given all of the incorporated uncertainties. Probabilistic FFS analysis can be an integral part of a risk-based inspection (RBI) protocol, where inspection is prioritized according to the risk of significant injury or economic loss.

Worldwide regulatory requirements entail that the FFS assessment must be based on recognized and generally accepted good engineering practices. Research conducted and knowledge gained during the past years has led to the formulation of international standards and procedures for conducting FFS assessments. Table 1 provides a list of major FFS procedures along with the addressed failure mechanisms and the related industry sector.

4.2 Methodology adopted in this study

An overview of the API 579 FFS assessment methodology [4.1] followed for all damage encountered in refineries, is given in Table 2. The organization of each assessment procedure in API 579 is consistent with this methodology. This assessment methodology has proven to be robust for all flaw and damage types that have been incorporated into API 579. Because of this success, when new sections are added to API 579, the template used for the development will be based on this assessment methodology.

Table 4.1: Major FFS procedures [4.4]

Procedure	Reference	Status	Industry sector	Failure mechanisms							
				Pitting	Fracture	Fatigue	Creep rupture	Metal loss	Environment assisted cracking	Mechanical damages	Fire damage
BS 7910	[4.7]	UK national procedure, published by BSI	General	N	Y	Y	Y	Y	Y	Y	N
API 579-1/ ASME FFS-1	[4.1]	Joint API/ASME standard	Downstream oil and gas facilities	Y	Y	Y	Y	Y	Y	Y	Y
FITNET	[4.8]	European document, superseded by BS 7910:2013	General	N	Y	Y	Y	Y	Y	Y	N
SINTAP	[4.9]	European document, superseded by FITNET	General	N	Y	Y	Y	Y	Y	N	N
B31.G	[4.10]	ASME Standard	Pipeline Transportation	N	N	N	N	Y	N	Y	N
R5	[4.11]	Maintained by the UK nuclear industry	General	N	Y	Y	Y	N	N	N	N
R6	[4.12]	Maintained by the UK nuclear industry	General	N	Y	Y	N	N	Y	N	N
RSE-M	[4.13]		Nuclear Power	N	Y	Y	Y	N	N	N	N

Table 4.2: Organization of each section in API 579

Step	Description
1	*Damage mechanism identification*- The first step in a FFS assessment is to identify the flaw type and cause of damage. FFS assessments should not be performed unless the cause of the damage can be identified. The original design and fabrication practices, materials of construction, service history, and environmental conditions can be used to estimate the likely cause of the damage. Once the flaw type is identified, the appropriate section of this document can be selected for the assessment

2	*Applicability and limitations of the FFS assessment procedures*- A decision on whether to proceed or not with the procedure should be made, according to the applicability and limitations of each procedure
3	*Data requirements*- The data required for FFS assessments depend on the flaw type or damage mechanism being evaluated. Data requirements may include: original equipment design data, information pertaining to maintenance and operational history, expected future service, and data specific to the FFS assessment such as flaw size, state of stress in the component at the location of the flaw, and material properties. Data requirements specific to a damage mechanism or flaw type are covered in the section containing the corresponding assessment procedures
4	*Assessment techniques and acceptance criteria*- Assessment techniques and acceptance criteria are provided in each section.
5	*Remaining life evaluation*- An estimate of the remaining life or limiting flaw size should be made. The remaining life is established using the FFS assessment procedures with an estimate of future damage rate (i.e. corrosion allowance). The remaining life can be used in conjunction with an inspection code to establish an inspection interval
6	*Remediation*- Remediation methods are provided in each section based on the damage mechanism or flaw type. In some cases, remediation techniques may be used to control future damage associated with flaw growth and/or material degradation
7	*In-service monitoring*- Methods for in-service monitoring are provided in each section based on the damage mechanism or flaw type. In-service monitoring may be used for those cases where, a remaining life and inspection interval cannot be adequately established because of the complexities associated damage mechanism and service environment
8	*Documentation*- The documentation of an FFS assessment should include a record of all data and decisions made in each of the previous steps to qualify the component for continued operation. Documentation requirements common to all FFS assessment procedures are given in Section 2 of API 579. Specific documentation requirements for a particular damage mechanism or flaw type are covered in the section containing the corresponding assessment procedures

For pressurized equipment in operating plants, API 579 [4.1] prescribes three levels of structural integrity evaluations. Levels 1–3 are progressively more sophisticated. Each assessment level provides a balance between the degree of conservatism, the amount of required input, the skills of the evaluator, and the complexity of the analysis. A general overview of each assessment level and its intended use are described below:

- Level 1: The assessments that are the most conservative screening criteria that generally include the use of charts and tables, which can be implemented by plant technicians with a minimum quantity of inspection and component information.
- Level 2: The assessments involve detailed calculations intended for use by plant engineering personnel, with the help of a recommended procedure. The assessment procedures included in this level are intended to provide a more detailed evaluation that produces results, less conservative than those from a Level 1 assessment. In Level 2, inspection information similar to that required for Level 1 are required; however, more detailed calculations are used in the evaluation. Level 2 assessments are typically conducted by plant engineers or specialists experienced and knowledgeable in performing FFS assessments.
- Level 3: The assessment procedures included in this level are intended to provide the most detailed evaluation that produces results that are less conservative than those from Level 2 assessment. In a Level 3 the most detailed inspection and component information is typically required, and the recommended analysis is based on numerical techniques such as the finite element method. The Level 3 assessment procedures are primarily intended to be undertaken by engineering specialists highly experienced in the field of Fracture Mechanics and Materials.

The FFS assessment procedures in API 579 cover both the current integrity of the component given an accumulated state of damage and the projected remaining life. If the results of a FFS assessment indicate that the equipment is suitable for the current operating conditions, the equipment can continue its operation, under the pre requirement that a proper inspection program is established. In case the results indicate that the equipment is not suitable for the current operating conditions, calculation methods are provided to rerate the component. For pressurized components (e.g. pressure vessels and piping) these calculation methods can be used to determine a reduced maximum allowable working pressure and/or coincident temperature. The remaining life calculation in API 579 is not intended to provide a precise estimate of the actual time to failure. Instead, the remaining life calculation is used to establish an appropriate inspection interval in conjunction with the governing inspection code and/or the in service monitoring plan, or the need for remediation.

The procedures in API 579 were developed to overcome the shortcomings of the former inspection codes for pressure vessels and piping which are mainly based on empirical data and past experience. Extensive validation based on both numerical analysis and physical testing has been applied to various damage modes such as metal loss and crack-like flaws.

The procedure is described in the flow chart depicted in Fig. 4.1.

The present study concerns the implementation of Level 2 FFS assessment in components that experienced creep due to long term high temperature exposure. The assessment can only be applied if the following requirements are satisfied:

- The history of the operating conditions, as well as, the documentation concerning future operating conditions are available.
- The component has been subjected in less or equal than 50 cycles of operation including startup and shutdown conditions, or less than that specified in the original design.
- The component does not contain any of the following flaws: LTA (Local Thin Area) or groove-like flaw, pitting damage, blister, HIC (Hydrogen Induced Cracking), or SOHIC (Stress Oriented Hydrogen Induced Cracking) damage, weld misalignment, out-of-roundness, or bulge that exceed the original design code tolerances, a dent or dent-gouge combination, a crack-like flaw, or microstructural abnormality such as graphitization or hydrogen attack.

As described below, one of the requirements for the evaluation of the FFS procedure is a precise description of the component operating history and future operational conditions. The future planned operating conditions can be readily defined. However, many times an adequate description of the past operating history cannot be made. To address this problem, the MPC Project Omega Program has developed a testing procedure to evaluate material parameters required for a remaining life assessment. The tests require removal of a material sample from a location in the component subject to the highest creep damage. This location is typically associated with the highest temperature and/or stress location. When an Omega Test is performed on a material sample from the component, the Omega material parameters are determined, and these parameters include the effects of creep damage associated with past operation. Consequently, by performing an Omega test, the remaining life problem is "shifted" such that the operating conditions up to the time of the test do not need to be evaluated to determine a remaining life. This feature of the MPC Omega Method provides a means to accurately account for creep damage from past operation without having to know how the component was operated. The assessment techniques developed under the MPC Project Omega program provide a methodology for estimating the remaining life of a component operating at high temperature that has been extensively used in the refining and petrochemical industry. The MPC Project Omega Method is a public domain assessment procedure with a proven record and associated property relations covering a wide range of materials used in the refining and petrochemical industry. In this methodology, a strain-rate parameter and multi-axial damage parameter (Omega) are used to predict the rate of strain accumulation, creep damage accumulation, and remaining time to failure as a function of stress state and temperature [4.14].

In the following paragraphs two Case Studies which implemented Level 2 assessment, are presented i.e.

Case Study 1: A bulging example of a gasifier experienced a temperature excursion for a short duration.

Case Study 2: A fired crude heater experienced a temperature excursion for a short duration

In both cases the refinery needs to know how much additional damage occurred to the components as well as to understand how the temperature excursion impacts the remaining life.

The calculations were performed in Mathematica. The relevant commands list is provided in the Annex.

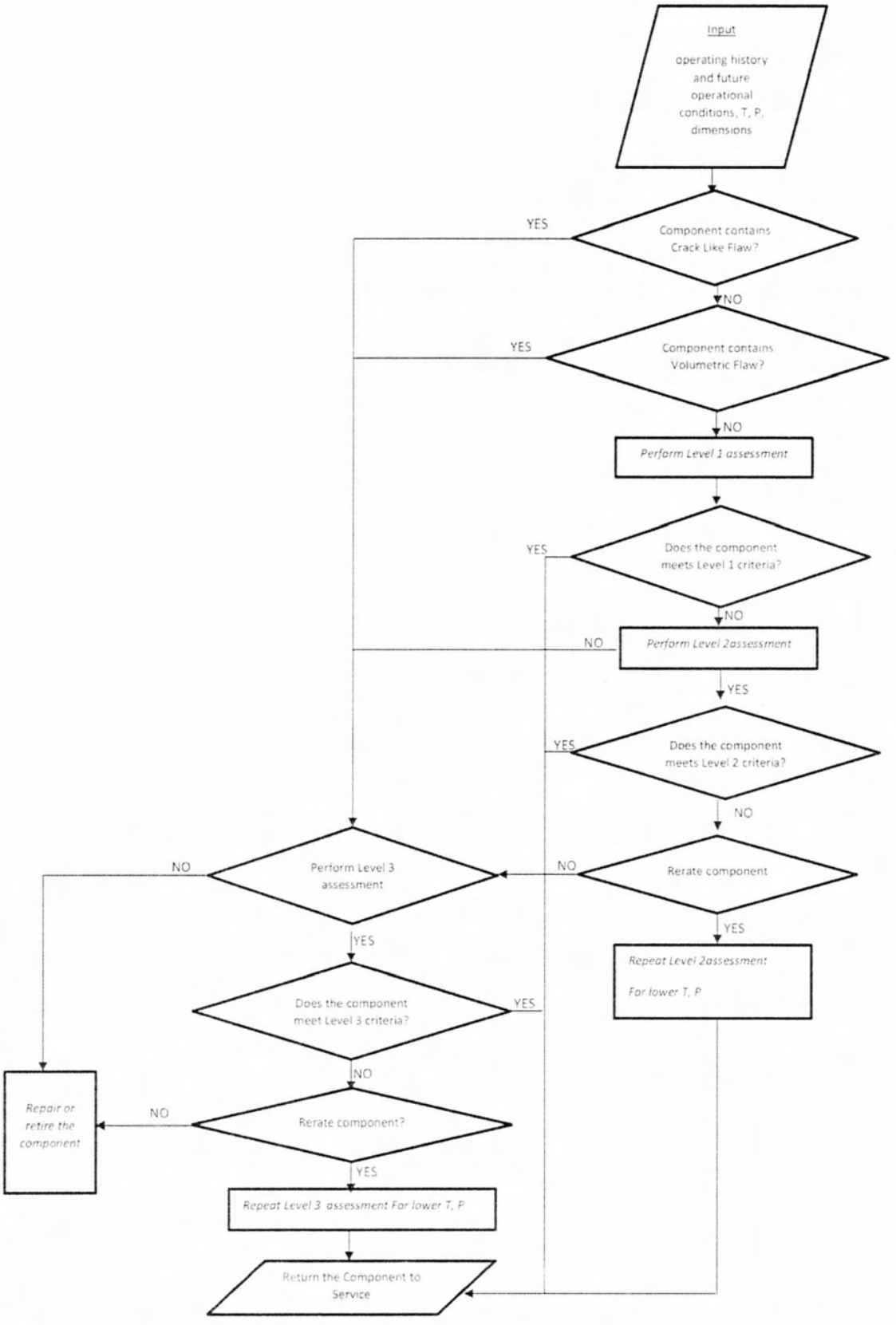

Figure 4.1: Overview of the Assessment Procedures, for the Evaluation of a Component in the Creep Range [1]

4.3 Case study 1: FFS for Bulging damage in a gasifier

The shell of the gasifier experienced a temperature excursion for a short duration. In this area a bulge (Fig. 4.2) had been formed during operation. The refinery needs to know how much additional damage occurred to the shell, therefore to understand how the excursion impacts the remaining life. This information will be used to support the decision if the gasifier will need to be replaced at an upcoming scheduled turn-around, or if the section of the gasifier containing the bulge, can last for certain period. The aim of this analysis is to evaluate the remaining life of the gasifier, using the Level 2 assessment procedures, and to determine if it is fit for service. The operation data as provided by the refinery are shown below. It is worth noting that the future expected time period of 3600 hours incorporated in the calculations represents the required time up to the next programmed shut down.

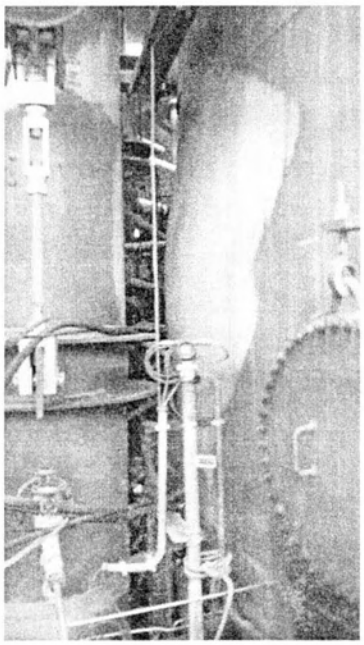

Figure 4.2: The bulging area of the gasifier

Gasifier Data

Component	= Cylinder
Material	= SA-516 Grade 70
Typical Condition (j=1)	= 0.38 MPa @ 343°C
Internal Diameter	= 13666 mm
Fabricated Thickness	= 26 mm
Future Corrosion Allowance (FCA)	= 1.5 mm
Weight	= 31625.7 kg
Capacity	= 486904.63 liters
Past Operating Time (j=1)	= 87600 hours
Future Expected Time (j=2)	= 3600 hours

Temperature Excursion Data

Excursion Pressure	= 0.38 MPa
Excursion Temperature	= 600 °C
Excursion Duration	= 3600 hours

Inspection Data

The gasifier shell has experienced hot spots in several areas, that causes bulging as depicted in Fig 1. The bulging area has been treated as an area with metal loss, within the original corrosion allowance due to the thickness reduction. Considering the inspection records, this is the first operational excursion into the creep range for this component. There are no circumferential weld seams in this section of the gasigier.

A Level 2 Assessment has to be performed according to paragraph 10.4.3 of API 579 [4.1].

The steps followed are described hereinafter:

STEP 1 – A load history, based on past operation and future planned operation, was determined. The load histogram included all significant operating loads and events that were applied to the component. The total number of operating cycles , M, was took into account. It is important to note that the loading conditions in the histogram were analyzed in the same order as the actual sequence of operations. According to API 579 [4.1] this must be followed, even if it entails breaking the loading condition into two or more analysis steps. The load history for the operation of the gasifier is given in Table 4.3.

Table 4.3: Load history for operation before (m=1) and after bulging (m=2)

	Past (m=1)	Future (m=2)
Pressure (MPa)	0.38	0.38
Temperature (°C)	343	600
Time (hours)	87600	3600

STEP 2 –The total cycle time, ^{m}t, of each operating cycle m, was divided in a number of time increments, ^{n}t. The total number of time increments, N, for each operating cycle, m, was defined. The time increments used to model the operating cycle should

be small enough to capture all significant variations in the operating cycle. The smaller the time increment, the more accurate the remaining life predication.

For this application, *N* was set to 2 because the condition for each sub-cycle was the same. In general, *N* should be set to match any change in pressure, temperature, or tube thickness. Each of the operating cycles in the load history was split into its respective sub-increments in Table 4.4.

Table 4.4: Load history and increments for operation before (m=1) and after bulging (m=2) of each period

Operating Cycle	Past (m=1)		Future (m=2)	
Sub-increment	n=1	n=2	n=1	n=2
Design Pressure (MPa)	0.38	0.38	0.38	0.38
Time (hours)	43800	43800	1800	1800

STEP 3 – The assessment temperature, ${}^{n}T$, for each time increment ${}^{n}t$ is given in Table 4.5.

Table 4.5: Design Temperature for each sub-increment

Operating Cycle	Past (m=1)		Future (m=2)	
Sub-increment	n=1	n=2	n=1	n=2
Design Pressure (MPa)	0.38	0.38	0.38	0.38
Design Temperature (°C)	343	343	600	600
Time (hours)	43800	43800	1800	1800

STEP 4 – The stress components ${}^{n}\sigma_{ij}$, for each time increment ${}^{n}t$ was determined as described below.

Initially, the shell dimension was checked to insure the shell is considered as thin-walled according to the definition given in paragraph 10.5.2.5 of API 579 [4.1].

$$\frac{OD}{t_{mean}} \geq 6$$

$$\frac{13692}{26} \geq 6$$

$$526.6 \geq 6$$

Since the thin-walled criterion was met, the mean diameter stress equations according to Table 10.2 [4.1] was applied.

$$ {}^{n}\sigma_1 = {}^{n}\sigma_{mean} = \frac{P(D_{mean})}{2t_{corr}} \quad (4.1) $$

$$ {}^{1}\sigma_1 = \frac{P(OD - t_{nom} + FCA)}{2(t_{nom} - FCA)} $$

$$ {}^{1}\sigma_1 = \frac{0.38(13692 - 26 + 1.5)}{2(26 - 1.5)} $$

$$ {}^{1}\sigma_1 = 107.7 MPa $$

$$ {}^{n}\sigma_2 = 0.5({}^{n}\sigma_{mean}) \quad (4.2) $$

$$ {}^{1}\sigma_2 = 0.5({}^{1}\sigma_1) $$

$$ {}^{1}\sigma_2 = 53.83 MPa $$

$$ {}^{n}\sigma_3 = 0.0 $$

$$ {}^{n}\sigma_e = 0.866({}^{n}\sigma_{mean}) $$

$$ {}^{1}\sigma_e = 0.866({}^{1}\sigma_1) $$

$$ {}^{1}\sigma_e = 0.866(107.7) $$

$$ {}^{1}\sigma_e = 93.24 MPa $$

The stress calculations for 2nd operating cycle (m=2) were different because of the reduced thickness (*t=25.6 mm*) in the bulging area. Therefore the values of the stresses were increased compared to the 1st operating cycle.

Table 4.6: Stress calculation for each operating cycle

Operating Cycle	Past (m=1)		Future (m=2)	
Sub-increment	n=1	n=2	n=1	n=2
Design Pressure (MPa)	0.38	0.38	0.38	0.38
Design Temperature (°C)	343	343	600	600
Time (hours)	43800	43800	1800	1800
${}^{n}\sigma_{xx} = {}^{n}\sigma_1$	107.7	107.7	109.45	109.45
${}^{n}\sigma_{yy} = {}^{n}\sigma_2$	53.83	53.83	54.72	54.72

${}^{n}\sigma_{zz} = {}^{n}\sigma_{3}$	0	0	0	0
${}^{n}\tau_{xy}$ (MPa)	0	0	0	0
${}^{n}\sigma_{e}$ (MPa)	93.24	93.24	94.78	94.78

STEP 5 –The protection of the component against plastic collapse was evaluated as shown below:

$$ {}^{n}\sigma_{ref}^{p} = \frac{{}^{n}P_b + ({}^{n}P_b^2 + 9\,{}^{n}P_l^{\,2})^{0.5}}{3} $$

$$ {}^{n}\sigma_{ref}^{p} = \frac{0 + (0^2 + 9(107.7^2))^{0.5}}{3} $$

$$ {}^{n}\sigma_{ref}^{p} = 107.7\ \text{MPa} $$

$$ \sigma_{ys}(343\,^{o}\text{C}) = 250\ \text{MPa} $$

$$ \sigma_{ys}(600\,^{o}\text{C}) = 170\ \text{MPa} $$

$$ {}^{n}\sigma_{ref}^{p} \le \min[0.75(\sigma_{ys}(343\,^{o}\text{C})), 0.75(\sigma_{ys}(600\,^{o}\text{C}))] $$

$$ {}^{n}\sigma_{ref}^{p} \le \min[0.75(250), 0.75(170)] $$

$$ 107.7 \le 127.5 $$

Since the primary load reference stress, ${}^{n}\sigma_{ref}^{p}$, is less than 75% of the minimum yield strength, the plastic collapse criteria were satisfied. The stress of the second operating cycle (m=2) also satisfies the criterion.

STEP 6 – Determination of the principal stresses.

Thin-walled shell experience a bi-axial stress state and the shear stress is zero, therefore, the principal stresses are given by the stress components calculated in STEP 4(${}^{n}\sigma_{xx} = {}^{n}\sigma_{1}$, ${}^{n}\sigma_{yy} = {}^{n}\sigma_{2}$, ${}^{n}\sigma_{zz} = {}^{n}\sigma_{3}$). The table provided at the end of STEP 4 includes, also, the principal stresses.

STEP 7 – Determination of the remaining life at the stress level ${}^{n}\sigma_{e}$ and temperature ${}^{n}T$ for time increment ${}^{n}t$ by utilizing creep rupture data for the material and designate this value as ${}^{n}L$.

The remaining life of a component, *L*, for a given stress state and temperature can be computed using the equations given below, as provided by the Omega method. In these equations, stress is in *ksi*, temperature in *°F*, and the remaining life and time in

hours. Material constants were taken from Annex F, Table F.30 in API 579 [4.1] for Carbon steel.

$A_0 = -16.3$

$A_1 = 38060$

$A_2 = -9165$

$A_3 = 1200$

$A_4 = -600$

$B_0 = -1.0$

$B_1 = 3060.0$

$B_2 = 135.0$

$B_3 = -760.0$

$B_4 = 247.0$

For a cylinder or cone $\alpha_\Omega = 2$.

The MPC Project Omega parameter is defined as $\beta_\Omega = \frac{1}{3}$.

The calculation for the remaining life at the stress level ${}^n\sigma_e$ and temperature ${}^nT$ for time increment ${}^nt$ is provided below.

The adjustment factors for creep ductility Δ_Ω^{cd} and creep strain Δ_Ω^{sr} were set to 0.0

$$S_l = \log_{10}\left({}^n\sigma_e\right)$$

$$S_l = \log_{10}\left((13.52)\right)$$

$$S_l = 0.884$$

$$\log_{10}\dot{\varepsilon}_{co} = -\left\{\left(A_0 + \Delta_\Omega^{sr}\right) + \left[\frac{1}{460 + {}^nT}\right]\left[A_1 + A_2 S_l + A_3 S_l^2 + A_4 S_l^3\right]\right\}$$

$$\log_{10}\dot{\varepsilon}_{co} = -\left\{\left(-16.3 + 0\right) + \left[\frac{1}{460 + 649.4}\right]\left[38060 + (-9165)(0.884) + (1200)(0.884)^2 + (-600)(0.884)^3\right]\right\}$$

$$\log_{10}\dot{\varepsilon}_{co} = -0.0894$$

$$\dot{\varepsilon}_{co} = 6.68 \times 10^{-12}\ {}^{1}/_{Hr}$$

$$\log_{10}\Omega = -\left\{\left(B_0 + \Delta_\Omega^{cd}\right) + \left[\frac{1}{460 + {}^nT}\right]\left[B_1 + B_2 S_l + B_3 S_l^2 + B_4 S_l^3\right]\right\}$$

$$\log_{10}\Omega = -\left\{\left(-1 + 0\right) + \left[\frac{1}{460 + 649.4}\right]\left[3060 + (135)(0.884) + (-760)(0.884)^2 + (247)(0.884)^3\right]\right\}$$

$$\log_{10}\Omega = 0.6737$$

$$\Omega = 30.5$$

$$n_{BN} = -\left\{\left[\frac{1}{460 + {}^{n}T}\right]\left[A_2 + 2A_3 S_l + 3A_4 S_l^2\right]\right\}$$

$$n_{BN} = -\left\{\left[\frac{1}{460 + 649.4}\right]\left[-9165 + 2(1200)(0.884) + 3(-600)(0.884)^2\right]\right\}$$

$$n_{BN} = 7.62$$

$$\Omega_n = \max\left[\left(\Omega - n_{BN}\right), 3.0\right]$$

$$\Omega_n = \max\left[\left(30.5 - 7.62\right), 3.0\right]$$

$$\Omega_n = 22.88$$

$$\delta_\Omega = \beta_\Omega\left(\frac{{}^{n}\sigma_1 + {}^{n}\sigma_2 + {}^{n}\sigma_3}{{}^{n}\sigma_e} - 1.0\right)$$

$$\delta_\Omega = \frac{1}{3}\left(\frac{15.62 + 7.81 + 0.0}{13.53} - 1.0\right)$$

$$\delta_\Omega = 0.244$$

$$\Omega_m = \Omega_n^{\delta_\Omega + 1} + \alpha_\Omega n_{BN}$$

$$\Omega_m = 22.88^{0.244+1} + 2(7.62)$$

$$\Omega_m = 64.35$$

$${}^{n}L = \frac{1}{\dot{\varepsilon}_{co}\,\Omega_m}$$

$${}^{1}L = \frac{1}{6.68 \times 10^{-12}(64.35)}$$

$${}^{1}L = 2.33 \times 10^{9}\ hours$$

The remaining life for the 2nd (n=2) increment of the 1st (m=1) operating cycle was identically calculated. The results differ for the 2nd (m=2) operating cycle, since the temperature and the thickness of the shell are different due to the bulging. The principal stresses as well as the equivalent stress of Eqs. (4.1) & (4.2) exhibited higher values in the second operating cycle (Table 4.7).

Table 4.7: Operating conditions for the 2nd operating cycle (m=2)

	Principal Stresses (ksi)			Equivalent Stress (ksi)	Temperature (F)
	σ_1	σ_2	σ_3	σ_e	T
Operating Cycle (m=2)	15.87	8.33	0	13.74	1112

The calculations, concern the 2nd operating cycle, are given below:

$$S_l = \log_{10}\left({}^{n}\sigma_e\right)$$

$$S_l = \log_{10}\left((13.74)\right)$$

$$S_l = 0.879$$

$$\log_{10}\dot{\varepsilon}_{co} = -\left\{\left(A_0 + \Delta_{\Omega}^{sr}\right) + \left[\frac{1}{460 + {}^{n}T}\right]\left[A_1 + A_2 S_l + A_3 S_l^2 + A_4 S_l^3\right]\right\}$$

$$\log_{10}\dot{\varepsilon}_{co} = -\left\{\left(-16.3 + 0\right) + \left[\frac{1}{460 + 1112}\right]\left[38060 + (-9165)(0.879) + (1200)(0.879)^2 + (-600)(0.879)^3\right]\right\}$$

$$\log_{10}\dot{\varepsilon}_{co} = -0.32$$

$$\dot{\varepsilon}_{co} = 7.6 \times 10^{-4}\ {}^{1}/_{Hr}$$

$$\log_{10}\Omega = -\left\{\left(B_0 + \Delta_{\Omega}^{cd}\right) + \left[\frac{1}{460 + {}^{n}T}\right]\left[B_1 + B_2 S_l + B_3 S_l^2 + B_4 S_l^3\right]\right\}$$

$$\log_{10}\Omega = -\left\{\left(-1 + 0\right) + \left[\frac{1}{460 + 1112}\right]\left[3060 + (135)(0.879) + (-760)(0.879)^2 + (247)(0.879)^3\right]\right\}$$

$$\log_{10}\Omega = 1.32$$

$$\Omega = 5.69$$

$$n_{BN} = -\left\{\left[\frac{1}{460 + {}^{n}T}\right]\left[A_2 + 2A_3 S_l + 3A_4 S_l^2\right]\right\}$$

$$n_{BN} = -\left\{\left[\frac{1}{460 + 1112}\right]\left[-9165 + 2(1200)(0.879) + 3(-600)(0.879)^2\right]\right\}$$

$$n_{BN} = 5.37$$

$$\Omega_n = \max\left[\left(\Omega - n_{BN}\right), 3.0\right]$$

$$\Omega_n = \max\left[\left(5.69 - 5.37\right), 3.0\right]$$

$$\Omega_n = 3$$

$$\delta_\Omega = \beta_\Omega \left(\frac{{}^n\sigma_1 + {}^n\sigma_2 + {}^n\sigma_3}{{}^n\sigma_e} - 1.0 \right)$$

$$\delta_\Omega = \frac{1}{3}\left(\frac{15.87 + 7.94 + 0.0}{13.75} - 1.0 \right)$$

$$\delta_\Omega = 0.244$$

$$\Omega_m = \Omega_n^{\delta_\Omega + 1} + \alpha_\Omega n_{BN}$$

$$\Omega_m = 5.69^{0.244+1} + 2(5.37)$$

$$\Omega_m = 14.67$$

$${}^nL = \frac{1}{\dot{\varepsilon}_{co}\,\Omega_m}$$

$${}^1L = \frac{1}{7.6 \times 10^{-4}(14.67)}$$

$${}^1L = 89.65 hours$$

The remaining life for the second increment (n=2) of the second operating cycle is calculated similarly.

STEP 8 – STEPS 3 through 7 for each time increment ${}^nt$ in the m^{th} operating cycle to determine the rupture time, ${}^nL$, were repeated for each increment. The results for each time period are shown in the Table 4.8.

Table 4.8: Rupture time, ${}^nL$, for each increment

Operating Cycle	Past (m=1)		Future (m=2)	
Sub-increment	n=1	n=2	n=1	n=2
Design Pressure (MPa)	3.94	3.94	3.94	3.94
Design Temperature (°C)	343	343	600	600
Time (hours)	43800	43800	1800	1800
${}^n\sigma_{xx} = {}^n\sigma_1$	107.7	107.7	109.45	109.45
${}^n\sigma_{yy} = {}^n\sigma_2$	53.83	53.83	54.72	54.72

${}^{n}\sigma_{zz} = {}^{n}\sigma_{3}$	0	0	0	0
${}^{n}\tau_{xy}$(MPa)	0	0	0	0
${}^{n}\sigma_{e}$(MPa)	93.24	93.24	94.78	94.78
Remaining Life ^{n}L (hours)	2.33×10^{9}	2.33×10^{9}	89.65	89.65

STEP 9 – The accumulated creep damage for all points in the m^{th} cycle using Equation (10.25) [4.1] was computed. In this equation, ${}^{n}t$ was defined as the time increment when the component is subjected to a stress level, ${}^{n}\sigma_{e}$, at a corresponding operating temperature ${}^{n}T$, and ${}^{n}L$ is the permissible life at this temperature based on material data.

$$ {}^{m}D_{c} = \sum_{n=1}^{N} \frac{{}^{n}t}{{}^{n}L} $$

$$ {}^{1}D_{c} = \frac{{}^{1}t}{{}^{1}L} + \frac{{}^{2}t}{{}^{2}L} = \frac{43800}{2.33\times10^{9}} + \frac{43800}{2.33\times10^{9}} = 3.7\times10^{-5} $$

STEP 10 –STEPS 2 through 9 for each of the operating cycles defined in STEP 1 were repeated. The results of each operating cycle are presented in the Table 4.9.

Table 4.9: Accumulated Creep damage for each period

Operating Cycle	Past (m=1)		Future (m=2)	
Sub-increment	n=1	n=2	n=1	n=2
Design Pressure (MPa)	3.94	3.94	3.94	3.94
Design Temperature (°C)	343	343	600	600
Time (hours)	43800	43800	1800	1800
${}^{n}\sigma_{xx} = {}^{n}\sigma_{1}$	107.7	107.7	109.45	109.45
${}^{n}\sigma_{yy} = {}^{n}\sigma_{2}$	53.83	53.83	54.72	54.72
${}^{n}\sigma_{zz} = {}^{n}\sigma_{3}$	0	0	0	0
${}^{n}\tau_{xy}$(MPa)	0	0	0	0
${}^{n}\sigma_{e}$(MPa)	93.24	93.24	94.78	94.78

Remaining Life ^{n}L (hours)	2.33×10^{9}	2.33×10^{9}	89.65	89.65
Damage $^{m}D_c$	3.7×10^{-5}		40.16	

STEP 11 –The total creep damage for all cycles of operation was computed.

$$D_c^{total} = \sum_{m=1}^{M} {}^{m}D_c \le D_c^{allow}$$

$$D_c^{total} = \sum_{m=1}^{2} {}^{m}D_c \le D_c^{allow}$$

$$D_c^{total} = {}^{1}D_c + {}^{2}D_c \le D_c^{allow} = 3.7\times10^{-5} + 40.16 \le 0.8$$

$$D_c^{total} = 40.16 > 0.8$$

STEP 12 – Since the total damage, D_c^{total}, was greater than the allowable creep damage, D_c^{allow}, then the life of the component was limited to the time corresponding to $D_c^{total} = D_c^{allow}$. The remaining life, for the selected future conditions, was calculated as follows.

$$D_c^{total} = D_c^{allow}$$

$${}^{1}D_c + {}^{2}D_c = D_c^{allow}$$

$$3.7\times10^{-5} + \frac{t}{89.65} = 0.8$$

$$t = 71.72 hours$$

The main result suggests that the component can continue safely its operation for 71.72 hours at 600 °C.

According to API 579 [4.1] a rerate of operational conditions is necessary in order to specify the temperature for which the gasifier can return to service. The pressure can't be changed because it is the operating condition of the gasifier. Therefore, the above calculations were repeated in order to determine the temperature where the gasifier can safely work. These calculations pointed out that the gasifier can return to service for 3600 hours more, if the operating temperature drops below 525 °C.

4.4 Case Study 2: FFS for a Fired crude heater

A fired crude heater experienced a temperature excursion for a short duration. The refinery needs to know how much additional damage occurred to the tubes, as well as, to understand how the excursion impacts the remaining tube life. This information will be used to support the decision if the heater will need to be re-tubed at an upcoming scheduled turn-around, or if the tubes are likely to last for another run. The purpose of the case study is to evaluate the remaining life of the tubes, employing the Level 2 assessment procedures, and determine if they are fit for service for another run.

Heater Tube Data

Component	= Cylinder
Material	= SA-335 Grade P22
Typical Condition (j=1)	= 1.45 MPa @ 600°C
Outside Diameter	= 220 mm
Fabricated Thickness	= 8.18 mm
Future Corrosion Allowance (FCA)	= 2.54 mm
Past Operating Time (j=1)	= 131400 hours
Future Expected Time (j=3)	= 43800 hours

Temperature Excursion Data

Excursion Pressure	= 1.45 MPa
Excursion Temperature	= 660 °C
Excursion Duration	= 336 hours

Inspection Data

There are no visual signs of damage to the tube, no bulging, metal loss, or excessive scale was noted. Looking through the inspection records, this is the first operational excursion into the creep range for this component. There are no circumferential weld seams in the fire box.

A multiple condition Level 2 Assessment for the component in creep service was performed according to paragraph 10.4.3 [4.1]. In this example, the tube bends are located outside the firebox, so only the cylindrical portion of the tubes was analyzed.

For the purposes of this example, the tubes were assumed to be adequately supported and the circumferential pressure stress was the limiting design condition.

The procedure comprised of 12 steps that are analyzed below:

STEP 1 – Determination a load history based on the past and the future planned operation. The load history is listed in Table 4.10.

Table 4.10: Load history for each period

	Past (m=1)	Excursion (m=2)	Future (m=3)
Pressure (MPa)	1.45	1.45	1.45
Temperature (°C)	600	660	600
Time (hours)	131400	336	43800

STEP 2 – The total cycle time, ${}^{m}t$, of each operating cycle m, was divided in a number of time increments, ${}^{n}t$. The total number of time increments, N, for each operating cycle, m, was defined. The time increments used to model the operating cycle should be small enough to capture all significant variations in the operating cycle. The smaller the time increment, the more accurate the remaining life predication.

For this application, N was set to 2 because the condition for each sub-cycle was the same. In general, N should be set to match any change in pressure, temperature, or tube thickness. Each of the operating cycles in the load history was split into its respective sub-increments in Table 4.11.

Table 4.11: Load history and increments of each period

Operating Cycle	Past (m=1)		Excursion (m=2)		Future (m=3)	
Sub-increment	n=1	n=2	n=1	n=2	n=1	n=2
Design Pressure (MPa)	1.45	1.45	1.45	1.45	1.45	1.45
Time (hours)	65700	65700	168	168	21900	21900

STEP 3 – The assessment temperature, ${}^{n}T$, for the time increment ${}^{n}t$ is shown in Table 4.12.

Table 4.12: Design Temperature for each sub-increment

Operating Cycle	Past (m=1)		Excursion (m=2)		Future (m=3)	
Sub-increment	n=1	n=2	n=1	n=2	n=1	n=2
Design Pressure (MPa)	1.45	1.45	1.45	1.45	1.45	1.45
Design Temperature (°C)	600	600	660	660	600	600
Time (hours)	65700	65700	168	168	21900	21900

STEP 4 – The stress components ${}^{n}\sigma_{ij}$, for each time increment ${}^{n}t$ was determined as described below.

Initially, the tube dimension was checked to insure the tube is considered as thin-walled according to the definition given in paragraph 10.5.2.5 of API 579 [4.1].

$$\frac{OD}{t_{mean}} \geq 6$$

$$\frac{8.625}{0.322} \geq 6$$

$$26.8 \geq 6$$

Since the thin-walled criterion is met, the mean diameter stress equations according to Tale 10.2 [4.1] are applicable.

For this example a fully-corroded thickness is used for simplicity. A more realistic approach is to calculate the stress as a function of the thickness according to the past and predicted corrosion rates. An example of this calculation is worked out below for the first sub-increment of the first operating cycle.

$$^{n}\sigma_1 = {}^{n}\sigma_{mean} = \frac{P(\mathrm{D}_{mean})}{2t_{corr}}$$

$$^{1}\sigma_1 = \frac{P(\mathrm{OD} - t_{nom} + \mathrm{FCA})}{2(\mathrm{t}_{nom} - FCA)}$$

$$^{1}\sigma_1 = \frac{1.45(8.625 - 0.322 + 0.1)}{2(0.322 - 0.1)}$$

$$^{1}\sigma_1 = 27.44MPa$$

$$^{n}\sigma_2 = 0.5(^{n}\sigma_{mean})$$

$$^{1}\sigma_2 = 0.5(^{1}\sigma_1)$$

$$^{1}\sigma_2 = 13.72MPa$$

$$^{n}\sigma_3 = 0.0$$

$$^{n}\sigma_e = 0.866(^{n}\sigma_{mean})$$

$$^{1}\sigma_e = 0.866(^{1}\sigma_1)$$

$$^{1}\sigma_e = 0.866(27.44)$$

$$^{1}\sigma_e = 23.76MPa$$

Table 4.13: Stress calculation for each operating cycle

Operating Cycle	Past (m=1)		Excursion (m=2)		Future (m=3)	
Sub-increment	n=1	n=2	n=1	n=2	n=1	n=2
Design Pressure (MPa)	1.45	1.45	1.45	1.45	1.45	1.45
Design Temperature (°C)	600	600	660	660	600	600
Time (hours)	65700	65700	168	168	21900	21900
$^{n}\sigma_{xx} = {}^{n}\sigma_1$	27.44	27.44	27.44	27.44	27.44	27.44
$^{n}\sigma_{yy} = {}^{n}\sigma_2$	13.72	13.72	13.72	13.72	13.72	13.72
$^{n}\sigma_{zz} = {}^{n}\sigma_3$	0	0	0	0	0	0
$^{n}\tau_{xy}$ (MPa)	0	0	0	0	0	0
$^{n}\sigma_e$ (MPa)	23.76	23.76	23.76	23.76	23.76	23.76

STEP 5 – Determine if the component has adequate protection against plastic collapse

Since the primary load reference stress, ${}^{n}\sigma_{ref}^{P}$, is less than 75% of the minimum yield strength, the plastic collapse criteria are satisfied. The stress in the component is constant in this example, therefore the results below are valid for all operating cycles and sub-increments.

$$ {}^{n}\sigma_{ref}^{P} = \frac{{}^{n}P_b + ({}^{n}P_b^2 + 9\,{}^{n}P_L^2)^{0.5}}{3} $$

$$ {}^{n}\sigma_{ref}^{P} = \frac{0 + (0^2 + 9(27.44^2))^{0.5}}{3} $$

$$ {}^{n}\sigma_{ref}^{P} = 27.44\,\text{MPa} $$

$$ \sigma_{ys}(600\,^{o}\text{C}) = 136.86\,\text{MPa} $$

$$ \sigma_{ys}(660\,^{o}\text{C}) = 103.65\,\text{MPa} $$

$$ {}^{n}\sigma_{ref}^{P} \le \min[0.75(\sigma_{ys}(600\,^{o}\text{C})), 0.75(\sigma_{ys}(660\,^{o}\text{C}))] $$

$$ {}^{n}\sigma_{ref}^{P} \le \min[0.75(136.86), 0.75(103.65)] $$

$$ 27.44 \le 77.74 $$

STEP 6 – Determination of the principal stresses.

Thin-walled tube experience a bi-axial stress state and the shear stress is zero, therefore, the principal stresses are given by the stress components calculated in STEP 4(${}^{n}\sigma_{xx} = {}^{n}\sigma_1, {}^{n}\sigma_{yy} = {}^{n}\sigma_2, {}^{n}\sigma_{zz} = {}^{n}\sigma_3$). The table provided at the end of STEP 4 includes, also, the principal stresses.

STEP 7 – Determination of the remaining life at the stress level ${}^{n}\sigma_e$ and temperature ${}^{n}T$ for time increment ${}^{n}t$ by utilizing creep rupture data for the material and designate this value as ${}^{n}L$. In these equations, stress is in *ksi*, temperature is °F, and the remaining life and time are in *hours*. Material constants according to Annex F, Table F.30 [4.1] in API 579 for Carbon steel are:

$A_0 = -21.86$

$A_1 = 50205$

$A_2 = -5436$

$A_3 = 500$

$A_4 = -3400$

$B_0 = -1.85$

$B_1 = 7205$

$B_2 = -2436$

$B_3 = 0.0$

$B_4 = 0.0$

For a cylinder or cone $\alpha_\Omega = 2$.

The MPC Project Omega parameter is defined as $\beta_\Omega = \frac{1}{3}$.

The calculation for the remaining life at the stress level ${}^n\sigma_e$ and temperature ${}^nT$ for time increment ${}^nt$ is provided below.

The adjustment factors for creep ductility Δ_Ω^{cd} and creep strain Δ_Ω^{sr} were set to 0.0

$$S_l = \log_{10}\left({}^n\sigma_e\right)$$

$$S_l = \log_{10}\left((3.442)\right)$$

$$S_l = 0.5368$$

$$\log_{10}\dot{\varepsilon}_{co} = -\left\{\left(A_0 + \Delta_\Omega^{sr}\right) + \left[\frac{1}{460 + {}^nT}\right]\left[A_1 + A_2 S_l + A_3 S_l^2 + A_4 S_l^3\right]\right\}$$

$$\log_{10}\dot{\varepsilon}_{co} = -\left\{\left(-21.86 + 0\right) + \left[\frac{1}{460 + 1115}\right]\left[50205 + (-5436)(0.5368) + (500)(0.5368)^2 + (-3400)(0.5368)^3\right]\right\}$$

$$\log_{10}\dot{\varepsilon}_{co} = -7.921$$

$$\dot{\varepsilon}_{co} = 1.199 \times 10^{-8}\ {}^{1}/_{Hr}$$

$$\log_{10}\Omega = -\left\{\left(B_0 + \Delta_\Omega^{cd}\right) + \left[\frac{1}{460 + {}^nT}\right]\left[B_1 + B_2 S_l + B_3 S_l^2 + B_4 S_l^3\right]\right\}$$

$$\log_{10}\Omega = -\left\{\left(-1.85 + 0.0\right) + \left[\frac{1}{460 + 1115}\right]\left[7205 + (-2436)(0.5368) + 0.0(0.5368)^2 + 0.0(0.5368)^3\right]\right\}$$

$$\log_{10}\Omega = 1.894$$

$$\Omega = 78.406$$

$$n_{BN} = -\left\{\left[\frac{1}{460 + {}^{n}T}\right]\left[A_2 + 2A_3 S_l + 3A_4 S_l^2\right]\right\}$$

$$n_{BN} = -\left\{\left[\frac{1}{460 + 1115}\right]\left[-5436 + 2(500)(0.5368) + 3(-3400)(0.5368)^2\right]\right\}$$

$$n_{BN} = 4.977$$

$$\Omega_n = \max\left[(\Omega - n_{BN}), 3.0\right]$$

$$\Omega_n = \max\left[(78.406 - 4.977), 3.0\right]$$

$$\Omega_n = 73.429$$

$$\delta_\Omega = \beta_\Omega\left(\frac{{}^{n}\sigma_1 + {}^{n}\sigma_2 + {}^{n}\sigma_3}{{}^{n}\sigma_e} - 1.0\right)$$

$$\delta_\Omega = \frac{1}{3}\left(\frac{3.974 + 1.987 + 0.0}{3.442} - 1.0\right)$$

$$\delta_\Omega = 0.244$$

$$\Omega_m = \Omega_n^{\delta_\Omega + 1} + \alpha_\Omega n_{BN}$$

$$\Omega_m = 73.429^{0.244+1} + 2(4.977)$$

$$\Omega_m = 219.43$$

$${}^{n}L = \frac{1}{\dot{\varepsilon}_{co}\,\Omega_m}$$

$${}^{1}L = \frac{1}{1.199 \times 10^{-8}(219.43)}$$

$${}^{1}L = 380090 hours$$

The remaining life for each other increment were calculated similarly.

STEP 8 –STEPS 3 through 7 for each time increment ${}^{n}t$ in the m^{th} operating cycle were repeated, in order to determine the rupture time, ${}^{n}L$, for each increment. The results for each time period are presented in Table 4.14.

Table 4.14: Rupture time, ${}^{n}L$, for each increment

Operating Cycle	Past (m=1)		Excursion (m=2)		Future (m=3)	
Sub-increment	n=1	n=2	n=1	n=2	n=1	n=2

Design Pressure (MPa)	1.45	1.45	1.45	1.45	1.45	1.45
Design Temperature (°C)	600	600	660	660	600	600
Time (hours)	65700	65700	168	168	21900	21900
${}^{n}\sigma_{xx} = {}^{n}\sigma_{1}$	27.44	27.44	27.44	27.44	27.44	27.44
${}^{n}\sigma_{yy} = {}^{n}\sigma_{2}$	13.72	13.72	13.72	13.72	13.72	13.72
${}^{n}\sigma_{zz} = {}^{n}\sigma_{3}$	0	0	0	0	0	0
${}^{n}\tau_{xy}$ (MPa)	0	0	0	0	0	0
${}^{n}\sigma_{e}$ (MPa)	23.76	23.76	23.76	23.76	23.76	23.76
Remaining Life ^{n}L (hours)	380090	380090	10330	10330	380090	380090

STEP 9 – The accumulated creep damage for all points in the m^{th} cycle were computed using Equation (10.25) [4.1].

$$ {}^{m}D_{c} = \sum_{n=1}^{N} \frac{{}^{n}t}{{}^{n}L} $$

$$ {}^{1}D_{c} = \frac{{}^{1}t}{{}^{1}L} + \frac{{}^{2}t}{{}^{2}L} = \frac{65700}{380090} + \frac{65700}{380090} = 0.346 $$

STEP 10 –STEPS 2 through 9, for each of the operating cycles defined in STEP 1, were repeated.

The results of each operating cycle are shown in Table 4.15.

Table 4.15: Accumulated Creep damage for each period

Operating Cycle	Past (m=1)		Excursion (m=2)		Future (m=3)	
Sub-increment	n=1	n=2	n=1	n=2	n=1	n=2
Design Pressure (MPa)	1.45	1.45	1.45	1.45	1.45	1.45
Design Temperature (°C)	600	600	660	660	600	600

Time (hours)	65700	65700	168	168	21900	21900
${}^{n}\sigma_{xx} = {}^{n}\sigma_{1}$	27.44	27.44	27.44	27.44	27.44	27.44
${}^{n}\sigma_{yy} = {}^{n}\sigma_{2}$	13.72	13.72	13.72	13.72	13.72	13.72
${}^{n}\sigma_{zz} = {}^{n}\sigma_{3}$	0	0	0	0	0	0
${}^{n}\tau_{xy}$ (MPa)	0	0	0	0	0	0
${}^{n}\sigma_{e}$ (MPa)	23.76	23.76	23.76	23.76	23.76	23.76
Remaining Life ${}^{n}L$ (hours)	380090	380090	10330	10330	380090	380090
Damage ${}^{m}D_c$	0.346		0.033		0.115	

STEP 11 –The total creep damage for all cycles of operation were computed.

$$D_c^{total} = \sum_{m=1}^{M} {}^{m}D_c \le D_c^{allow}$$

$$D_c^{total} = \sum_{m=1}^{3} {}^{m}D_c \le D_c^{allow}$$

$$D_c^{total} = {}^{1}D_c + {}^{2}D_c + {}^{3}D_c \le D_c^{allow} = 0.346 + 0.033 + 0.115 \le 0.8$$

$$D_c^{total} = 0.494 \le 0.8$$

STEP 12 – The creep damage prediction is complete for this location in the component. In this case, since the total damage, $D_c^{total} = 0.494$, is lower than the allowable damage, the component is acceptable for continued operation for five more years (m=3). The remaining life for operation can be determined solving the following equation:

$$D_c^{total} = D_c^{allow}$$

$$\frac{65700}{380090} + \frac{65700}{380090} + \frac{168}{10330} + \frac{168}{10330} + \frac{t}{380090} = 0.8$$

$$t = 160018 hours$$

So the remaining life of the tubes is 18 years.

Larson-Miller Parameter Approach

Alternative STEP 7 – The remaining life at the stress level using the Larson-Miller parameter were determined, using data according to Annex F, Table F.31 [4.1]. SA335Grade P22 material

Table 4.16: Data for SA335GradeP22

Parameters	Minimum Larson Miller Parameter LMP_m	Average Larson Miller Parameter LMP_a
A_0	43.98	43.49
A_1	-0.846	-0.602
A_2	-40.48	-28.04
A_3	0.262	0.206
A_4	15.37	10.98
A_5	0.0496	0.0283
A_6	0.66	0.36
C_{LMP}	20.0	20.0

Calculation of Remaining life with minimum Larson Miller Parameter:

$$LMP_m = \frac{A_0 + A_2 + \sqrt{S_{eff}} + A_4 S_{eff} + A_6 S_{eff}^{1.5}}{1 + A_1\sqrt{S_{eff}} + A_3 S_{eff} + A_5 S_{eff}^{1.5}}$$

The estimation of remaining life were estimated using the following equations:

$$Log_{10}^{n}[L] = \frac{1000 LMP\left({}^{n}S_{eff}\right)}{\left({}^{n}T + 460\right)} - C_{LMP}$$

Where

$${}^{n}S_{eff} = \frac{{}^{n}\sigma_e}{1000}\exp\left[0.24\left(\frac{J_1}{S_s} - 1\right)\right]$$

$$J_1 = {}^{n}\sigma_1 + {}^{n}\sigma_2 + {}^{n}\sigma_3$$

$$S_s = ({}^{n}\sigma_1^{\,2} + {}^{n}\sigma_2^{\,2} + {}^{n}\sigma_3^{\,2})^{0.5}$$

$$J_1 = 3.974 + 1.987 + 0 = 5.961$$

$$S_s = \sqrt{3.974^2 + 1.987^2 + 0^2} = 4.443$$

$${}^{n}S_{eff} = 3.442\exp\left[0.24\left(\frac{5.961}{4.443} - 1\right)\right] = 3.736$$

Calculation of remaining life using the **minimum Larson- Miller parameter** data

$$LMP_{\min} = \frac{A_0 + A_2\sqrt{S_{eff}} + A_4 S_{eff} + A_6 S_{eff}^{1.5}}{1 + A_1\sqrt{S_{eff}} + A_3 S_{eff} + A_5 S_{eff}^{1.5}} =$$

$$= \frac{43.98 + (-40.48)\sqrt{3.736} + (15.37)(3.736) + (0.66)(3.736)^{1.5}}{1 - 0.846\sqrt{3.736} + 0.262(3.736) + 0.0496(3.736)^{1.5}}$$

$$= 39.79$$

$$Log_{10}L = \left[\frac{1000LMP_{\min}}{T + 460} - C_{LMP}\right] = \frac{1000(39.79)}{1115 + 460} - 20 = 5.26$$

$$^1L = 183889 hours$$

$$^1t = 65700 hours$$

So the life fraction for the first sub-increment is calculated as follows: $\left(\frac{65700}{183889}\right) = 0.357$

Similarly the life fraction for the other sub-increment can be calculated using the above equations. The calculated life fractions are: 0.357, 0.034, 0.034, 0.119, 0.119, so the total damage is:

$$D_C^{total} = [0.357 + 0.357 + 0.034 + 0.034 + 0.119 + 0.119] = 1.02 \geq 0.8$$

Therefore, the component is not acceptable for continuing operation according to calculations using the equations of minimum Larson-Miller parameter.

Calculation of remaining life using the **average Larson-Miller parameter** data.

$$LMP_{avg} = \frac{A_0 + A_2\sqrt{S_{eff}} + A_4 S_{eff} + A_6 S_{eff}^{1.5}}{1 + A_1\sqrt{S_{eff}} + A_3 S_{eff} + A_5 S_{eff}^{1.5}} =$$

$$= \frac{43.49 + (-28.04)\sqrt{3.736} + (10.98)(3.736) + (0.36)(3.736)^{1.5}}{1 - 0.601\sqrt{3.736} + 0.206(3.736) + 0.028(3.736)^{1.5}} = 40.72$$

$$Log_{10}L = \left[\frac{1000LMP_{\min}}{T + 460} - C_{LMP}\right] = \frac{1000(40.72)}{1115 + 460} - 20 = 5.85$$

$$^1L = 717489 hours$$

$$^1t = 65700 hours$$

Life fraction for the first sub-increment: $\left(\frac{65700}{717489}\right) = 0.092$

For the other 5 sub-increments, the life fractions are: 0.092, 0.00967, 0.00967, 0.03, 0.03. The total creep damage is:

$$D_C^{total} = [0.092 + 0.092 + 0.00967 + 0.00967 + 0.03 + 0.03] = 0.35 \leq 0.8$$

Therefore, the component is acceptable for continuing operation according to calculations using the equations of average Larson-Miller parameter.

4.5 Conclusions

The API 579 -1 /ASME FFS procedure was employed to analyze the structural integrity of pressurized equipment used in high temperature applications in oil refineries.

Level 2 assessment was conducted in two separate case studies selected from the recent activities of the Materials Laboratory.

In the first case study a Level 2 assessment concerning the bulging damage of a gasifier was conducted and real operational conditions were integrated in the calculations. A full calculation procedure was presented, and according to the results the refinery was allowed to rerate the component after certain time period under specified temperature and pressure conditions.

In the second case study a fired crude heater was assessed in order to determine the remaining life fraction of the tubes. The remaining life fraction was also calculated by using the Larson- Miller approach. FFS coincides to the LM approach in case that the average LM parameter was considered. If the minimum LM parameter was taken into the calculations the two approaches differ with the LM approach to be at the conservative side. The LMP method predicted longer creep lives than the Omega method when based on average creep strength values but not when based on the minimum creep strength curve or the lower bound of the creep strength property scatter band. These results are in agreement with the literature [4.15]. It is worth noting that in both approaches the wall thickness considered stable with no corrosion consideration.

4.6 Terms & Definitions

A_i material coefficients for the MPC Project Omega strain-rate-parameter, see Annex F, Table F.30 [4.1]

a_Ω triaxiality parameter based on the state of stress for MPC Project Omega Life Assessment Model.

B_i material coefficients for the MPC Project Omega Omega-parameter, see Annex F, Table F.30 [4.1]

β_Ω MPC Project Omega parameter to 0.33

C_{LMP} Larson Miller Constant in Annex F, Table F.31 [4.1]

D_{mean} mean diameter of a cylinder or sphere

D_c^{allow} allowable creep damage

${}^m D_c$ creep damage for the mth operating cycle

D_c^{total} total creep damage considering all operating cycles.

Δ_Ω^{sr} adjustment factor for creep strain rate to account for the material scatter band in the Project Omega Model, a range of −0.5 for the bottom of the scatter band to +0.5 for the top of the scatter band can be used

δ_Ω MPC Project Omega parameter

ε_c accumulated creep strain

$\dot{\varepsilon}_c$ creep strain rate

$\dot{\varepsilon}_{co}$ initial creep strain rate at the start of the time period being evaluated based on the stress state and temperature (see Annex F, paragraph F.7.3); note, the units of measure for computing this parameter must be *ksi* and ^oF

J_1 term used to compute ${}^n S_{eff}$

${}^n L$ rupture time for the loading history for the n^{th} time increment.

LMP_{avg} average Larson Miller parameter

$LMP_{\min}$ minimum Larson Miller parameter

m current operating cycle number

M total number of operating cycles

N total number of time increments in an operating cycle

n_{BN} Bailey-Norton coefficient ($n_{BN} = -dLog\,\dot{\varepsilon}_c / dLog\sigma$)evaluated at the reference stress in the current load increment, used in the MPC Project Omega Life Assessment Model.

$^{n}P_{L}$ primary local membrane stress for the nth time increment

$^{n}P_{b}$ primary bending stress for the nth time increment

$^{n}S_{eff}$ effective stress used to compute the remaining life in terms of the Larson-Miller parameter for the n^{th} time increment.

S_{l} log base 10 of the effective stress

S_{s} term used to compute $^{n}S_{eff}$

σ_{e} effective stress

$^{n}\sigma_{ref}$ reference stress for the n^{th} time increment

σ_{ys} yield strength at the assessment temperature

$^{n}\sigma_{ij}$ applied stress components for the i^{th} time step

T temperature

^{n}T temperature for the n^{th} time increment.

^{m}t total time in the m^{th} cycle

^{n}t time increment or load duration for use in the damage calculation

Ω uniaxial Omega damage parameter (see Annex F, paragraph F.7.1.1) [4.1].; note, the units of measure for computing this parameter must be *ksi* and *oF* .

Ω_{m} multiaxial Omega damage parameter (see Annex F, paragraph F.7.1.1) [4.1].

Ω_{n} adjusted uniaxial Omega damage parameter.

4.7 References

[4.1] API 579-1/ASME FFS-1. Fitness-for-service. 2nd ed. 2007. Washington, USA

[4.2] Tantichattanont P, Adluri SMR, Seshadri R. Fitness-for-service assessment of spherical pressure vessels with hot spots. Int J. Pres. Ves. Pip. 2007;84:762-772

[4.3] Sinha RK, Sinha SK, Madhusoodanan K. Fitness for service assessment of coolant channels of Indian PHWRs. J. of Nucl. Mat. 2008;383:14-21

[4.4] Shekari E, Khan F, Ahmed S. A predictive approach to fitness-for-service assessment of pitting corrosion. Int J. Pres. Ves. Pip. 2015;xxx:1-9

[4.5] B. Dogan. Fitness for service of welded components under creep and creep-fatigue loading. Int J. Pres. Ves. Pip. 2010;87:656-663

[4.6] Alegre JM, Bravo PM, Cuesta II. Fatigue design of wire-wound pressure vessels using ASME-API 579 procedure. Eng. Fail. Anal. 2010;17:748-759

[4.7] BSI. BS 7910: guide to methods for assessing the acceptability of flaws in metallic structures. UK: British Standards Institution; 2013.

[4.8] FITNET. Fitness-for-service procedure final draft MK8. European Fitness-forService Thematic Network (FITNET); 2008.

[4.9] SINTAP. Structural integrity assessment procedure for European industry. 1999.

[4.10] ASME. ASME B31.G: Manual for determining the remaining strength of corroded pipelines. American Society of Mechanical Engineers; 2012.

[4.11] EDF. Energy, R5: assessment procedure for the high temperature response of structures. 2003. Gloucester, UK.

[4.12] EDF. Energy, R6: assessment of the integrity of structures containing defects. 2006. Gloucester, UK.

[4.13] RSE-M Code. Rules for in-service inspection of nuclear power plant components. 2010th ed. Paris: AFCEN; 2010.

[4.14] Prager M. Development of the MPC Omega Method for Life Assessment in the Creep Range. J. Pressure Vessel Technol.1995;117(2):95-103

[4.15] Jorge L. Hau and Antonio Seijas, Furnace Tube Life Assessment as Impacted by the Methodology Used , NACE Corrosion 2008, paper No. 8547

5. Carburization of High- Temperature steels: A simulation- based ranking of materials carburization resistance*

5.1 Introduction

Carburization is a high-temperature corrosion problem experienced in industrial processes such as ethylene production, natural gas reforming and coal gasification. The phenomenon takes place mainly in the petrochemical industry, where ethylene is produced in pyrolysis furnaces by thermal cracking of hydrocarbons in a steam hydrocarbon mixture at temperatures up to 1100°C. In this cracking process, coke deposition occurs at the inner walls of the cracking tubes. In steam reformers natural gas or other hydrocarbons are converted by catalytic reaction on Ni-catalysts to CO and H_2 and carburization of tube walls is observed after over heating or excessive carbon activities. In industrial heat-treating furnaces for carburizing of steels, carburization of carrying grates and furnace walls is also observed. Components of the CO_2-cooled nuclear reactors may be carburized by CO_2, and the heat exchangers of helium reactors may be carburized by impurities such as CO and CH_4 in the helium gas. In coal gasification and in waste incineration plants carburization is possible, however sulfidation and corrosion by chlorine would be more severe processes [5.1, 5.2]. Carburization takes place at high temperatures, and results in deterioration of Fe, Ni, and Co-base alloys. There are several damage processes caused by carburization, such as internal carbide formation in high-alloy steels in carbonaceous environments and metal dusting, a disintegration of metallic materials into a dust of graphite and metal particles in strongly carburizing atmospheres [5.3, 5.4].

Carbon is transferred from the gas atmosphere through the porous coke at the alloy surface, where it diffuses in the interior and forms alloy carbides. Under most service conditions the materials are protected against carburization by an oxide layer, which serves as a barrier against carbon diffusion. The diffusion of carbon into the surface of a steel tube exposed to the combustion environment is enhanced by oxide-scale cracking and spallation and by operation at temperatures above the design specifications. The exposure of fresh metal to the carburizing environment enhances the carbon penetration. The oxide scale may crack or spall due to temperature changes during operation. In addition, a reducing atmosphere acts against the stability of the protective Cr_2O_3. There have been several experimental studies of carburization in the recent literature. Swaminathan et al. [5.5] studied the carburization failure of cast HK40+Nb alloy tubes of an air pre-heater unit in a petrochemical industry. The tubes failed prematurely after 13000 h in service

* This work has been published to Engineering Failure Analysis 2015 (51) 29-36

because of carburization attack from the flue gas on the inner wall side. Nawancy [5.6] examined pyrolysis furnace tubes made of HP45 heat-resistant steel casting to handle carbonaceous gases at about 850 °C in a petrochemical plant. These tubes developed longitudinal cracks after 22000 h. Yin [5.7] studied the thermodynamics of carburization of 310 stainless steel exposed in carbon-rich CH_4/H_2 atmosphere for 500 h indicating that 1000 °C is an approximate limiting temperature, below which the environment exhibits a mixed oxidizing/carburizing behavior, while above this temperature a reducing/carburizing behavior is established. Kaya [5.8] investigated the carburization phenomenon in two tubular materials made from Fe–Cr–Ni-based HK40 alloy after a service life of approximately 25000 h in an ethylene pyrolysis furnace. Catastrophic failures due to carburization of 9Cr-1Mo, 13CrMo44, 321H and TP304H steels were also reported in the literature for service life well below the design life [5.9- 5.11]. Carburization failures due to extremely high temperatures have also been reported. Kaewkumsai et al. [5.12] reported a failure of an AISI 310 tube just one month after installation due to exposure to temperatures 200-250 °C above the design temperature. Hamid et al. [5.13] reported longitudinal cracks that in extreme cases penetrated the entire tube thickness. In this case the failure was due to a combination of creep and carburization attack because of exposure of the tube to an extremely high temperature. In addition to the experimental work, several theoretical works on carburization attack have been performed [5.1, 5.8, 5.15- 5.17] mainly on the effect of alloy composition, carbon activity and temperature on the development of the carburization front.

Despite the theoretical and experimental work as well as the failure cases reported in the literature, carburization is not taken into account quantitatively in the design codes. For example, the API 530 standard used for the calculation of heater-tube thickness in petroleum refineries [5.14] provides guidelines for selection of tube materials based solely on criteria for creep resistance. Carburization is only mentioned as a potential mechanism that could limit the service life of the tubes. The aim of the present work is to provide a ranking of carburization resistance of the steels listed in the API 530 standard through a simulation of the carburization process. Simulations were performed by employing the computational kinetics software DICTRA [5.18], which can handle diffusion-controlled transformations, such as the alloy carbide formation during carbon diffusion. The carburization resistance was ranked according to the time required for the carburization front to reach the mid-thickness of the tubes. There are certain limitations under which the present model is applied. The first is related to the absence of a protective oxide layer at the surface. This situation is true when the oxide has spalled or under low partial oxygen pressure. Therefore, only carbon diffusion has been considered, without any oxygen diffusion and associated internal oxidation. The second limitation has to do with carbon activity at the surface. The carbon activity considered is established by the equilibrium of the steel surface with the gas phase. A carbon activity of 1 was applied

as a boundary condition. This means that internal carbon deposition and metal dusting is not considered.

5.2 Methodology and calculations

A planar one-dimensional unit cell, depicted in Fig. 5.1 was employed for the simulations. The length *L* of the cell was taken equal to the thickness of the tube wall, 3mm. The simulation was performed under the following assumptions:

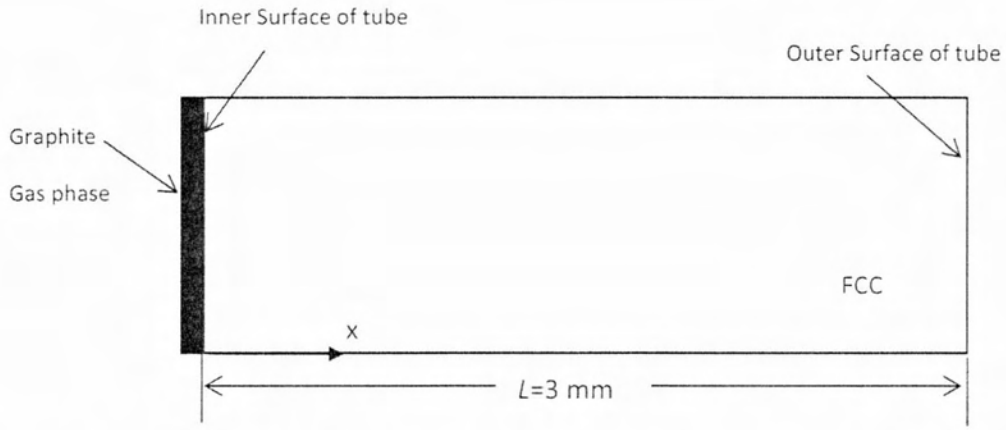

Figure 5.1: Geometrical model showing the unit cell implemented for the carburization simulations. *L* is the thickness of the tube.

a) Carbon is transferred from the gas atmosphere, through the porous coke, to the alloy surface.
b) No oxide layer was considered in order to simulate carburization under low oxygen partial pressure or oxide spallation conditions.
c) The temperature and concentration dependence of the diffusion coefficient of carbon was taken into account.
d) Formation of alloy carbides was taken into account.

Under these assumptions, the concentration profile of the alloying elements in the *x* direction is described by the diffusion equation (Fick's 2nd law) as

$$\frac{\partial c_k}{\partial t} = -\frac{\partial J_k}{\partial x} \tag{5.1}$$

where c_k is the concentration and J_k is the diffusive flux of the component *k*.

The fluxes J_k are given by the Fick-Onsager law, for diffusion in multicomponent systems, which for *n* components takes the form

$$J_k = \sum_{j=1}^{n-1} D_{kj}^{n} \frac{\partial c_j}{\partial x} \tag{5.2}$$

Where D_{kj}^{n} is the diffusion coefficient matrix, incorporated in DICTRA.

The boundary conditions at the left boundary (inner tube surface) are

$$a_C = 1 \tag{5.3}$$

$$\left.\frac{\partial c_k}{\partial x}\right|_{x=0} = 0 \quad \text{for } k \neq C \tag{5.4}$$

Where is α_c the carbon activity. The system is closed (zero flux) for all elements except for carbon. At the right boundary (outer tube surface) the boundary conditions are

$$\left.\frac{\partial c_k}{\partial x}\right|_{x=L} = 0 \tag{5.5}$$

I.e. the system was considered to be closed for all elements.

For the solution of the diffusion equation (5.1) both thermodynamic and kinetic data are required. These data were retrieved from relevant thermodynamic and kinetic (mobility) databases. The diffusion coefficient in equation (5.2) was calculated by multiplying the respective mobilities with the relevant thermodynamic factor calculated by the Thermo-Calc computational thermodynamics software [5.19]. The thermodynamic database employed was the TCFE6 database for ferrous alloys, implemented in Thermo-Calc. The mobility database was the MOBFE2 database for ferrous alloys implemented in DICTRA. The initial composition of the steels used in the simulations is given in Table 1. These steels are listed in the API 530 standard and are used as tubing materials for high-temperature service. There are two group of steels in Table 5.1, ferritic Cr-Mo steels (P22, P21, P5, P9) and austenitic stainless steels (304, 316, 316L, 321, 347). Steels 321 and 347 are stabilized with Ti and Nb

respectively. The phases considered for the simulation were the FCC austenite phase as the matrix phase and the alloy carbides $M_{23}C_6$, M_7C_3 and MC. These carbides were considered to precipitate during carburization in the austenitic matrix.

Table 5.1: Chemical composition (wt%) of the steels under evaluation according to API 530. Values in parentheses indicate the compositions used for the simulations.

Steel grade	C	Mn	Si	P	S	Cr	Ni	Mo	Ti	Nb
P22	0.05-0.15 (0.1)	0.3-0.6 (0.4)	0.5 max (0.4)	0.025	0.025	1.9-2.6 (2.25)	-	0.87-1.13 (1)	-	
P21	0.05-0.15 (0.1)	0.3-0.6 (0.4)	0.5max (0.4)	0.025	0.025	2.65-3.35 (3)	-	0.8-1.06 (1)	-	
P5	0.15max (0.1)	0.3-0.6 (0.4)	0.5max (0.4)	0.025	0.025	4-6 (5)	-	0.45-0.65 (0.5)	-	
P5b	0.15max (0.1)	0.3-0.6 (0.4)	1-2 (1.5)	0.025	0.025	4-6 (5)	-	0.45-0.65 (0.5)	-	
P9	0.15max (0.1)	0.3-0.6 (0.4)	0.25-1 (0.6)	0.025	0.025	8-10 (9)	-	0.9-1.1 (1)	-	
304	0.08	2	1max (0.8)	0.04max	0.03max	18-20 (18)	8-11 (10)	-	-	
316	0.08max (0.08)	2	0.75max (0.7)	0.04max	0.03max	16-18 (16)	8-11 (10)	2-3 (2)	-	
316L	0.035max (0.03)	2	0.75max (0.7)	0.04max	0.03max	16-18 (16)	10-15 (10)	2-3 (2)	-	
321	0.08max (0.08)	2	0.75max (0.7)	0.04max	0.03max	16-18 (16)	9-13 (10)	-	0.4-0.6 (0.5)	
347	0.08max (0.05)	2max (1)	0.75max (0.6)	0.04max	0.03max	17-20 (18)	9-13 (10)	-	-	1

5.3 Results and discussion

5.3.1 Experimental validation

Following Engstrom et al. [5.20], the methodology described above was validated with experimental data for a Ni-25Cr (wt%) alloy exposed at 850°C for 1000 hours in a carburizing atmosphere with a carbon activity $a_c = 1$.

The carbon profile established within the tube wall is shown in Fig. 5.2a. In the same diagram the experimental carbon profile determined by Bongartz et al. [5.21] is superimposed. A good agreement is exhibited between calculated and experimental

values. In addition the profile of the volume fraction of the alloy carbides M_7C_3 and M_3C_2 is depicted in Fig. 5.2b, and is compared with the experimentally determined carbide distribution taken from Quadakkers et al. [5.22]. Again the agreement between calculated and experimental values is good. The presence of a 'discontinuity' of the carbon profile, in Fig. 5.2a, at about 0.5mm is attributed to the transformation from M_7C_3 to M_3C_2 carbide with increasing carbon. This experimental validation allows the implementation of the methodology in carburization simulations of the steels listed in Table 5.1.

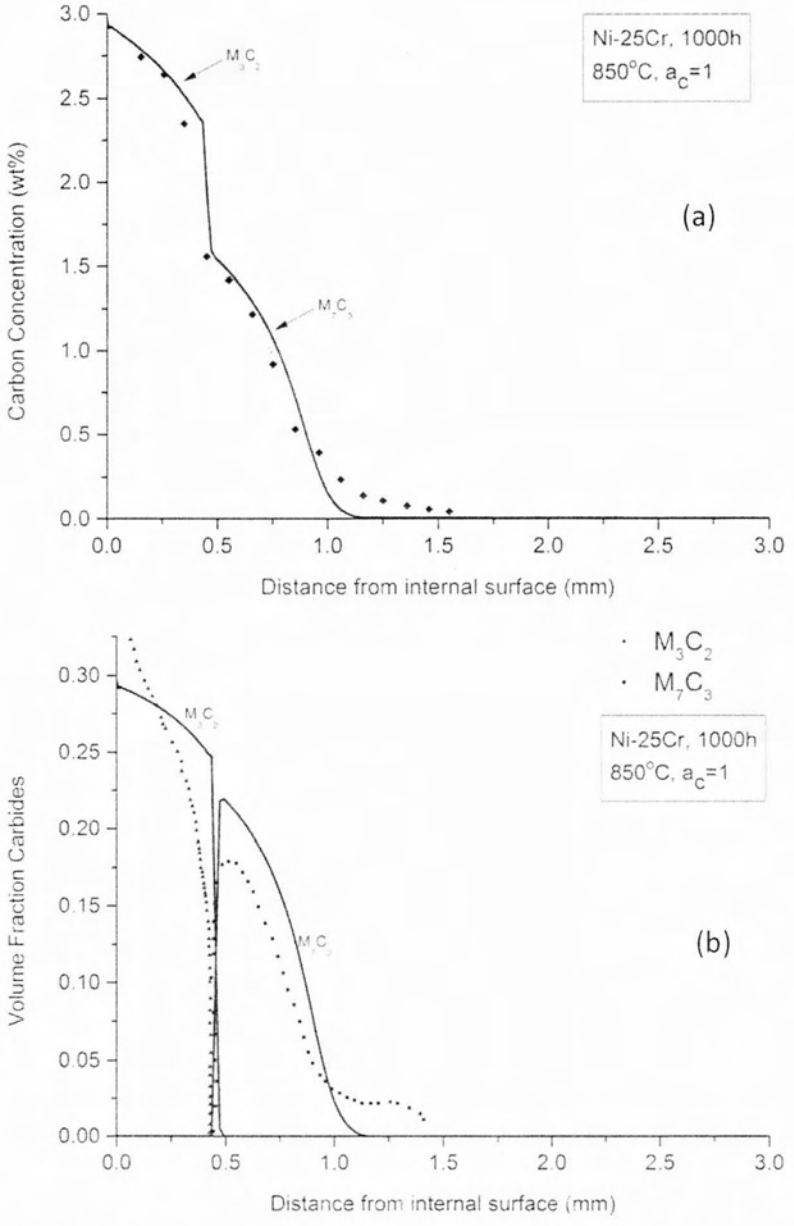

Figure 5.2: (a) Comparison of calculated (solid line) and experimental (dotted line) [5.21] carbon concentration profile and (b) comparison of calculated (solid line) and experimental (dotted line) [5.22] carbide volume fraction profile for Ni-25Cr alloy exposed for 1000h at 850°C with unit carbon activity.

5.3.2 Representative calculations for 316 steel

Carburization simulations were carried out for all steels of Table 5.1. Representative calculations for the 316 austenitic stainless steel will be discussed in this section. The simulation was performed for a temperature of 800°C. In Fig. 5.3a carbon concentration with distance from the inner surface of the tube is shown. The x-axis of the diagram corresponds to the tube wall thickness. The time required for the carburization front to reach a distance equal to half the thickness of the tube wall, termed carburization mid-thickness time $t_{1/2}$, is introduced to express the carburization resistance. From Fig. 5.3a it is depicted that the carbon profile reaches mid-thickness at a time of 222.2 hours. At the same time, as depicted in Fig. 5.3b, the carbide front reaches mid-thickness. As carbon diffuses in the tube, it enriches the austenitic matrix and carbides are being formed in the carburized regions. Initially $M_{23}C_6$ (M=Cr, Fe) is formed, but as carbon concentration increases with time, the $M_{23}C_6$ is replaced by the M_7C_3 carbide. In addition to Quadakkers et al. [5.22], this transformation has been documented experimentally by Kaya [5.8].

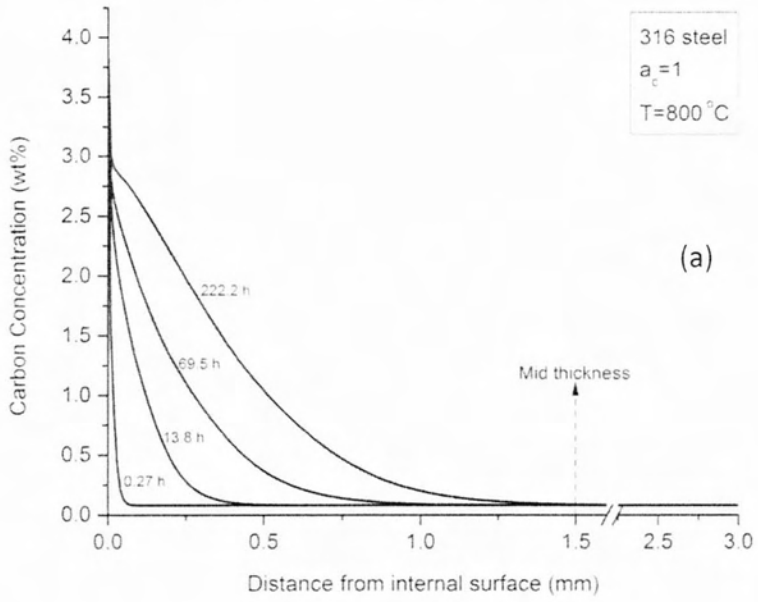

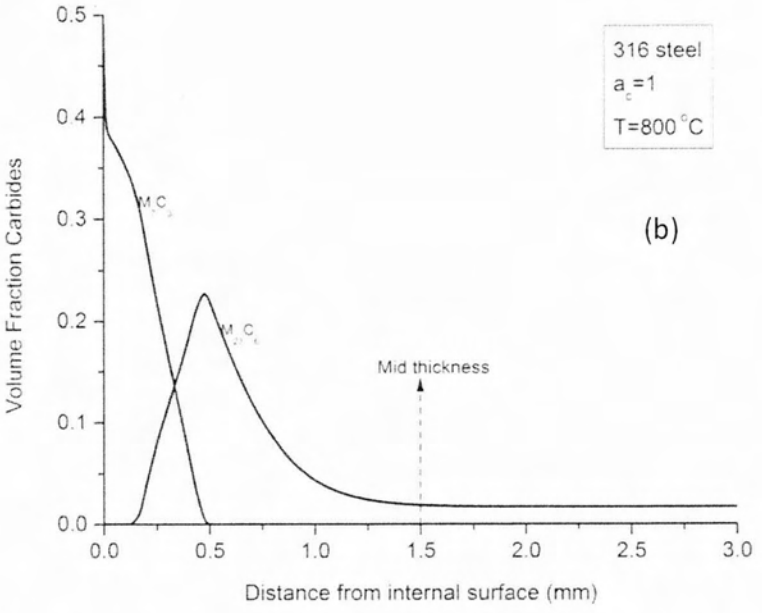

Figure 5.3: Carburization simulation for 316 steel at 800°C. (a) Evolution of carbon concentration profile with time. Carburization mid-thickness time is 222.2 h. (b) Profile of volume fraction carbides for 222.2 h carburization time

It is also important to monitor chromium depletion from the austenite matrix in the carburized regions, since this affects the oxidation resistance of the tube material. The chromium profile in the tube wall for the mid-thickness time $t_{1/2} = 222.2$ hours is shown in Fig.5.4. The Cr depletion corresponds to 0.5 wt% Cr at the inner surface of the tube.

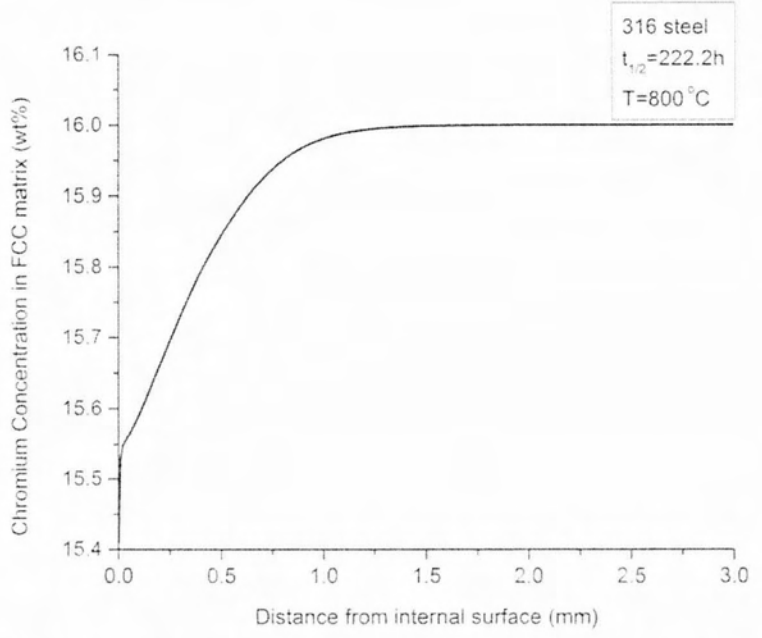

Figure 5.4: Chromium profile for the carburization mid-thickness time of 222.2 h for 316 steel at 800°C.

Temperature has a significant impact on carburization kinetics as demonstrated in Fig. 5.5, where calculations were performed for the temperature range 600-800°C. The carburization mid-thickness time $t_{1/2}$ of tubes is reduced rapidly with temperature.

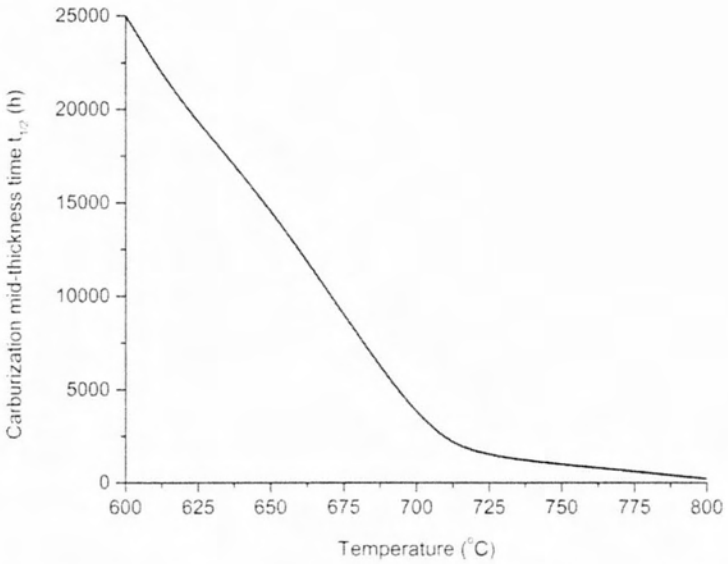

Figure 5.5: Effect of temperature on the carburization mid-thickness time for 316 steel.

5.3.3 Ranking of carburization resistance

The calculated carburization mid-thickness time $t_{1/2}$ for the steels listed in Table 5.1 is depicted in Figs. 5.6 and 5.7 for service temperatures 600 and 800 oC respectively. The steels are grouped in two classes, ferritic and austenitic. The austenitic grades exhibit a much longer mid-thickness time than the ferritic grades at both temperatures.

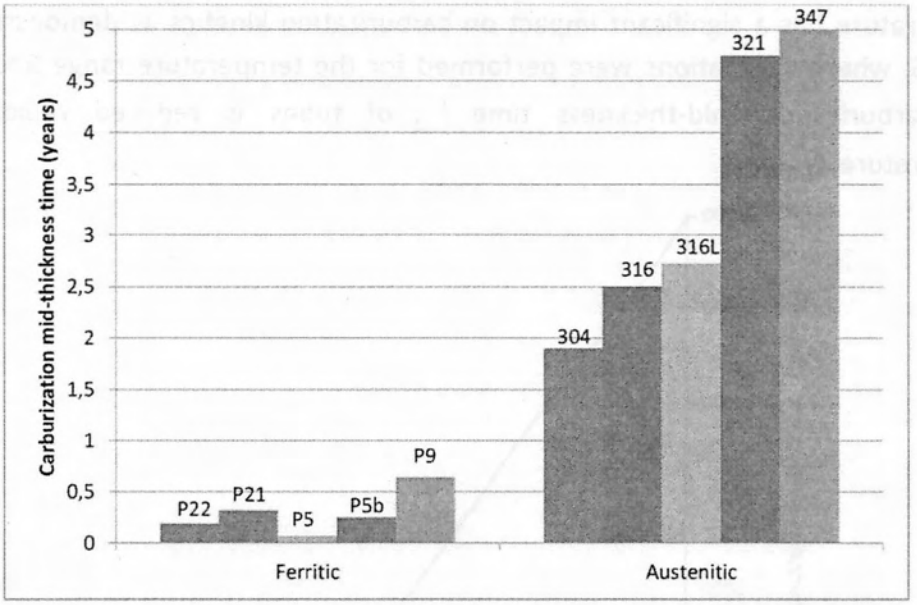

Figure 5.6: Calculated carburization mid-thickness time, (3mm tube thickness), for API 530 steels at 600°C .

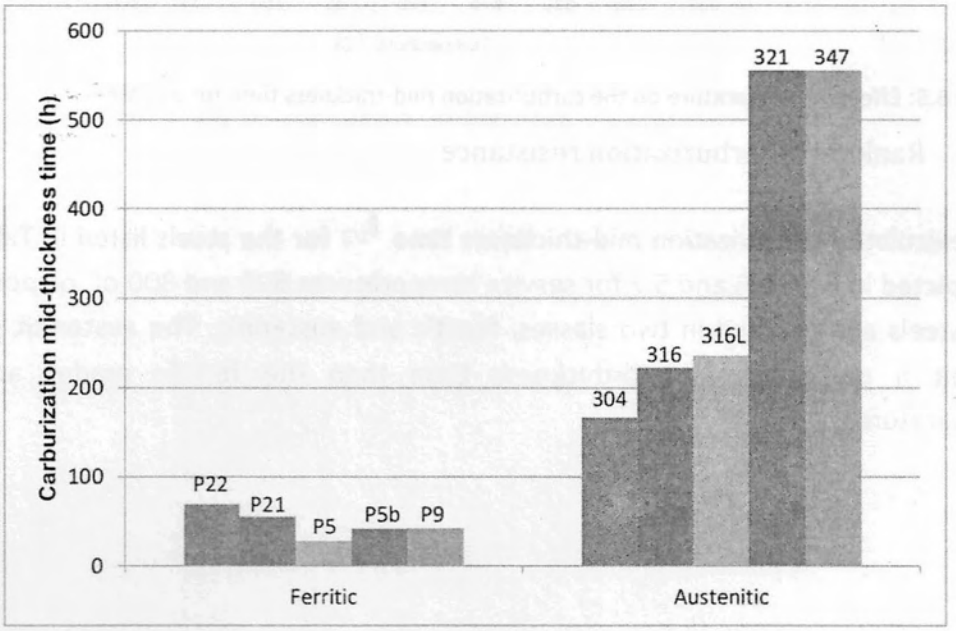

Figure 5.7: Calculated carburization mid-thickness time, (3mm tube thickness), for API 530 steels at 800°C.

This behavior is attributed to the lower diffusion coefficient of carbon in the FCC matrix. The differences between the steels of the austenitic group are larger than those of the ferritic group. The ferritic steels exhibit more or less similar carburization resistance. Nevertheless some variations should be discussed. At 600°C the P9 steel has the longest carburization mid-thickness time. This is attributed to the high Cr content, which in combination with the higher Mo content results in slower carbon diffusion. In addition the P5 steel exhibits the lowest carburization resistance due to the lower Mo content. The behavior is different at the higher

temperature of 800°C. The acceleration of diffusion at high temperature dominates the composition effects on carbon diffusion, and the carburization front is determined by the formation of carbides, which in turn depends on the available amount of Cr in the steel. Therefore, at 800°C the P22 steel exhibits the longest carburization mid-thickness time among the ferritic steels. As discussed above the austenitic steels possess a much higher carburization resistance than the ferritic grades. Regarding the non-stabilized grades 304, 316 and 316L, carburization resistance is raised by addition of Mo (316 vs 304) and lower carbon (316L vs 316). The stabilized grades 321 and 347 exhibit the highest carburization resistance among the austenitic steels. This is attributed to the formation of MC carbides, preventing the diffusion of carbon at higher depth from the surface. In order to validate this observation a carburization simulation was carried out at 800°C for the composition of steel 321 with and without addition of Ti. The results are shown in Fig. 5.8 where the carbide profiles are depicted for t=555.5h corresponding to the mid-thickness time for 321 steel.

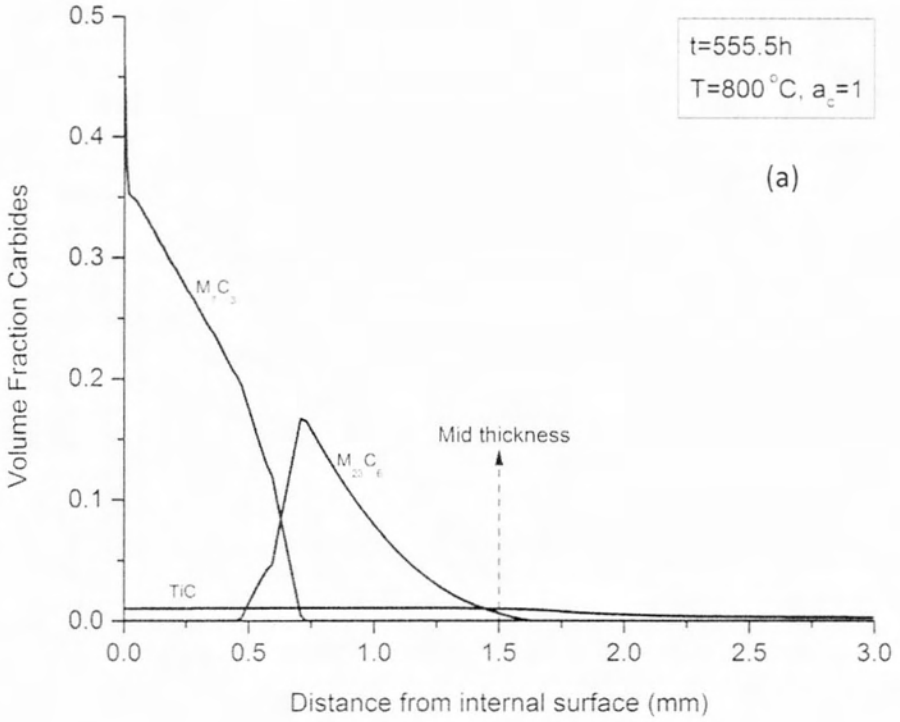

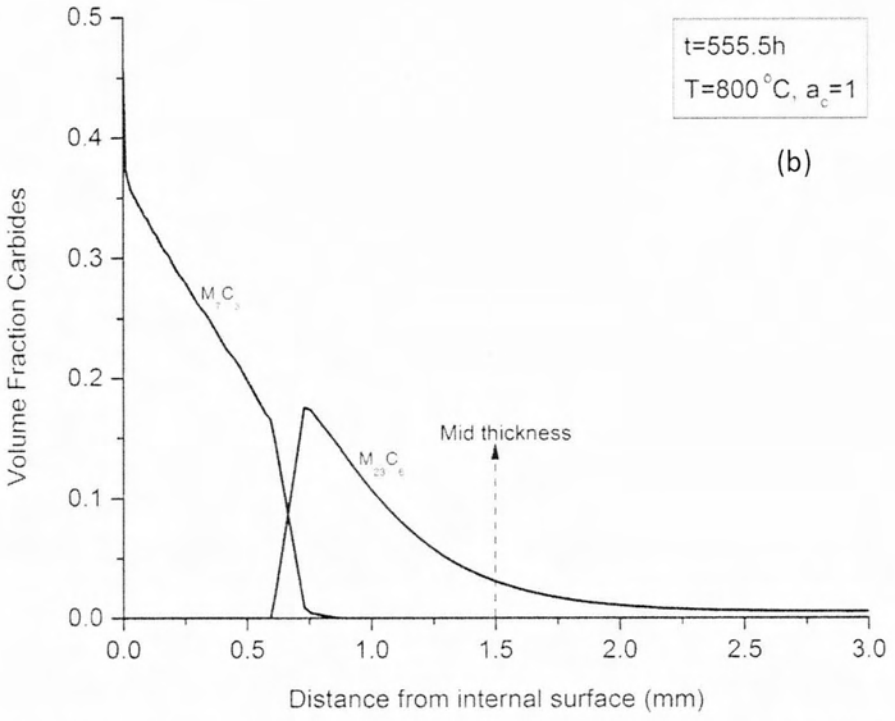

Figure 5.8: Comparison of carbide volume fraction profiles for the carburization mid-thickness time of 555.5 h for 321 steel at 800°C. (a) 321 steel, (b) 321 steel composition without Ti addition.

It is evident that for the steel without the Ti addition the carbide front goes beyond mid-thickness and reaches a much greater distance from the surface of the steel. There is a counter effect of MC carbides that requires attention. The interfaces between the MC carbides and the alloy matrix could provide a high diffusivity path and accelerate the diffusion of carbon in a way similar to that reported by Motin et al. [5.23] for the case of SiO_2 precipitates in Fe-Si alloys. However because of the low volume fraction of MC carbides this effect should be small.

The results presented above indicate that simulation of carburization could be a valuable tool in alloy selection for carburization resistance and for the development of suitable maintenance procedures for the timely replacement of tubes operating at high temperature

5.4 Conclusions

Carburization simulations were carried out for the heat-resistant steels referred to the API-530 standard by applying a model for carbon diffusion with the concurrent formation of alloy carbides. The method was validated experimentally. From the results presented above, the following conclusions can be drawn.

- The carburization layer is composed from $M_{23}C_6$ and M_7C_3 carbides. The M_7C_3 carbide is associated with higher carbon contents below the surface. In the Ti

or Nb stabilized austenitic grades, MC carbides form, leading to improvement of the carburization resistance.

- The austenitic grades exhibit a higher carburization resistance than the ferritic grades at all temperatures.
- The ferritic grades exhibit similar carburization resistance. Alloy composition has a stronger effect at lower service temperatures (600°C) where carburization resistance increases with Cr and Mo content. The acceleration of diffusion at high temperatures (800°C) dominates the composition effects on carbon diffusion, and the carburization front is determined by the formation of carbides, which in turn depends on the available amount of Cr in the steel.
- In the austenitic grades, the highest carburization resistance is exhibited by the stabilized grades 321 and 347. Regarding the non-stabilized grades, carburization resistance is raised by addition of Mo (316 vs 304) and lower carbon (316L vs 316).

5.5 References

[5.1] Forseth S, Kofstad P. Metal dusting phenomenon during carburization of Fe-Ni-Cr alloys at 850–1000°C. Mater. Corros. 1995;46:201-06.

[5.2] Matamala G, Canete P. Carburization of Fe-Ni-Cr Alloys in CH4-H2 Atmospheres between 900 and 1100°C. Revista Latinoamericana de Metalurgia y Materiales 1998;8:67-72.

[5.3] Grabke HJ, Wolf I. Carburization and oxidation. Mater. Sci. Eng. A 1987;87:23-33.

[5.4] Guttmann V, Burgel R. Effect of a carburizing environment on the creep behaviour of some austenitic steels. In Corrosion resistant materials for coal conversion systems. 1982;423-38.

[5.5] Swaminathan J, Singh R, Gunjan MR, Chattoraj I. Failure analysis of air pre-heater tubes of a petrochemicals plant. Eng. Fail. Anal. 2009;16:2371–81.

[5.6] Tawancy HM, Degradation of mechanical strength of pyrolysis furnace tubes by high-temperature carburization in a petrochemical plant. Eng. Fail. Anal. 2009;16:2171–78.

[5.7] Yin R, Carburization of 310 stainless steel exposed at 800–1100°C in 2%CH4/H2 gas mixture. Corros. Sci. 2005;47:1896–10.

[5.8] Kaya AA. Microstructure of HK40 alloy after high-temperature service in oxidizing/carburizing environment II. Carburization and carbide Transformations. Mater. Charact. 2002;49:23 – 34.

[5.9] Ju GJ, Wu WZ, Dai SH. Failure of 9Cr-1Mo tubes in a feed furnace of dehydrogenation unit. Int J. Pres. Ves. Pip. 1997;74:199-04.

[5.10] Tanner GM. Metal dusting (catastrophic carburization) of a waste boil heat tube. Eng. Fail. Ana.l 1994;1:289-06.

[5.11] D. Lopez-Lopez, Wong-Moreno A, Martinez L. Carburization processes involved in boiler-tube failures. Corros. Sci. 1993;35:1151-58.

[5.12] Kaewkumsai S, Khonraeng W, Sathirachinda N. High temperature failure of natural gas feed burner pipe. Eng. Fail. Anal. 2013;27:74–83.

[5.13] Hamid AU, Tawancy HM, Mohammed ARI, Abbas NM. Failure analysis of furnace radiant tubes exposed to excessive temperature. Eng. Fail. Anal. 2006;13:1005–21.

[5.14] API Standard 530. Calculation of heater tube thickness in petroleum refineries. 5th Edition, American Petroleum Institute, 2003.

[5.15] Young DJ, Carburization and metal dusting. Sheir's Corrosion.2010;1:272-303.

[5.16] Li H, Zheng Y, Benum LW, Oballa M, Chen W. Carburization behaviour of Mn–Cr–O spinel in high temperature hydrocarbon cracking environment. Corros. Sci. 2009;51:2336-41.

[5.17] Matsukawa C, Hayashi S, Yakuwa H, Kishikawa T, Narita T, Ukai S. High-temperature carburization behaviour of HASTELLOY X in CH4 gas. Corros. Sci. 2011;53:3131–38.

[5.18] Agren J. Computer simulations of diffusional reactions in complex steels. I.S.I.J. International 1992;32:291-96.

[5.19] Sundman B, Jansson B, Andersson JO. The Thermo-Calc databank system. CALPHAD 1985;9:153-90.

[5.20] Engstrom A, Hoglund L, Agren J, Computer simulation of diffusion in multicomponent systems. Metal. Mater. Trans. A 1994;25A:1127-1134.

[5.21] Bongartz K, Schulten R, Quadakkers WJ, Nickel H. Finite difference model describing carburization in high temperature alloys. Corrosion 1986;42:390-97.

[5.22] Quadakkers WJ, Schulten R, Bongartz K, Nickel H. A mathematical model describing carburization in multielement alloy systems. 10th Int. Conf. on Metal Corrosion, Madras, India 1987.

[5.23] Motin MAA, Zhang J, Young DJ, Simultaneous corrosion of Fe-Si alloys by carbon and oxygen. J. Electroch. Soc. 2010;157:C375-C381.

6. Conclusions

In this work an attempt was made for the consideration of creep and carburization phenomena which may cause catastrophic failures in oil refineries upon their evolution. API codes have been developed since ... and are revised regularly integrated update developments and experience towards the development of safer guidelines. Generating know-how in this area is a contribution to the further development of these codes.

API 530 was adopted for the minimum thickness evaluation of 347 austenitic stainless steel. The whole procedure was demonstrated in detail and the influence of the working temperature, as well as the initial design consideration, on the tube thickness were demonstrated.

The remaining life fraction of a gasifier shell was calculated according to API 530 using the LM method. Taking into account the results the shell has consumed a small portion of its service life before the temperature excursions.

API 530 suggests safe operational time periods in strong relation to the maximum temperature attained, while above the design limit (540 °C) cannot be used for any prediction purposes.

Microstructural assessment performed both by replica and common metallography technics indicated that locally the maximum temperature during the incidence excided the design limit of the CS. Phenomena as pearlite spheroidization, as well as grain coarsening were detected associated with local softening.

The bulk tensile properties showed that the CS's tensile properties are maintained well above the specified limits.

The API 579 -1 /ASME FFS procedure was employed to analyze the structural integrity of pressurized equipment used in high temperature applications in oil refineries. Level 2 assessment was conducted in two separate case studies taken from the recent activities of the Materials Laboratory.

In the first case study a bulging damage in a gasifier was considered with FFS and real operational conditions were integrated in the calculations. According to them the refinery was allowed to rerate the component after certain time period under specified temperature and pressure conditions.

In the second case study a fired crude heater was assessed in order to determine the remaining life fraction of the tubes. The remaining life was also calculated by using the Larson- Miller approach. FFS confines with the LM approach in case that the average LM parameter was considered. If the minimum LM parameter was taken into the calculations the two approaches differ.

Carburization simulations were carried out for the heat-resistant steels referred to the API-530 standard using thermodynamic and kinetic calculations. The

carburization layer is composed from $M_{23}C_6$ and M_7C_3 carbides. The M_7C_3 carbide is associated with higher carbon contents below the surface. In the Ti or Nb stabilized austenitic grades, MC carbides form, leading to improvement of the carburization resistance. The austenitic grades exhibit a higher carburization resistance than the ferritic grades at all temperatures. The ferritic grades exhibit similar carburization resistance. Alloy composition has a stronger effect at lower service temperatures (600°C) where carburization resistance increases with Cr and Mo content. The acceleration of diffusion at high temperatures (800°C) dominates the composition effects on carbon diffusion, and the carburization front is determined by the formation of carbides, which in turn depends on the available amount of Cr in the steel. In the austenitic grades, the highest carburization resistance is exhibited by the stabilized grades 321 and 347. Regarding the non-stabilized grades, carburization resistance is raised by addition of Mo (316 vs 304) and lower carbon (316L vs 316).

Annex

Calculation of the minimum thickness of tubes working at high temperatures.

Material : 347 and 347 H (18 Cr – 10 Ni – Nb)

Calculations are performed according to API 530

Parameters being used are :

- δ_{cr} : stress thickness, expressed in mm
- T_d : maximum temperature of metal tube, expressed in °C
- p : elastic/rupture design gauge pressure, expressed in MPa
- D_0 : outside diameter, expressed in mm
- δ_{ca} : corrosion allowance, expressed in mm
- t : operating time used as a basis for tube design
- σ_{el} : elastic allowable stress, expressed in MPa, at the design metal temperature
- σ_r : rupture allowable stress, expressed in MPa, at the design metal temperature
- δ_{min} : minimum thickness, expressed in mm, including corrosion allowance
- f_{corr} : corrosion fraction

Give the maximumum temperature of the metal tube, expressed in °C

```
Td = 705;
```

Give the outside diameter, expressed in mm

```
D0 = 168.3;
```

Give the elastic design gauge pressure or the the rupture design rupture pressure,expressed in MPa

```
p = 5.8;
```

Operating time used as basis for tube design, expressed in hours (x 10^3)

```
t = 100;
```

Give the corrosion allowance, expressed in mm

```
δCA = 3.2;
```

```
(*Digitize function of Elastic allowable stress,
σel, p.79, Fig. E17, API 530*)
σel[x_] :=
  125.46213 - 4.5 * 10^8 / (859.90165 * √(Pi / 2)) * Exp[-2 * ((x - 2656.20187) / 859.90165)^2];

(*Digitize function of Rupture allowable stress,
```

```
σr, 100*10^3h, p.79, Fig. E17, API 530*)
σr[x_, 100] := 76619.59143 * Exp[-x / 91.9845] + 1.23268;
(*Digitize function of Rupture allowable stress,σr, 60*10^3h,
p.79, Fig. E17, API 530*)
σr[x_, 60] := 52818.4372 * Exp[-x / 99.72] - 2.3078;

(*Digitize function of Rupture allowable stress,
σr, 40*10^3h, p.79, Fig. E17, API 530*)
σr[x_, 40] := 68681.72742 * Exp[-x / 97.2893] - 1.11634;

(*Digitize function of Rupture allowable stress,σr, 20*10^3h,
p.79, Fig. E17, API 530*)
σr[x_, 20] := 70516.03676 * Exp[-x / 98.95159] - 1.20069;

(*Digitize function of Yield strength,σy,p.79,Fig. E17, API 530*)
σy[x_] := -38648.13801 + 38788.69888 / (1 + Exp[(x - 1399.55523) / 88.24103]);

(*Digitize function of Corrosion Fraction,fcorr, p.5, Fig. 1, API 530*)
f[x_] := 0.65429 *
   x^0.22044  ;

If[Td < 590,
 (*elastic design*)
 If[σel[Td] < σy[Td],
  δσ,e = p * D0 / (2 σel[Td] + p);
  δmin = δσ,e + δCA;
  Print[Text["Minimum thickness:  "], δmin, Text[" mm"]],
  Print[Text["Wrong alloy"]]],

 (*rupture design*)
 δσ,r = p * D0 / (2 σr[Td, t] + p);
 B = δCA / δσ,r;

 δmin,r = δσ,r + f[B] * δCA;

 δσ,e = p * D0 / (2 σel[Td] + p);
 δmin,e = δσ,e + δCA;

 If[δmin,r > δmin,e, Print[Text["Minimum thickness:  "], δmin,r, Text[" mm"]],
  Print[Text["Minimum thickness:  "], δmin,e, Text[" mm"]]]]
```

Minimum thickness: 13.7345 mm

Larson – Miller

Material : P22

CalculationsareperformedaccordingtoAPI579

Parametersbeingusedare :

– T_i : temperature for each operating period , expressedin °F

– P : operating pressure, expressed in MPa

– D_0 □ : outside diameter, expressed in mm

– FCA : future corrosion allowance, expressedin mm

– t_i : operating time for each period

– t : thickness

Give the maximumum temperature of the metal tube, expressed in °F

```
T1 = 1112;
T2 = 1220;
T3 = 1112;
```

Give the orating preassure, expressed in mm

```
P = 1.45;
```

Give the outside Diameter, expressed in mm

```
OD = 220;
```

Give the thickness, expressed in mm

```
t = 8.18;
```

Give the Future Corrosion Allowance

```
FCA = 2.54;
```

Give the Past operating time, expressed in hours

```
t1 = 131 400;
```

Give the Excursion operating time, expressed in hours

```
t2 = 336;
```

Give the Future operating time, expressed in hours

```
t3 = 43800;
```

LM

$$\sigma_{1,1} = \frac{P\,(OD - t + FCA)}{2\,(t - FCA)} * 0.1450377;$$

$$\sigma_{2,1} = \frac{\sigma_{1,1}}{2};$$

$$\sigma_{3,1} = 0;$$

$$\sigma_{e,1} = 0.866 * \sigma_{1,1}$$

$$\sigma_{1,2} = \frac{P\,(OD - t + FCA)}{2\,(t - FCA)} * 0.1450377;$$

$$\sigma_{2,2} = \frac{\sigma_{1,2}}{2};$$

$$\sigma_{3,2} = 0;$$

$$\sigma_{e,2} = 0.866 * \sigma_{1,2};$$

$$\sigma_{1,3} = \frac{P\,(OD - t + FCA)}{2\,(t - FCA)} * 0.1450377;$$

$$\sigma_{2,3} = \frac{\sigma_{1,2}}{2};$$

$$\sigma_{3,3} = 0;$$

$$\sigma_{e,3} = 0.866 * \sigma_{1,3};$$

3.461

$$A_0 = 43.49;$$

$$A_1 = -0.602;$$

$$A_2 = -28.04;$$

$$A_3 = 0.206;$$

$$A_4 = 10.98;$$

$$A_5 = 0.028;$$

$$A_6 = 0.36;$$

$$C_{lmp} = 20;$$

$$B_0 = 43.98;$$

$$B_1 = -0.846;$$

$$B_2 = -40.48;$$

$$B_3 = 0.262;$$

$$B_4 = 15.37;$$

$$B_5 = 0.0496;$$

$$B_6 = 0.66;$$

$$J_{1,1} = \sigma_{1,1} + \sigma_{2,1} + \sigma_{3,1};$$

$$S_{s,1} = \sqrt{\sigma_{1,1}^{\,2} + \sigma_{2,1}^{\,2} + \sigma_{3,1}^{\,2}} \;\; // \; N;$$

$$S_{eff,1} = \sigma_{e,1}\, Exp\left[0.24\left(\frac{J_{1,1}}{S_{s,1}} - 1\right)\right];$$

$$LMP_{m1} = \frac{B_0 + B_2 * \sqrt{S_{eff,1}} + B_4 * S_{eff,1} + B_6 * S_{eff,1}^{\,1.5}}{1 + B_1 * \sqrt{S_{eff,1}} + B_3 * S_{eff,1} + B_5 * S_{eff,1}^{\,1.5}};$$

$$LMP_1 = \frac{A_0 + A_2 * \sqrt{S_{eff,1}} + A_4 * S_{eff,1} + A_6 * S_{eff,1}^{1.5}}{1 + A_1 * \sqrt{S_{eff,1}} + A_3 * S_{eff,1} + A_5 * S_{eff,1}^{1.5}};$$

$$L_{m1} = 10^{\left(\frac{1000 * LMP_{m1}}{T_1 + 460} - C_{Imp}\right)};$$

$$L_1 = 10^{\left(\frac{1000 * LMP_1}{T_1 + 460} - C_{Imp}\right)};$$

$$J_{1,2} = \sigma_{1,2} + \sigma_{2,2} + \sigma_{3,2};$$

$$S_{s,2} = \sqrt{\sigma_{1,2}^2 + \sigma_{2,2}^2 + \sigma_{3,2}^2} \quad // \; N;$$

$$S_{eff,2} = \sigma_{e,2} \, Exp\left[0.24 \left(\frac{J_{1,2}}{S_{s,2}} - 1\right)\right];$$

$$LMP_{m2} = \frac{B_0 + B_2 * \sqrt{S_{eff,2}} + B_4 * S_{eff,2} + B_6 * S_{eff,2}^{1.5}}{1 + B_1 * \sqrt{S_{eff,2}} + B_3 * S_{eff,2} + B_5 * S_{eff,2}^{1.5}};$$

$$LMP_2 = \frac{A_0 + A_2 * \sqrt{S_{eff,2}} + A_4 * S_{eff,2} + A_6 * S_{eff,2}^{1.5}}{1 + A_1 * \sqrt{S_{eff,2}} + A_3 * S_{eff,2} + A_5 * S_{eff,2}^{1.5}};$$

$$L_{m2} = 10^{\left(\frac{1000 * LMP_{m2}}{T_2 + 460} - C_{Imp}\right)};$$

$$L_2 = 10^{\left(\frac{1000 * LMP_2}{T_2 + 460} - C_{Imp}\right)};$$

$$J_{1,3} = \sigma_{1,3} + \sigma_{2,3} + \sigma_{3,3};$$

$$S_{s,3} = \sqrt{\sigma_{1,3}^2 + \sigma_{2,3}^2 + \sigma_{3,3}^2} \quad // \; N;$$

$$S_{eff,3} = \sigma_{e,3} \, Exp\left[0.24 \left(\frac{J_{1,3}}{S_{s,3}} - 1\right)\right];$$

$$LMP_{m3} = \frac{B_0 + B_2 * \sqrt{S_{eff,3}} + B_4 * S_{eff,3} + B_6 * S_{eff,3}^{1.5}}{1 + B_1 * \sqrt{S_{eff,3}} + B_3 * S_{eff,3} + B_5 * S_{eff,3}^{1.5}};$$

$$LMP_3 = \frac{A_0 + A_2 * \sqrt{S_{eff,3}} + A_4 * S_{eff,3} + A_6 * S_{eff,3}^{1.5}}{1 + A_1 * \sqrt{S_{eff,3}} + A_3 * S_{eff,3} + A_5 * S_{eff,3}^{1.5}};$$

$$L_{m3} = 10^{\left(\frac{1000 * LMP_{m3}}{T_3 + 460} - C_{Imp}\right)};$$

$$L_3 = 10^{\left(\frac{1000 * LMP_3}{T_3 + 460} - C_{Imp}\right)};$$

$$\frac{t_1}{L_1} + \frac{t_2}{L_2} + \frac{t_3}{L_3};$$

$$\frac{t_1}{L_{m1}} + \frac{t_2}{L_{m2}} + \frac{t_3}{L_{m3}};$$

$$If\left[\frac{t_1}{L_1} + \frac{t_2}{L_2} + \frac{t_3}{L_3} > 0.8,$$

```
 Print[Text["The component is NOT acceptable for continuing
```

```
    operation according to calculations using equations
    of AVERAGE Larson- Miller parameter"]], Print[
  Text["The component is acceptable for continuing operation according to
    calculations using equations of AVERAGE Larson- Miller parameter"]]]
```

$$\text{If}\left[\frac{t_1}{L_{m1}} + \frac{t_2}{L_{m2}} + \frac{t_3}{L_{m3}} > 0.8, \text{Print}[\text{Text}[\text{"The component is NOT acceptable}\right.$$

```
    for continuing operation according to calculations using
    equations of MINIMUM Larson- Miller parameter"]], Print[
  Text["The component is not acceptable for continuing operation according to
    calculations using equations of MINIMUM Larson- Miller parameter"]]]
```

The component is acceptable for continuing operation
according to calculations using equations of AVERAGE Larson– Miller parameter

The component is NOT acceptable for continuing operation
according to calculations using equations of MINIMUM Larson– Miller parameter

Fittness for Service for component with bulging

Calculations are performed according to API579

Parameters being used are :

- T_i : temperature of metal tube, expressed in °C
- p : elastic / rupture design gauge pressure, expressed in MPa
- OD : outside diameter, expressed in mm
- FCA : future corrosion allowance, expressedin mm
- t_i : operating time for each period
- r_i : thickness for each period

Give the maximumum temperature of the metal tube, expressed in °F

$T_1 = 649;$

$T_2 = 977;$

Give the Past operating time, expressed in hours

$t_1 = 87\,600;$

Give the outside Diameter, expressed in mm

$OD = 168;$

Give the thickness before for t_1, expressed in mm

$r_1 = 26;$

Give the thickness before for t_2, expressed in mm

$r_2 = 25.4;$

Give the Future operating time, expressed in hours

$t_2 = 3600;$

Give the orating preassure, expressed in MPa

$P = 0.45;$

Give the Material constants according to Annex F, Table F.30 [4.1] in API 579

$A_0 = -16.3;$

$A_1 = 38\,060;$

$A_2 = -9165;$

$A_3 = 1200;$

$A_4 = -600;$

$B_0 = -1;$

$B_1 = 3060;$

$B_2 = 135;$

$B_3 = -760;$

$B_4 = 247;$

Calculation of the principal Stresses, expressed in ksi

$$\sigma_{1,1} = \frac{P\,(OD - r_1 + FCA)}{2\,(t - FCA)} * 0.1451;$$

$$\sigma_{2,1} = \frac{\sigma_{1,1}}{2};$$

$$\sigma_{3,1} = 0;$$

$$\sigma_{e,1} = 0.866 * \sigma_{1,1};$$

$$\sigma_{1,2} = \frac{P\,(OD - r_2 + FCA)}{2\,(t - FCA)} * 0.1451;$$

$$\sigma_{2,2} = \frac{\sigma_{1,2}}{2};$$

$$\sigma_{3,2} = 0;$$

$$\sigma_{e,2} = 0.866 * \sigma_{1,2};$$

For cylinder or cone:

$$a_\omega = 2;$$

The MPC Project Omega Method parameter is:

$$\beta_\omega = \frac{1}{3};$$

MPC Project Omega Method

$$S_{1,1} = \text{Log}[\sigma_{e,1},\ 10]$$

$$\varepsilon_{co,1} = 10^{-\left(A_0 + \frac{1}{460 + T_1}\left(A_1 + A_2 * S_{1,1} + A_3 * S_{1,1}^2 + A_4 * S_{1,1}^3\right)\right)};$$

$$\ddot{Y}_1 = 10^{\left(B_0 + \frac{1}{460 + T_1}\left(B_1 + B_2 * S_{1,1} + B_3 * S_{1,1}^2 + B_4 * S_{1,1}^3\right)\right)};$$

$$\eta_{BN,1} = -\left(\left(\frac{1}{460 + T_1}\right)\left(A_2 + 2\,A_3 * S_{1,1} + 3\,A_4 * S_{1,1}^2\right)\right);$$

$$\ddot{Y}_{n,1} = \text{Max}[\ddot{Y}_1 - \eta_{BN,1},\ 3];$$

$$\delta_{\omega,1} = \beta_\omega\left(\frac{\sigma_{1,1} + \sigma_{2,1} + \sigma_{3,1}}{\sigma_{e,1}} - 1\right);$$

$$\ddot{Y}_{m,1} = \ddot{Y}_{n,1}^{\delta_{\omega,1}+1} + a_\omega * \eta_{BN,1};$$

$$L_1 = \frac{1}{\varepsilon_{co,1} * \ddot{Y}_{m,1}};$$

$$S_{1,2} = \text{Log}[\sigma_{e,2},\ 10];$$

$$\varepsilon_{co,2} = 10^{-\left(A_0 + \frac{1}{460 + T_2}\left(A_1 + A_2 * S_{1,2} + A_3 * S_{1,2}^2 + A_4 * S_{1,2}^3\right)\right)};$$

$$\ddot{Y}_2 = 10^{\left(B_0 + \frac{1}{460 + T_2}\left(B_1 + B_2 * S_{1,2} + B_3 * S_{1,2}^2 + B_4 * S_{1,2}^3\right)\right)};$$

$$\eta_{BN,2} = -\left(\left(\frac{1}{460 + T_2}\right)\left(A_2 + 2\,A_3 * S_{1,2} + 3\,A_4 * S_{1,2}^2\right)\right);$$

$$\ddot{Y}_{n,2} = \text{Max}[\ddot{Y}_2 - \eta_{BN,2},\ 3];$$

$$\delta_{\omega,2} = \beta_\omega\left(\frac{\sigma_{1,2} + \sigma_{2,2} + \sigma_{3,2}}{\sigma_{e,2}} - 1\right);$$

$$\ddot{Y}_{m,2} = \ddot{Y}_{n,2}^{\delta_{\omega,2}+1} + a_\omega * \eta_{BN,2};$$

$$L_2 = \frac{1}{\varepsilon_{co,2} * \ddot{Y}_{m,2}};$$

$$\frac{t_1}{L_1} + \frac{t_2}{L_2};$$

$$\text{If}\left[\frac{t_1}{L_1} + \frac{t_2}{L_2} > 0.8,\ \text{Print}[\text{Text}[\text{"A rerate is needed"}]],\ \text{Print}[\text{Text}[\text{"The component can return to service"}]]\right]$$

The component can return to service

Fittness for Service for component with excursion time period

Calculations are performed according to API579

Parameters being used are :

- T_i : temperature for each operating period , expressedin °F
- P : operating pressure, expressed in MPa
- OD : outside diameter, expressed in mm
- FCA : future corrosion allowance, expressed in mm
- t_i : operating time for each period

Give the maximumum temperature of the metal tube, expressed in °F

$T_1 = 1112;$

$T_2 = 1220;$

$T_3 = 1112;$

Give the orating preassure, expressed in MPa

$P = 1.45;$

Give the outside Diameter, expressed in mm

$OD = 220;$

Give the thickness, expressed in mm

$t = 8.18;$

Give the Future Corrosion Allowance

$FCA = 2.54;$

Give the Past operating time, expressed in hours

$t_1 = 131\,400;$

Give the Excursion operating time, expressed in hours

$t_2 = 336;$

Give the Future operating time, expressed in hours

$t_3 = 43\,800;$

Give the Material constants according to Annex F, Table F.30 [4.1] in API 579

$A_0 = -21.86;$
$A_1 = 50\,205;$
$A_2 = -5436;$
$A_3 = 500;$
$A_4 = -3400;$
$B_0 = -1.85;$
$B_1 = 7205;$
$B_2 = -2436;$
$B_3 = 0;$
$B_4 = 0;$

For cylinder or cone:

$a_\omega = 2;$

The MPC Project Omega Method parameter is:

$\beta_\omega = \frac{1}{3};$

MPC Project Omega Method

$$\sigma_{1,1} = \frac{P\,(OD - t + FCA)}{2\,(t - FCA)} * 0.1451;$$
$$\sigma_{2,1} = \frac{\sigma_{1,1}}{2};$$
$$\sigma_{3,1} = 0;$$
$$\sigma_{e,1} = 0.866 * \sigma_{1,1}$$

$$\sigma_{1,2} = \frac{P\,(OD - t + FCA)}{2\,(t - FCA)} * 0.1451;$$
$$\sigma_{2,2} = \frac{\sigma_{1,2}}{2};$$
$$\sigma_{3,2} = 0;$$
$$\sigma_{e,2} = 0.866 * \sigma_{1,2};$$

$$\sigma_{1,3} = \frac{P\,(OD - t + FCA)}{2\,(t - FCA)} * 0.1451;$$
$$\sigma_{2,3} = \frac{\sigma_{1,2}}{2};$$
$$\sigma_{3,3} = 0;$$
$$\sigma_{e,3} = 0.866 * \sigma_{1,3};$$

$$S_{1,1} = \text{Log}[\sigma_{e,1},\ 10]$$
$$\varepsilon_{co,1} = 10^{-\left(A_0 + \frac{1}{460 + T_1}\left(A_1 + A_2 * S_{1,1} + A_3 * S_{1,1}^2 + A_4 * S_{1,1}^3\right)\right)};$$
$$\ddot{Y}_1 = 10^{\left(B_0 + \frac{1}{460 + T_1}\left(B_1 + B_2 * S_{1,1} + B_3 * S_{1,1}^2 + B_4 * S_{1,1}^3\right)\right)};$$
$$\eta_{BN,1} = -\left(\left(\frac{1}{460 + T_1}\right)\left(A_2 + 2\,A_3 * S_{1,1} + 3\,A_4 * S_{1,1}^2\right)\right);$$
$$\ddot{Y}_{n,1} = \text{Max}[\ddot{Y}_1 - \eta_{BN,1},\ 3];$$

$$\delta_{\omega,1} = \beta_\omega \left(\frac{\sigma_{1,1} + \sigma_{2,1} + \sigma_{3,1}}{\sigma_{e,1}} - 1 \right);$$

$$\ddot{Y}_{m,1} = \ddot{Y}_{n,1}^{\delta_{\omega,1}+1} + a_\omega * \eta_{BN,1};$$

$$L_1 = \frac{1}{\varepsilon_{co,1} * \ddot{Y}_{m,1}};$$

$$S_{1,2} = \text{Log}[\sigma_{e,2}, 10];$$

$$\varepsilon_{co,2} = 10^{-\left(A_0 + \frac{1}{460+T_2}\left(A_1 + A_2 * S_{1,2} + A_3 * S_{1,2}^2 + A_4 * S_{1,2}^3\right)\right)};$$

$$\ddot{Y}_2 = 10^{\left(B_0 + \frac{1}{460+T_2}\left(B_1 + B_2 * S_{1,2} + B_3 * S_{1,2}^2 + B_4 * S_{1,2}^3\right)\right)};$$

$$\eta_{BN,2} = -\left(\left(\frac{1}{460 + T_2}\right)\left(A_2 + 2\,A_3 * S_{1,2} + 3\,A_4 * S_{1,2}^2\right)\right);$$

$$\ddot{Y}_{n,2} = \text{Max}[\ddot{Y}_2 - \eta_{BN,2}, 3];$$

$$\delta_{\omega,2} = \beta_\omega \left(\frac{\sigma_{1,2} + \sigma_{2,2} + \sigma_{3,2}}{\sigma_{e,2}} - 1 \right);$$

$$\ddot{Y}_{m,2} = \ddot{Y}_{n,2}^{\delta_{\omega,2}+1} + a_\omega * \eta_{BN,2};$$

$$L_2 = \frac{1}{\varepsilon_{co,2} * \ddot{Y}_{m,2}};$$

$$S_{1,3} = \text{Log}[\sigma_{e,3}, 10];$$

$$\varepsilon_{co,3} = 10^{-\left(A_0 + \frac{1}{460+T_3}\left(A_1 + A_2 * S_{1,3} + A_3 * S_{1,3}^2 + A_4 * S_{1,3}^3\right)\right)};$$

$$\ddot{Y}_3 = 10^{\left(B_0 + \frac{1}{460+T_3}\left(B_1 + B_2 * S_{1,3} + B_3 * S_{1,3}^2 + B_4 * S_{1,3}^3\right)\right)};$$

$$\eta_{BN,3} = -\left(\left(\frac{1}{460 + T_3}\right)\left(A_2 + 2\,A_3 * S_{1,3} + 3\,A_4 * S_{1,3}^2\right)\right);$$

$$\ddot{Y}_{n,3} = \text{Max}[\ddot{Y}_3 - \eta_{BN,3}, 3];$$

$$\delta_{\omega,3} = \beta_\omega \left(\frac{\sigma_{1,3} + \sigma_{2,3} + \sigma_{3,3}}{\sigma_{e,3}} - 1 \right);$$

$$\ddot{Y}_{m,3} = \ddot{Y}_{n,3}^{\delta_{\omega,3}+1} + a_\omega * \eta_{BN,3};$$

$$L_3 = \frac{1}{\varepsilon_{co,3} * \ddot{Y}_{m,3}};$$

$$\frac{t_1}{L_1} + \frac{t_2}{L_2} + \frac{t_3}{L_3};$$

```
If[ t1/L1 + t2/L2 + t3/L3 > 0.8, Print[Text["A rerate is needed" ]],
 Print[Text["The component can return to service" ]]]
```